

ISOLATION OF CARDAMONIN,
PINOSTROBIN CHALCONE FROM THE
RHIZOMES OF *BOESENBERGIA ROTUNDA*
AND THEIR CYTOTOXIC EFFECTS AGAINST
COLON CANCER HT29 AND BREAST
CANCER MDA-MB-231 CELL LINES

IBRAHIM AWAD MOHAMMED

UMP

MASTER OF SCIENCE

UNIVERSITI MALAYSIA PAHANG

UNIVERSITI MALAYSIA PAHANG

DECLARATION OF THESIS AND COPYRIGHT

Author's Full Name : IBRAHIM AWAD MOHAMMED

Date of Birth : 2ND JANUARY, 1992

Title : ISOLATION OF CARDAMONIN, PINOSTROBIN
CHALCONE FROM THE RHIZOME OF
BOESENBERGIA ROTUNDA AND THEIR CYTOTOXIC
EFFECTS AGAINST COLON CANCER HT29 AND
BREAST CANCER MDA-MB-231 CELL LINES

Academic Session : SEM 2 2018/2019

I declare that this thesis is classified as:

- CONFIDENTIAL (Contains confidential information under the Official Secret Act 1997)*
- RESTRICTED (Contains restricted information as specified by the organization where research was done)*
- OPEN ACCESS I agree that my thesis to be published as online open access (Full Text)

I acknowledge that Universiti Malaysia Pahang reserves the following rights:

1. The Thesis is the Property of Universiti Malaysia Pahang
2. The Library of Universiti Malaysia Pahang has the right to make copies of the thesis for the purpose of research only.
3. The Library has the right to make copies of the thesis for academic exchange.

Certified by:

(Student's Signature)

(Supervisor's Signature)

A2893476
New IC/Passport Number
Date:

DR. MOHAMMED NADEEM AKHTAR
Name of Supervisor
Date:

NOTE: * If the thesis is CONFIDENTIAL or RESTRICTED, please attach a thesis declaration letter.

SUPERVISOR'S DECLARATION

We hereby declare that we have checked this thesis and, in our opinion,, this thesis is adequate in terms of scope and quality for the award of the degree of Master of Science

(Supervisor's Signature)

Full Name : DR. MOHAMMED NADEEM AKHTAR

Position : ASSOCIATE PROFESSOR

Date :

(Co-supervisor's Signature)

Full Name : DR. HAZRULRIZAWATI ABD HAMID

Position : ASSOCIATE PROFESSOR

Date :

STUDENT'S DECLARATION

I hereby declare that the work in this thesis is based on my original work except for quotations and citations which have been duly acknowledged. I also declare that it has not been previously or concurrently submitted for any other degree at Universiti Malaysia Pahang or any other institutions.

(Student's Signature)

Full Name : IBRAHIM AWAD MOHAMMED

ID Number : MSK17001

Date :



UMP

ISOLATION OF CARDAMONIN, PINOSTROBIN CHALCONE FROM THE
RHIZOMES OF *BOESENBERGIA ROTUNDA* AND THEIR CYTOTOXIC
EFFECTS AGAINST COLON CANCER HT29 AND BREAST CANCER MDA-
MB-231 CELL LINES



IBRAHIM AWAD MOHAMMED

Thesis submitted in fulfilment of the requirements
for the award of the degree of
Master of Science

UMP

Faculty of Industrial Science & Technology

UNIVERSITI MALAYSIA PAHANG

JUNE 2019

ACKNOWLEDGEMENTS

I am very grateful to God the Almighty, the Most Gracious and the Most Merciful for giving me this chance and guiding me through. I am extremely grateful and would like to express my sincere gratitude to my supervisor, Assoc. Prof. Dr. Muhammad Nadeem Akhtar for his creative ideas, invaluable guidance, continued encouragement, constant support and time spent in making this project possible. He had provided me with his professional opinions and judgments in helping me able to analyze and interpreting the spectral data. I am sincerely gratifying for his guidance and his tolerance on my mistakes during this final year project.

I would also like to express my gratitude to Dr. Seema Zareen as well as Universiti Malaysia Pahang. I also would like to express special thanks to lab assistants and officers of Faculty of Industrial Sciences and Technology, UMP for their helps during this project. Besides that, thanks for the Central Laboratory UMP for providing NMR services. I would like to give my appreciations to my course mates who had helped me during my master projects. Together we had shared the knowledge and help each other during this project would definitely leave a great memory in my undergraduate study life. I also would like to express special thanks to my father and my mother and my sisters.



UMP

ABSTRAK

Boesenbergia rotunda adalah contoh tumbuhan herba perubatan yang secara tradisinya digunakan dalam rawatan pelbagai penyakit yang mengancam nyawa seperti diuretik, disentri, keradangan, gangguan afrodisiak dan gangguan gastrointestinal. Produk semulajadi dari tumbuh-tumbuhan perubatan, sama ada sebagai sebatian tulen atau ekstrak bersandar, menyediakan peluang tanpa had untuk ubat-ubatan baru kerana terdapatnya banyak kepelbagaian kimia. Disebabkan peningkatan permintaan untuk kepelbagaian kimia dalam program skrining, mencari ubat-ubatan terapeutik dari produk semulajadi, minat terutamanya dalam tumbuhan yang boleh dimakan telah berkembang di seluruh dunia. Dalam kajian ini bioaktif sebatian telah diekstrak dan selepas itu terpencil dari akar *Boesenbergia rotunda* menggunakan teknik pengekstrakan pelarut. Sebatian yang disintesis dicirikan oleh spektrometri UV-Visible, Spektrofotometri Inframerah Inframerah Inframerah (FTIR), spektrometri Resonans Magnetik Spektrometri Gas (GC-MS) dan Resonans Magnetik NMR (NMR). Ekstrak tersebut kemudiannya tertakluk kepada analisis sitotoksik untuk mengkaji aktiviti biologi ekstrak. Ekstrak bioaktif dan heksana dan ekstrak kloroform tertumpu pada kromatografi lajur dan nipis. Enam unsur bahan kimia utama, pinostrobin (1), chalcone pinostrobin (2), cardamonin (3), 4,5-dihydrokawain (4) pinocembrin (5), dan alpinetin (6) diasingkan daripada rizom *Boesenbergia rotunda*. Semua unsur-unsur kimia ditapis dengan sel-sel kanser payudara triple-negatif manusia (MDA-MB-231) dan sel-sel sel kanser HT-29 dengan menggunakan 3-(4,5-dimetilthiazol-2-yl)-2,5-Ujian diphenyltetrazolium bromide (MTT) secara in vitro. Kompaun kardamonin (3), ($IC_{50} = 5.62 \pm 0.61$ dan $4.44 \pm 0.66 \mu\text{g} / \text{mL}$) dan chalcone pinostrobin (2), ($IC_{50} = 20.42 \pm 2.23$ dan $22.51 \pm 0.42 \mu\text{g} / \text{mL}$) terhadap sel-sel kanser kolon MDA-MB-231 dan HT-29. Kesan sitotoksik kardamonin (3), chalcone pinostrobin (2) dan flavokawain B (FKB) juga dibandingkan dan digambarkan oleh penyelidikan molekul dok untuk menubuhkan hubungan struktur-aktiviti. Struktur semua sebatian disokong dengan bantuan teknik crystallographic X-ray $^1\text{H-NMR}$, GC-MS, IR, UV dan tunggal. Penemuan ini dapat membantu meningkatkan penemuan ubat masa depan terhadap kanser payudara dan garis sel kanser kolon (H29). Hasil kajian menunjukkan bahawa *B. rotunda* rhizome mempunyai potensi dalam aplikasi ubat dan nutraseutikal. Selain itu, ini memberikan maklumat asas mengenai kehadiran sebatian yang dihasilkan dalam budaya in vitro yang penting untuk manipulasi lanjut jalur metabolik dalam kajian lain yang berkaitan

ABSTRACT

Boesenbergia rotunda is an example of medicinal herbal plants which has been traditionally employed in the treatment of many life-threatening ailments such as diuretic, dysentery, inflammation, aphrodisiac and gastrointestinal disorder. Natural products from medicinal plants, either as pure compounds or as standardized extracts, provide unlimited opportunities for new drug leads because of the huge availability of chemical diversity. Due to an increasing demand for chemical diversity in screening programs, seeking therapeutic drugs from natural products, interest particularly in edible plants has grown throughout the world. In this study bioactive compounds were extracted and thereafter isolated from the root of *Boesenbergia rotunda* using solvent extraction techniques. The synthesized compounds were characterized by using UV-Visible, Fourier Transform Infrared spectrophotometry (FTIR), Gas Chromatography-Mass Spectrometry (GC-MS) and Nuclear Magnetic Resonance (NMR) spectrometry. The extracts were thereafter subjected to cytotoxic analysis to study the biological activities of the extracts. The bioactive extracts hexane and chloroform extracts were subjected to column and thin chromatography. Six major chemicals constituents, pinostrobin (1), pinostrobin chalcone (2), cardamonin (3), 4,5-dihydrokawain (4) pinocembrin (5), and alpinetin (6) were isolated from the rhizomes of the *Boesenbergia rotunda*. All the chemical constituents were screened against the human triple-negative breast cancer cell (MDA-MB-231) and HT-29 colon cancer cell lines by using 3-(4,5-dimethylthiazol-2-yl)-2,5-diphenyltetrazolium bromide (MTT) assay *in vitro*. The compound cardamonin (3), ($IC_{50} = 5.62 \pm 0.61$ and 4.44 ± 0.66 $\mu\text{g/mL}$) and pinostrobin chalcone (2), ($IC_{50} = 20.42 \pm 2.23$ and 22.51 ± 0.42 $\mu\text{g/mL}$) were found to be potential natural cytotoxic compounds against MDA-MB-231 and HT-29 colon cancer cell lines, respectively. Cytotoxic effects of cardamonin (3), pinostrobin chalcone (2) and flavokawain B (FKB) were also compared and visualized by the molecular docking studies to establish the structure-activity relationship. The structures of all compounds were supported with the aid of $^1\text{H-NMR}$, GC-MS, IR, UV and single X-ray crystallographic techniques. These findings could help to improve the future drug discovery against breast cancer and colon cancer cell lines (H29). The result of the study suggests that *B. rotunda* rhizome has a potential in drug and nutraceutical applications. Moreover, this provides a baseline information on the presence of the compounds produced in *in vitro* cultures which is crucial for further manipulation of the metabolic pathway in other relevant studies

TABLE OF CONTENT

DECLARATION	
TITLE PAGE	
ACKNOWLEDGEMENTS	ii
ABSTRAK	iii
ABSTRACT	iv
TABLE OF CONTENT	v
LIST OF TABLES	ix
LIST OF FIGURES	x
LIST OF ABBREVIATIONS	xii
CHAPTER 1 INTRODUCTION	1
1.1 Research Background	1
1.2 Problem Statement	3
1.3 Research Objectives	4
1.4 Scope of Study	4
CHAPTER 2 LITERATURE REVIEW	6
2.1 Overview	6
2.2 Pharmacological Significance and Phytochemical Application of the Plant	7
2.3 Overview of Anti-radical Metabolites in <i>Boesenbergia rotunda</i>	13
2.4 Soxhlet Extraction	15
2.5 Isolation and Purification of Bioactive Constituents	16
2.6 Physicochemical Characterization Plants Metabolites	17
2.7 Molecular Docking	19

CHAPTER 3 METHODOLOGY	20
3.1 Sample Preparation	20
3.2 Reagents	20
3.3 Extraction Process	20
3.4 Characterization of Isolated <i>Compounds</i>	22
3.4.1 Ultraviolet-Visible Photometry Analysis	22
3.4.2 Gas Chromatography-Mass Spectroscopy (GC-MS) Analysis	22
3.4.3 Fourier transform infrared spectroscopy (FTIR)	22
3.4.4 Nuclear Magnetic Resonance Spectroscopy	23
3.5 Cell Viability Assay	23
3.5.1 Cell Line and Culture	23
3.5.2 Validation and Detection of Cell Viability Using MTT Assay	24
3.6 Computational Molecular Docking Studies	24
CHAPTER 4 RESULTS AND DISCUSSION	26
4.1 Overview of Preliminary Estimation of Extract Yield and Purified Fractions	26
4.2 Results of Pinostrobin (1) Characterization	26
4.2.1 UV-Vis Spectrometry Analysis of Pure Pinostrobin (1)	26
4.2.2 Functional Group Analysis of Single Pure Pinostrobin (1)	27
4.2.3 ¹ H Nuclear Magnetic Resonance (NMR) for a Pure Pinostrobin (I)	29
4.2.4 Gas Mass Spectrometry Determination of Pinostrobin (1)	30
4.2.5 Results of X-ray Crystallography Analysis of Pinostrobin (1)	32
4.3 Isolation and purification of Pinostrobin Chalcone (2)	33
4.3.1 UV-Vis Spectrophotometry Analysis of Pinostrobin Chalcone (2)	33
4.3.2 Functional Group Analysis of Single Pure Pinostrobin chalcone	34

4.3.3	¹ H Nuclear Magnetic Resonance (NMR) for Pinostrobin chalcone (2)	34
4.3.4	Gas Mass Spectrometry Determination of Pure Pinostrobin chalcone (2)	36
4.4	Characterization Results for Cardamonin (3)	36
4.4.1	UV-Vis Spectrometry Analysis of Cardamonin (3)	37
4.4.2	Functional Group Analysis of Single Pure Cardamonin (3)	37
4.4.3	¹ H Nuclear Magnetic Resonance (NMR) for a Pure Cardamonin (3)	38
4.4.4	Gas Mass Spectrometry Determination of Cardamonin (3)	39
4.5	Results of Pure 5, 6-dehydrokawain (4) Characterization	40
4.5.1	UV-Vis Spectrometry Analysis of 5,6-dehydrokawain (4)	40
4.5.2	Functional Group Analysis of Single Pure 5,6-dehydrokawain (4)	40
4.5.3	¹ H Nuclear Magnetic Resonance (NMR) for a Pure 5,6-dehydrokawain (4)	41
4.5.4	Gas Mass Spectrometry Determination of Pure 5,6-dehydrokawain (4)	42
4.6	Results of Pure 5,7-dihydroxyflavanone (5) Characterization	43
4.6.1	UV-Vis Spectrometry Analysis of 5,7-dihydroxyflavanone (5)	43
4.6.2	Functional Group Analysis of 5,7-dihydroxyflavanone (5)	44
4.6.3	¹ H Nuclear Magnetic Resonance for 5,7-dihydroxyflavanone (5)	45
4.6.4	Gas Mass Spectrometry Determination of 5,7-dihydroxyflavanone (5)	46
4.7	Results of Alpinetin (6) Characterization	47
4.7.1	UV-Vis Spectrometry Analysis of Pure Alpinetin (6)	47
4.7.2	Functional Group Analysis of Single Pure Alpinetin (6)	48
4.7.3	¹ H Nuclear Magnetic Resonance (NMR) of Alpinetin (6)	49
4.7.4	Gas Mass Spectrometry Determination of Pure Alpinetin (6)	51

4.8	Results of Flavokawain B (FKB) (7)	51
4.8.1	UV-Vis Spectrometry Analysis of Pure FKB (7)	52
4.8.2	Functional Group Analysis of FKB (7)	52
4.8.3	^1H Nuclear Magnetic Resonance (NMR) of FKB (7)	53
4.9	Cytotoxic Effects on Colon H-29 and Breast MDA-MB-231 Cancer Cell Line	54
4.10	Results of Molecular Docking Studies	57
CHAPTER 5 CONCLUSION		60
5.1	Conclusion	60
5.2	Recommendation	61
REFERENCES		62
APPENDIX A RESULT OF ^1H Nuclear Magnetic Resonance NMR		69



UMP

LIST OF TABLES

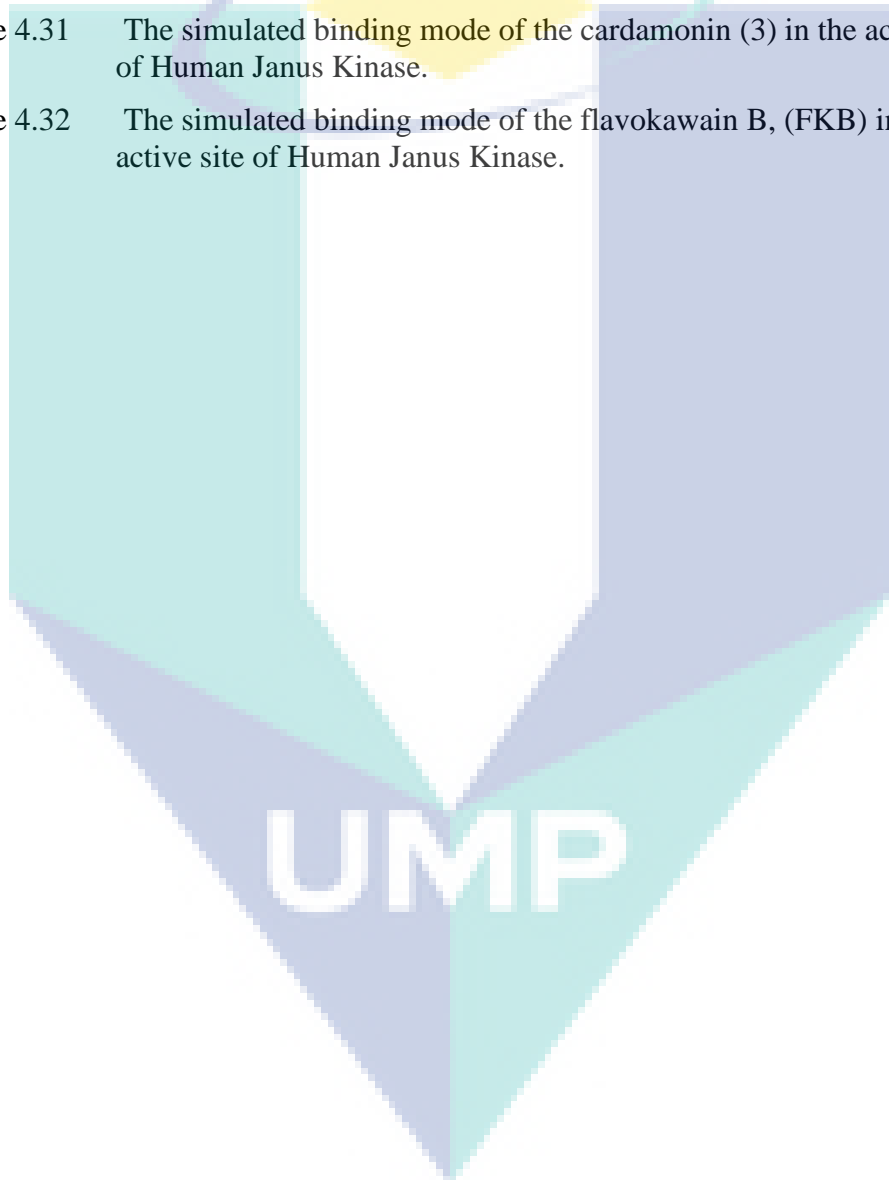
Table 2.1	Selected bioactive compounds from rhizomes of <i>B. rotunda</i>	8
Table 3.1	The placement and refinement methods and scoring functions used in the docking studies of the FKB derivatives 2,3 and FKB in the active site of the human Janus Kinase B; PDB: 3KRR.	25
Table 4.1	FTIR characteristics of a single pure pinostrobin (1)	28
Table 4.2	¹ H & ¹³ C NMR data of Pinostrobin compound (1)	30
Table 4.3	Crystal data and parameters for the structure refinement of Pinostrobin (1)	32
Table 4.4	NMR data of pure pinostrobin chalcone (2)	35
Table 4.5	NMR data of Cardamonin (3)	39
Table 4.6	¹ H & ¹³ C NMR data of 5,6-Dehydrokawain (4).	42
Table 4.7	Major functional groups present in 5,7-dihydroxyflavanone (5)	45
Table 4.8	¹ H & ¹³ C NMR data of compound (5)	45
Table 4.9	Major functional groups present in Alpinetin (6)	49
Table 4.10	¹ H & ¹³ C NMR data of Alpinetin	50
Table 4.11	NMR data of pure FKB (7)	54
Table 4.12	IC ₅₀ values of 1-6 and Flavokavain B types against H-29 and MDA-MB-231 cell lines.	54

UMP

LIST OF FIGURES

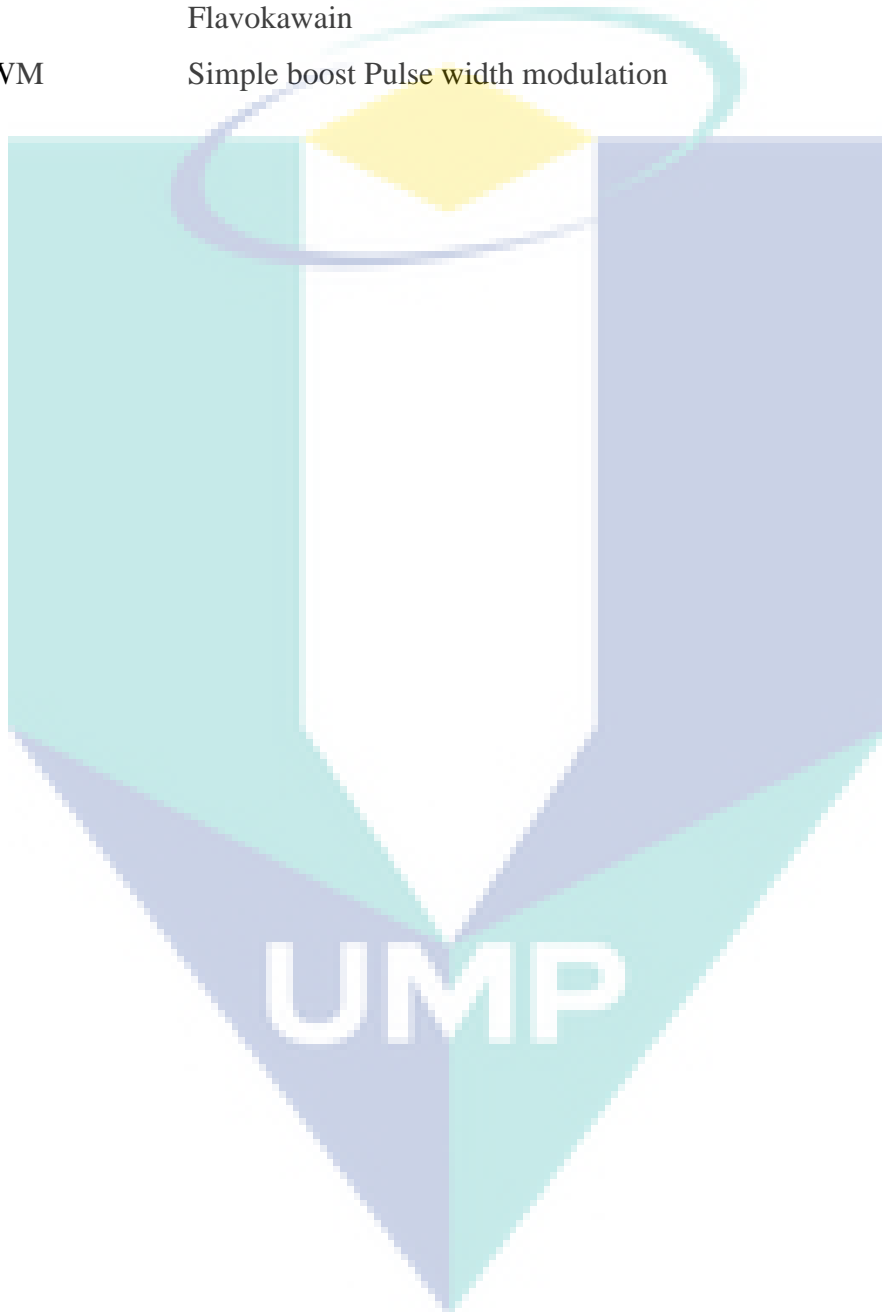
Figure 1.1	B. rotunda (a) Whole plant (b) Rhizome	2
Figure 2.1	Structures of Antioxidant Compounds	10
Figure 2.2	Compounds responsible for anti-inflammatory properties	11
Figure 2.3	Soxhlet apparatus	15
Figure 3.1	Flow diagram of extraction scheme for B. rotunda	21
Figure 4.1	UV-Vis spectrum of the chemical constituent isolated from B. rotunda	27
Figure 4.2	FT-IR functional groups in pure compound	28
Figure 4.3	The structure of pinostrobin (1)	29
Figure 4.4	ORTEP diagram of Pinostrobin (1)	30
Figure 4.5	GC-MS spectrum of single pure compound isolated from B. rotunda	31
Figure 4.6	UV spectrum of pure pinostrobin chalcone (2)	33
Figure 4.7	IR spectrum of pure pinostrobin chalcone (2)	34
Figure 4.8	Structure of pure pinostrobin chalcone (2)	35
Figure 4.9	GC-MS spectrum of pure pinostrobin chalcone (2)	36
Figure 4.10	UV spectrum of compound (3)	37
Figure 4.11	IR spectrum of compound (3)	38
Figure 4.12	Structure of pure Cardamonin (3)	38
Figure 4.13	UV-Vis spectrum of pure 5,6-dehydrokawain (4)	40
Figure 4.14	The structure of 5,6-dehydrokawain (4)	41
Figure 4.15	GC-MS spectrum of 5,6-dehydrokawain (4)	42
Figure 4.16	UV-VIS spectrum of pure 5,7-dihydroxyflavanone (5)	43
Figure 4.17	FTIR spectrum of purified 5,7-dihydroxyflavanone (5)	44
Figure 4.18	Mass spectrum of single pure 5,7-dihydroxyflavanone	46
Figure 4.19	Chemical structure of 5,7-dihydroxyflavanone (5).	47
Figure 4.20	UV-VIS spectrum of single alpinetin (6)	47
Figure 4.21	FTIR spectrum of purified Alpinetin (6)	48
Figure 4.22	ORTEP diagram of alpinetin (6).	50
Figure 4.23	Spectrum of compound Alpinetin	51
Figure 4.24	UV spectrum of FKP (7)	52
Figure 4.25	IR spectrum of pure (FKB)	52
Figure 4.26	Structure pure FKB (7).	53
Figure 4.27	Structure of compound 2, 3 and 4	55

Figure 4.28	Effect of natural compounds on the viability of MDA-MB-231 breast cancer cell line at 48 hours as determined by MTT assay. Each data point represents the mean of two independent experiments \pm SD.*significantly different from the control ($p < 0.05$).	56
Figure 4.29	Effect of natural compounds on the viability of HT-29 colon cancer cell line at 48 hours as determined by MTT assay. Each data point represents the mean of two independent experiments \pm SD.*significantly different from the control ($p < 0.05$).	56
Figure 4.30	The simulated binding mode of the pinostrobin chalcone (2) in the active site of Human Janus Kinase.	57
Figure 4.31	The simulated binding mode of the cardamonin (3) in the active site of Human Janus Kinase.	58
Figure 4.32	The simulated binding mode of the flavokawain B, (FKB) in the active site of Human Janus Kinase.	59



LIST OF ABBREVIATIONS

FTIR	Fourier transform infrared
GC-MS	Gas chromatography mass spectrometry
UV-ViS	Ultra violet
FKB	Flavokawain
SBPWM	Simple boost Pulse width modulation



CHAPTER 1

INTRODUCTION

1.1 Research Background

The World Health Organization (WHO) reported that over 80% of the world population uses herbal products as an alternative medicine, food supplements and as nutraceutical products (WHO, 2013). The use of these herbal products for health-related purposes has therefore experienced a sporadic surge between 1995 and 2008 (Zanariah et al., 2016). The medicinal value of many plants has therefore drawn the attention of researchers to focus on unveiling their therapeutic potentials. According to an estimate, one-quarter of the commonly used medicines contain compounds isolated from plants (Mageed, 2000) and according to World Health Organization, a large chunk of these natural plants have been discovered to have high medicinal values. Thus, herbal medicine has led to the discovery of a number of new drugs, and non-drug substances.

Boesenbergia rotunda (Figure 1.1) commonly known as finger-root, lesser galangal or Chinese ginger, is a medicinal and culinary herb from China and Southeast Asia (Ongwisespaiboon and Jiraungkoorskul, 2017). It belongs to the family *Zingiberaceae* usually used for nutritional and medicinal purposes (Salama et al., 2012). This plant has been used in the treatment of many diseases such as colic and gastrointestinal disorder, diuretic, dysentery, inflammation and aphrodisiac (Ongwisespaiboon and Jiraungkoorskul, 2017). Many researchers have elucidated and unraveled the medicinal properties of *B. rotunda* such as antioxidant and neuroprotective (Shindu et al., 2006), anti-inflammatory (Chatsumpun, et al., 2017), anti-mutagenic (Trakoontivakorn et al., 2001), anti-cancer (Kirana et al., 2007), anti-dermatophytic (Bhamarapavati et al., 2000), antibacterial (Voravuthikunchai et al.,

2005), chemopreventive and anti-*Helicobacter pylori* (Bhamarapravati et al., 2003), and anti-dengue 2 virus NS3 protease (Kiat et al., 2006) activities.

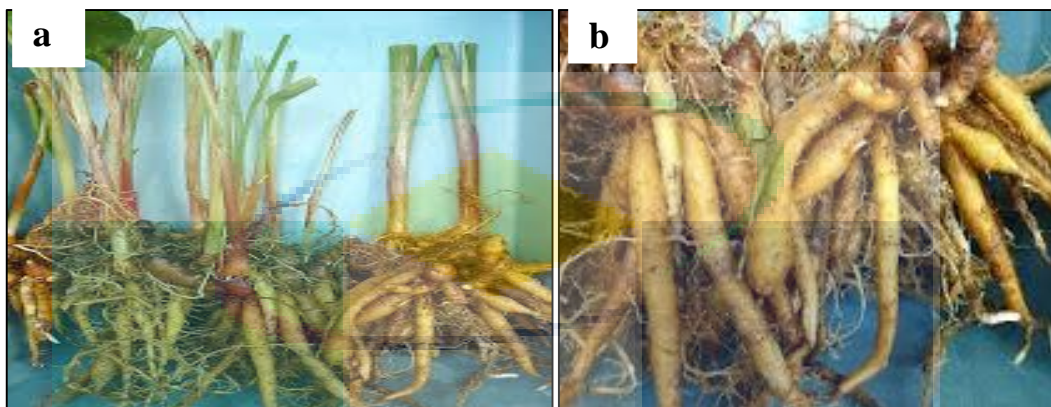


Figure 1.1 *B. rotunda* (a) Whole plant (b) Rhizome

Source: Mahmood et al., (2010)

Moreover, the numerous medicinal properties of *B. rotunda* due to the presence of many bioactive compounds such as flavonoid compound named pinostrobin, three flavanones (pinostrobin, pinocembrin and alpinetin) and two chalcones (cardamonin and boesenbergin A) (Aishwarya, 2017). The methanol-based extracts obtained from *B. rotunda* rhizomes was has been reported to have bioactive compounds such as quercetin and kaempferol, which are known to be responsible for their antioxidant and anti-inflammatory properties (Rho et al., 2011). Ching et al., (2007) reported that the extracts obtained using hexane and chloroform contains three flavanones (pinostrobin, pinocembrin, and alpinetin) and two chalcones (cardamonin and boesenbergin).

Various methods, such as saponification, heating under reflux, Soxhlet extraction and others are commonly used. The other modern extraction techniques include solid-phase micro-extraction, supercritical-fluid extraction, pressurized-liquid extraction, microwave-assisted extraction, solid-phase extraction, and surfactant-mediated techniques, which possess certain advantages. These are the reduction in organic solvent consumption and in sample degradation, elimination of additional sample clean-up and concentration steps before chromatographic analysis, improvement in extraction efficiency, selectivity, and kinetics of extraction. The ease of automation for these techniques also favours their usage for the extraction of plants materials (Sahin et al., 2017).

Moreover, isolation, identification and characterization of a single constituent is often a tedious process since the extracts that are usually obtained are a combination of complex bioactive compound with different polarities. To therefore obtain pure compound from plant extracts there is therefore a need to find a separation techniques method that is cost effective viz: thin layer liquid chromatography (TLC), column chromatography (CC), flash chromatography (FC), Sephadex chromatography(SC) and high performance liquid chromatography(HPLC).The pure compounds are then subjected to further physicochemical analyses such as Fourier-transform infrared spectroscopy (FTIR), UV-visible, Infrared (IR), and Nuclear Magnetic Resonance (NMR) (Sasidharan et al., 2011).

1.2 Problem Statement

Breast and colon cancer is one of the leading causes of death worldwide and every year number of new cases is expected to rise by about 70% over year. They are the second leading cause of death globally, and was responsible for 8.8 million deaths in 2015 (Mustapa et al., 2015). Globally, nearly 1 in 6 deaths is due to cancer. Approximately 70% of deaths from cancer occur in low- and middle-income countries (Yu et al., 2016). Natural products are an important source of medicinal drugs. Several drugs have been invited from medicinal plants. Plant natural product chemistry has played an important role in generating a large number of drug compounds.

Recently, it has been reported in the literature that approximately 49% molecules that were introduced as new pharmaceuticals chemical were either natural products or semi-synthetic analogues or synthetic products based on natural product models (Nuurul et al., 2016). Our aim is to develop new herbal remedies as well as newly synthesized compounds, which will allow for the practical applications of crude extracts of plants and synthesized compounds in order to discover new pharmaceuticals. It should be noted that an in-vivo data on the anti-ulcer effect of *B. rotunda* rhizomes is limited. In this study based on the importance of pharmaceutical formulation from medicinal plants, new drug was synthesized into new drugs and products, which could be used for breast cancer treatment. To achieve this goal, crude extracts of *B. rotunda* was screened.

1.3 Research Objectives

The overall aim of this study is to isolate and identify the bioactive compounds in *B. rotunda* roots. Following are the objectives of this study:

- i. To extract bioactive constituents from *B. rotunda* using Soxhlet extraction method.
- ii. To purify, isolate and characterize the bioactive compounds using column chromatography techniques.
- iii. To explore the cytotoxic properties of the *B. rotunda* against colon (H29) and breast cancer cell lines (MDA-MB-231).

1.4 Scope of Study

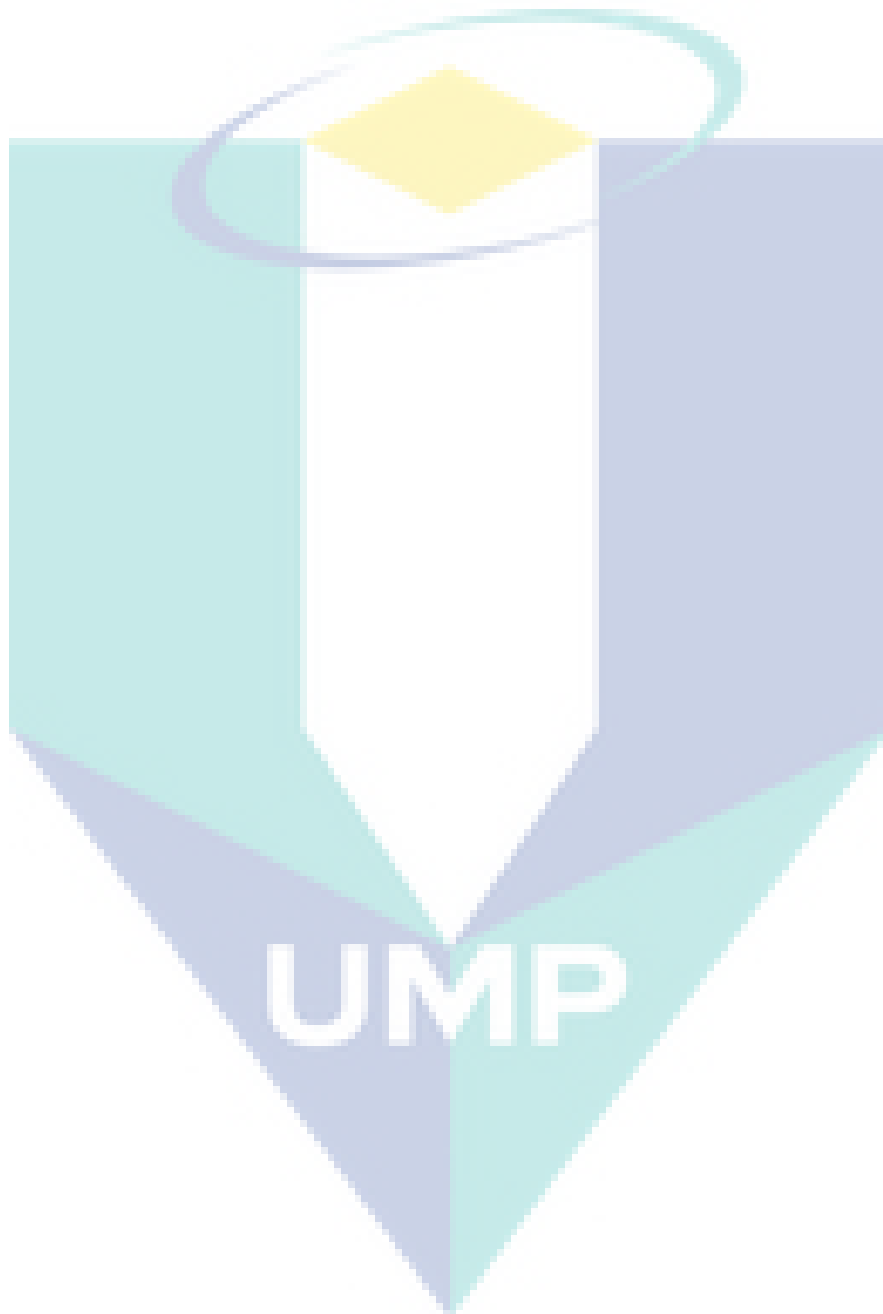
The following scopes were used in achieving the above research objectives:

The scopes of this research project are mainly divided into five stages. The first stage involved the collection of the plants and the subsequent extraction using Soxhlet extraction technique. The second stage involved the purification and isolation of important metabolites using the thin layer chromatography. The third stage involved the characterization of the isolated compounds using NMR, GC-MS, UV-Vis, FTIR and single X-ray crystallography spectroscopic techniques. Moreover, in the fourth stage, cytotoxicity properties of the pure compounds were screened against breast cancer cell lines MCF-7 and MDA-MB231. Lastly, the structure-activities relationships between different substituent's functional groups were established using the molecular docking.

Thesis Layout

This thesis is organized into five chapters. Chapter 1 gave the general overview of this research, encompassing the research objectives, and scope of study. Chapter 2 explored the literature on previous but related work. In Chapter 3 the materials, reagent, equipment, extraction and purification processes, biological protocols and physicochemical characterization employed were carefully presented. The step-by-step procedure for the phytochemical profiling, total phenolic content determination, antioxidant, cytotoxic, SEM, FTIR, and BET analyses were presented in detail. Chapter 4 presented the results of bioactive compound isolation, free radical scavenging activities, FTIR, GC-MS, NMR, X-ray crystallography, molecular studies and cell viability assays..

Chapter 5 concluded and highlighted the contribution of this current work and proffered recommendations for future work.



CHAPTER 2

LITERATURE REVIEW

2.1 Overview

The *B. rotunda* is a type of herb that belongs to *Zingiberaceae* family which commonly found in tropical countries such as Thailand, Malaysia, Indonesia and Myanmar (Atun et al., 2017). It is commonly called temu kuncih as and traditionally used as medicinal and culinary herb in Southeast Asia. It belongs to the order of Zingiberales herbaceous ground flora plants in the rainforest. There are approximately 150 species of this family with about 23 species found in Peninsular Malaysia (Ibrahim et al., 2010). It grows in damp, shade parts of the hill slopes or lower land as thickets or scattered plants. Zingiberaceae family can be easily recognized by their characteristics such as fleshy rhizomes especially when they were crushed and their aromatic leaves (Ching et al., 2007).

Mostly, this species is found in very damp, usually close to streams or in wet spongy ground and shaded areas (Jing et. al., 2013). *B. rotunda* is a small perennial plant about 15-40cm height. The leaves are light green and broad in size. Each shoot consists of elliptic oblong red sheathed leaves while the rhizomes are small globular shaped central subterraneous and the tissues of the tuber are softer, looser and waterier than the central rhizomes. Different variety of *B. rotunda* gives different colour of tubers and central rhizome (Eng-Chong et al., 2012).

The finger-root of *B. rotunda* has been reported for the treatment of peptic-ulcer, colic, oral diseases, urinary disorders, dysentery and inflammation (Saralamp et al., 1996). The neuroprotective, anti-inflammatory, anti-mutagenic, anticancer, chemopreventive, and anti-dermatophytic of this plant has also been investigated. There

is therefore a necessity to isolate important bioactive constituents from this important tropical plant at higher purity. This plant is very useful in treatment of various diseases.

B. rotunda is commonly used in Southeast Asia as food spices or condiments, increasing appetite, trigger for producing milk, as well as in folk medicine. Traditionally, this plant is used by people for therapeutic purposes against inflammation, aphthous ulcer, oral diseases, dry mouth, stomach discomfort, dysentery, leucorrhoea, cancer, and kidney disorder (Morikawa et al., 2008). Meanwhile, the rhizomes of *B. rotunda* are given to the women after childbirth. From all the researches done before, they showed that the rhizomes of *B. rotunda* contained active compounds which act as antioxidant, antibacterial, anti-inflammatory, antitumor, antifungal, analgesic, anti-pasmodic and insecticidal activities (Aishwarya, 2017).

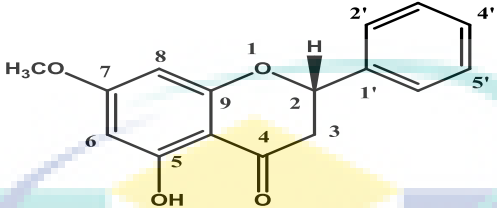
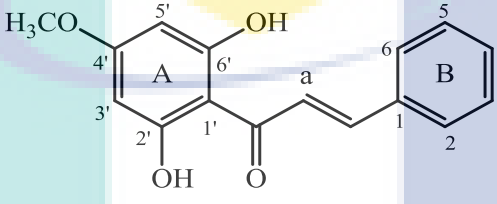
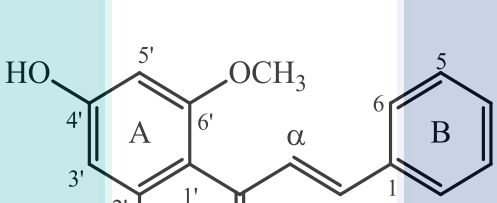
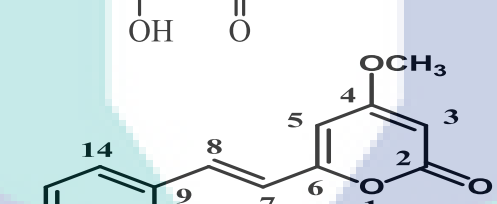
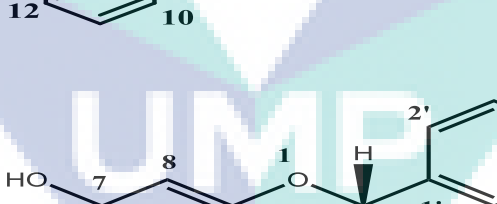
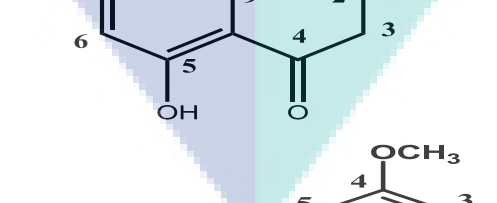
2.2 Pharmacological Significance and Phytochemical Application of the Plant

The pharmacological significance of this plant is mainly due to the presence of flavonoid, flavones, essential oil and chalcones (Trakoontivakorn et al., 2001). Fahey and Stephenson (2002) reported that pinostrobin (flavonone) has various activities including elevating the activity of an antioxidant enzyme, antispasmodic agent, reduce estrogen-induced cell proliferation, decreasing spontaneous contractions of intestinal smooth muscle and also mediating anti-inflammatory (Meckes et al., 1998, Le Bail et al., 2000, Wu et al., 2002).

Cardamonin (flavonoid) displayed anti-HIV-1 protease inhibition (Tewtrakul et al., 2003) and was also found to be analgesic and antipyretic (Pathong et al., 1989). Panduratin A (flavonoid) was found to reduce the development of human breast cancer and colon adenocarcinoma cell (Kirana et al., 2007), inhibit dengue-2 virus protease activity (Kiat et al., 2006), anti-aging activity (Shim et al., 2009) and have potential antibacterial and antiviral activities (Rukayadi et al., 2010, Wu et al., 2011). The major phytochemicals constituents are presented in Table 2.1 based on the previous researches. Kirana et al., (2007), screened eleven species of Zingiberaceae and found out that *B. rotunda* and *Zingiber aromaticum* exhibited the highest inhibition toward breast cancer and the human colon cancer cell growth. *B. rotunda* therefore possessed the strongest

inhibitory effect against breast cancer, cervical cancer, ovarian cancer and colon cancer (Ling et al., 2011).

Table 2.1 Selected bioactive compounds from rhizomes of *B. rotunda*

Compound	Structure	References
Pinostrobin (1)		Wangkangwan et al., (2009)
Pinotrobin chalcone (2)		Morikawa et al., (2008)
Cardamonin (3)		Tretrakul et al., (2009)
5,6-dehydrokawain (4)		Morikawa et al., (2008)
5,7-dihydroxyflavone (5)		Isa et al., (2012) Ching et al., (2007)
Alpinetin (6)		Wangkangwan et al., (2009)

The presence of panduratin A from *B. rotunda* has the ability to inhibit the growth of prostate cancer lines in a time and dose-dependent manner, which revealed its potentials therapeutic agent against prostate cancer (Yun et al., 2006). Also, Sukari et al., (2007) reported that panduratin A exhibited inhibitory activity against lung cancer cell and could act as antileukemic agent. He listed five flavonoid derivatives such as pinostrobin, pinocembrin, cardamonin, alpinetin and boesenbergin A, as responsible for the inhibitory properties.

The isolation and purification of *B. rotunda* rhizomes therefore resulted in the production and identification of isopanduratin A constituents using ^1H NMR. This bioactive component possesses inhibitory properties against S. Mutans which qualifies it as anti-cariogenic agents. Moreover, the presence of free radical usually results in pathological disturbances. Shindu et al., (2006) reported that the extracts from *B. rotunda* rhizome contain antioxidant components such as, 2¹,6¹-dihydroxy-4¹-methoxychalcone, 5,7-dihydroxyflavanone, 2¹,4¹-dihydroxy-6³-methoxychalcone, (-)-panduratinA, (-)-4-hydroxypanduratin A, and 5-hydroxy-7-methoxyflavanone as illustrated in Figure 2.1 below. Moreover, the isolation of -panduratin A and hydroxypanduratin A, the chloroform extract of *B. rotunda* rhizomes, were found to exhibit strong anti-inflammatory activities compared to the other extracted compounds which are sakuranetin, pinostrobin, pinocembrin, and dihydro-5,6-dehydrokawain as illustrated in the Figure 2.2.

B. rotunda exhibited anti-inflammatory activity through the inhibition of nitric oxide where nitric oxide acts as an inflammatory inter-mediator within human metabolic processes there by providing a defence against intracellular and extracellular stimulants. Also, the hydroxypanduratin A and panduratin A from *B. rotunda* extract showed strong inhibitory activity against nitric oxide as investigated by Tewtrakul et al., (2009/2003). Boonjaraspinyo et al. (2010) proved that rhizomes of *B. rotunda* could inhibit inflammation caused by *Opisthorchis viverrini* which spread through consumption of raw and uncooked fish. Furthermore, the *B. rotunda* extract proved as antiulcer effect with its pure compound, pinostrobin (Abdelwahab et al., 2011 & 2013). Peptic ulcers are one of the most terminal diseases of the digestive system, which has been commonly diagnosed in many part of the world (Sánchez-Mendoza et al., 2011).

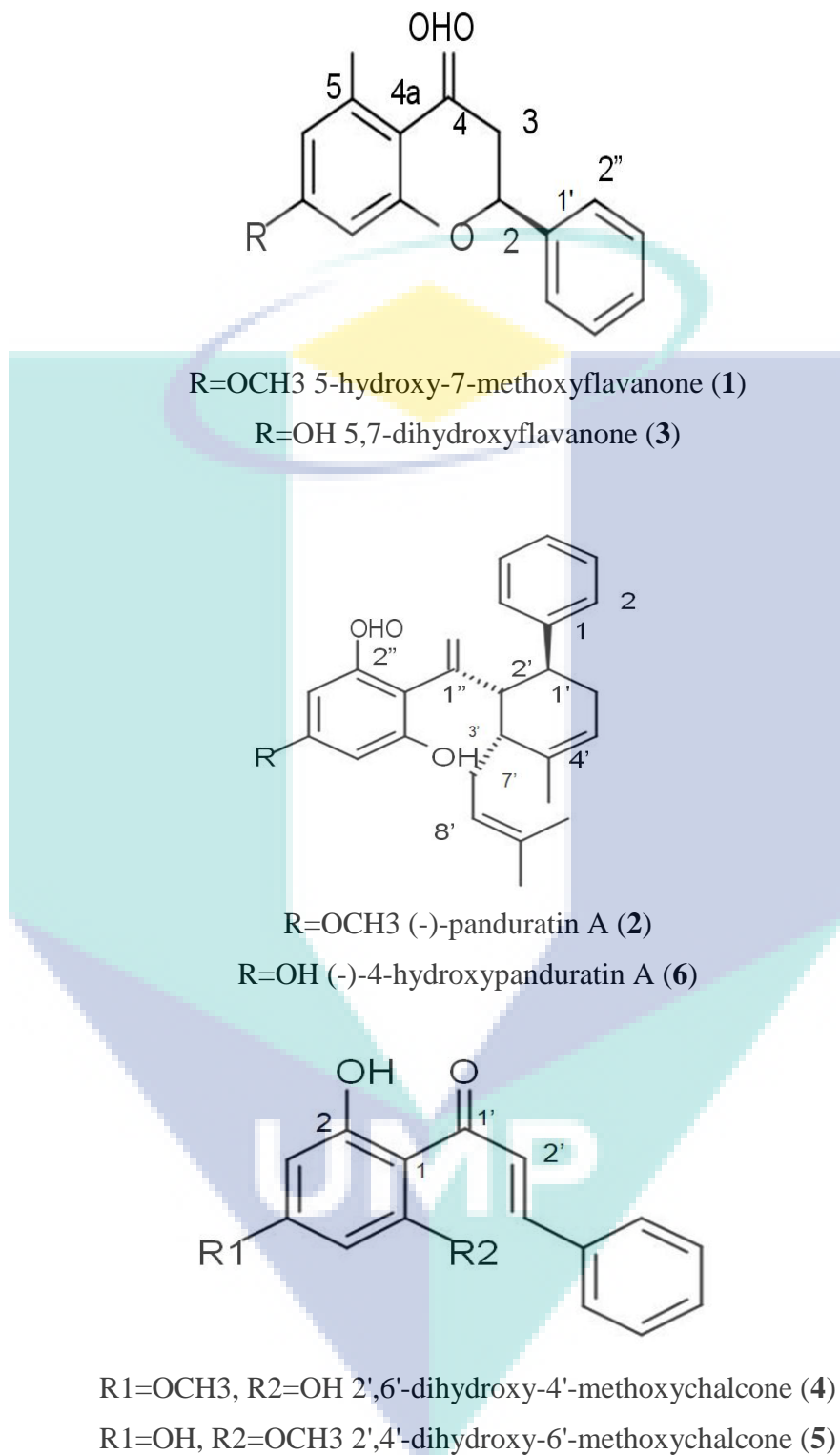


Figure 2.1 Structures of Antioxidant Compounds

Source: Shindu et al., (2006)

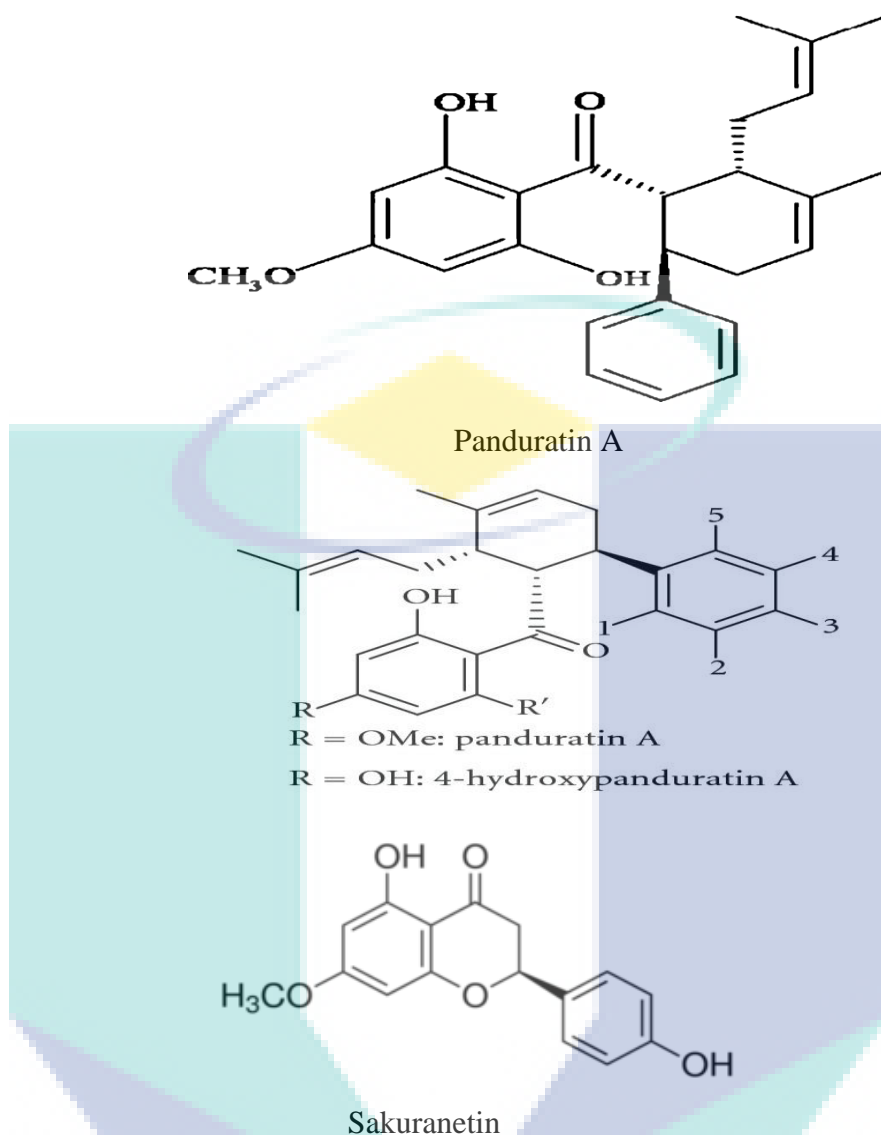


Figure 2.2 Compounds responsible for anti-inflammatory properties

The failure of the mucosa to act against the stomach gastric acid is regarded as the major cause of peptic ulcer (Bucciarelli et al., 2010). The exposure of human to hazardous chemicals has greatly increased the prevalence to gastric attacks (Chaturvedi et al., 2007). This has been estimated that approximately one-fifth of the world population suffer from this deadly disease. Moreover, the *Helicobacter pylori* infection is regarded as one of the major causes of peptic ulcer. Here, the formation of peptic ulcer could be traced to the meal-stimulated gastrin levels which lead to a reduction in the production of gastric mucus and in the secretion of duodenal mucosal bicarbonate. In spite of the availability of many synthetic drugs for the treatment of peptic ulcer, researcher has proposed a natural source (Bucciarelli et al., 2010). *B. rotunda* rhizomes of this plant have been known for a potential natural cure for peptic ulcer. It has been previously used for the

treatment of diseases such as colic, oral diseases, urinary disorders, dysentery and inflammation (Saralamp et al., 1996). Various researches has suggested *B. rotunda* as being neuroprotective, anti-inflammatory, anti-mutagenic, anticancer, chemopreventive, anti-dermatophytic, anti-*Helicobacter pylori* and anti-dengue-2 virus NS3 protease (Bhamarapravati et al., 2003). This anti-ulcer property is attributed to the presence of group of bioactive compounds such as isolated three flavanones, pinostrobin, pinocembrin and alpinetin and two chalcones, cardamonin and boesenbergin A from the rhizomes of *B. rotunda* (Ching et al., 2007). Ethanol is known to induce the risk of gastric ulcer in animals. Hence, its administration when utilised due to its easy and rapid penetration ability into the gastric mucosa. As the mucosal permeability increases, the vasoactive products are released. This causes vascular damage, and gastric cell necrosis later results into ulcer formation. It has been reported that the free radicals (i.e. oxygen) the ethanol produced play a significant role in the gastric damage (Mahmood et al., 2005/2010). In this study, the application of medicinal plants to prevent and treat many ailments is rapidly evolving globally (Ashidi et al., 2010).

In addition, the anti-parasitic activities of *B. rotunda* extract against *Giardia lamblia* was investigated by Sawangjaroen et al. (2005). A protozoan parasite known as giardiasis is responsible for the small intestine inflammation experience during ddiarrhoea. Sawangjaroen and friends showed that extraction of *B. rotunda* with chloroform and extraction of *B. rotunda* with methanol had IC50 value between 20 μ g/mL and 100 μ g/mL this showed that *B. rotunda* has bioactive compounds which can prevent giardiasis. Furthermore, the extract from *B. rotunda* has been reported to possess anti-aging properties. This is attributed to the presence of bioactive derivative of cyclohexenyl chalcone called 4-hydroxyanduratin A. Shim et al., (2008, 2009) reported that this bioactive derivative showed a UV induction effect in MMP-1 expression. UV radiations which induce elevated expression of MMP-1 were controlled when treated with 4-hydroxyanduratin A.

The pinostrobin content from the roof of *B. rotunda* has shown an antimicrobial capacity against *Helicobacter pylori*. This bacterium has been reported to be responsible for health conditions like gastritis, dyspepsia and peptic ulcer which has been linked to the development of colon cancer and gastric. Bhamarapravati et al., (2006) reported that the pinostrobin and red oil from the roots of *B. rotunda* was found to exhibit anti-H. pylori

activities. Rukayadi et al., (2009) reported that the panduratin A constituent in *B. rotunda* was found to exhibit antimicrobial activity against *Staphylococcus* strains. This is a gram positive cocci bacterium usually found in the human respiratory tract and on the skin with ability to cause skin infection, respiratory disease and food poisoning. Phongpaichit et al., (2005) reported that the chloroform extract of *B. rotunda* has the capacity to obstruct the propagation of *Candida neoformans* and *Microsporium gypseum*. However, it showed low effect against *C. albicans* through the antifungal assay. From the disc diffusion assay, the plant extract of *B. rotunda* showed the smallest diameter range as compared to other plant extracts.

Kim et al., (2011) reported that panduratin A act as AMP-activated protein kinase (AMPK) activator. This enzyme helps in the regulation of cellular energy through the activation of LKB1 and Ca²⁺/calmodulin-dependent protein kinase kinase β (CaMKK β). The activation of this enzyme could result in the activation of fatty acid oxidation-related genes. This prevents the lipid synthesis through the reduction of sterol regulatory element-binding protein-1c (SREBP-1c). These consequently increase the fatty acid oxidation thereby resulting in weight loss in vivo obese mouse model. It also plays a role as anti-photo aging agent. *B. rotunda* contained cyclohexenyl chalcone compound; derive of panduratin A which is 4-hydroxypanduratin A. The 4-hydroxypanduratin has effect in UV-induced MMP-1 expression. UV radiations which induce elevated expression of MMP-1 was controlled on treatment of 4-hydroxypanduratin A at nontoxic concentration to human skin fibroblast cells in vitro (0.001 - 0.1 μ M) compared to UV-irradiated control (Shim et al., 2008).

2.3 Overview of Anti-radical Metabolites in *Boesenbergia rotunda*

Free radicals are electrically charged molecules, with an unpaired electron which causes them to seek out and capture electrons from other substances in order to neutralize themselves (Alara et al., 2017). Although the initial attack causes the free radical to become neutralized, another free radical is formed in the process which causes a chain reaction. And until subsequent free radicals are deactivated, thousands of free radical reactions can occur within seconds of the initial reaction. Cell damage caused by free radicals appears to be a major contributor to aging and to degenerative diseases of aging such as cancer, cardiovascular disease, cataracts, immune system decline, and brain

dysfunction (Olalere et al., 2017). Fortunately, the free radical formation is controlled naturally by various beneficial compounds known as antioxidants. The limited availability of antioxidants in the body results in damages that can become debilitating and cumulative (Badwaik, Borah and Deka, 2015).

Many secondary metabolites are known to be active compounds with free radical scavenging properties, thereby reducing the risk of cancer. They are able to act for antioxidants either as hydrogen donating or as electron acceptor. Take for instance the hydroxyl groups in the phenolic compounds are good hydrogen donors which donate hydrogen that can react with reactive oxygen and nitrogen species leading to the formation of new radicals. The formation of new radicals with a great stability is thus generated (Pereira et al., 2009).

The flavonoids on the other hand are a group of compounds which has medicinal functions such as in the inhibition of auxin, defense against UV light, and in coloring of flowers. This is due to the presence of phyto-compounds such as pinostrobin which has been investigated to improve antioxidant activities of enzymes, attack inflammation, and reduce estrogen-induced cell damage. Flavonoids are of great value in industrial applications and this is due to their medicinal properties. The flavonoids derived through chemical synthesis have been reported to have toxic effects. It is vital to ensure continuous supply of plant source in order to meet the commercial demand. *B. rotunda* is traditionally propagated by vegetative techniques using a rhizome segment. However, this method is slow, time-consuming, and not economically viable as the collection of rhizome for industrial applications could limit the starting material for propagation (Atun, Handayani and Frindryani, 2017). Thus, it is essential to develop in vitro propagation method for obtaining sustainable, optimized sources of plant-derived bioactive compounds. The morphogenic potential and regenerative capacity of *B. rotunda* from in vitro cell cultures have been reported, but a detailed analysis of the productive competency and biosynthetic pathway of flavonoids has remained elusive. We have thus examined and compared the production of various flavonoids and chalcones produced in conventional propagated (CP) and in vitro-derived (CPA) field-grown plants of *B. rotunda*. The highest yields of bioactive compounds obtained from different organs of *B. rotunda* can thus be identified and exploited for medicinal use.

2.4 Soxhlet Extraction

There are different ways of extracting bioactive compounds from medicinal plants, conventional and non-conventional methods. Conventional methods are exhaustive hydro-distillation, maceration, solvent extraction, decoction, percolation, infusion, and soxhlet (Handa et al., 2008). Soxhlet extraction has been a well-established technique which possesses a great performance when compared with other conventional extraction methods except that it is well applied to the extraction of thermolabile compound (Luque et al., 1998). In soxhlet apparatus shown in Figure 2.1, the plant materials are placed in a porous or thimble-holder of strong filter paper, which is filled with condensed fresh solvent from a distillation flask. When the level of the liquid overflow, the liquid contents siphon back into the distillation flask in which the extracted solutes are carrying back into the bulk liquid. Fresh solvent passes back into the plant solid bed while the solutes are left in the flask. This operation is repeated until a complete extraction is achieved (Handa et al., 2008).

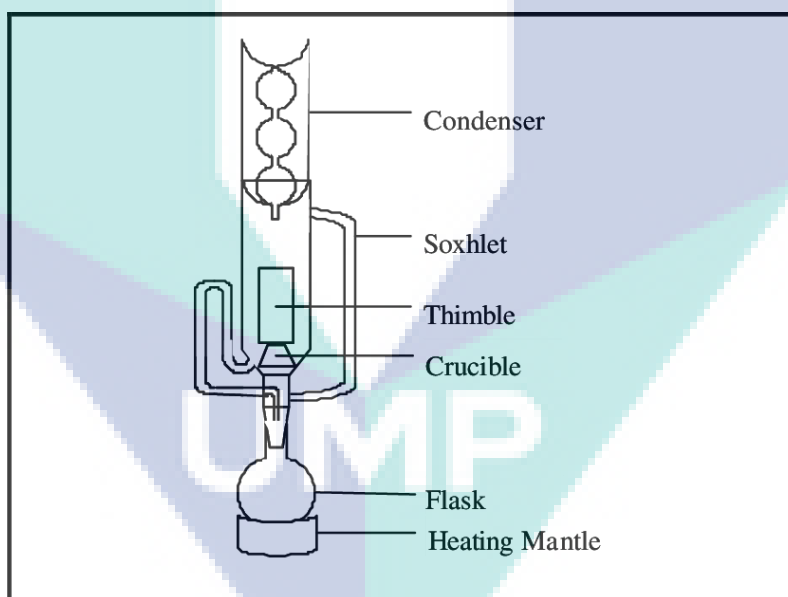


Figure 2.3 Soxhlet apparatus

Source: Sham et al., (2015)

One of the advantages of this method is that only one batch of solvent used is recycled instead of larger portions of warm solvent passing through the sample. After the extraction process, the solvent is removed mostly by using a rotary evaporator, extracted compound can be collected and the non-soluble portion of the extracted solid remains in the thimble will be discarded (Handa et al., 2008). Likewise, when compare this method

to other conventional methods, the larger yields can be extracted with a much smaller quantity of solvent (Luque et al., 1998).. These effects can boost an economy in terms of energy, time, and financial inputs (Shams et al., 2015).

2.5 Isolation and Purification of Bioactive Constituents

The process of separation, isolation and purification of bioactive compounds from natural product has resulted in the emergence of many high quality pharmaceutical products (Kirana et al., 2007). The use of an appropriate method for bioactive compounds identification is to screen the plant matrix for biological properties such as antioxidant, antibacterial, or cytotoxicity. The combined with simplicity, specificity, speed and cost effectiveness of in-vitro methods over the in-vivo makes them a desirable assay. The use of animal experiment is however expensive, time consuming, and are prone to ethical controversies. There are other factors that make it difficult to get appropriate protocols in the isolation and characterization of certain bioactive compounds. This could be attributed to different parts in the plant containing different molecules with divers' chemical structures and physicochemical properties. In isolating and characterizing bioactive phytochemicals in natural products, the collection of plant material is of paramount importance (Haroune et al., 2015). The collection of plant materials involves obtaining the ethno-botanical information of the targeted compounds. The extracts can then be obtained using various solvent which will invariable aid the isolation and purification of the active compounds responsible for the bioactivity. An important method of isolation and purification of active compounds is through the use of a column chromatographic techniques or High-Pressure Liquid Chromatography (HPLC) which accelerates the process of purification. The identification of the purified compounds can be achieved using different varieties of spectroscopic techniques such as UV-visible, Infrared (IR), Nuclear Magnetic Resonance (NMR), and mass spectroscopy (Atun and Frindryani, 2017).

The thin-layer and column chromatographic (TLC) methods had been used previously for the purification in the purification of many bioactive compounds. The merit of this method is in their simplicity, cost effectiveness, and availability at different stationary phases. The most valuable material used for this process are, alumina, cellulose, silica and polyamide. The plant matrix is made up of complex aggregation of

phytochemicals which usually results in difficulties in separation. To therefore make the process of separation easy, increasing polarity using multiple mobile phases is desirable for an effective separation. Moreover, the thin-layer chromatography (TLC) has its application in the analysis of different fractions of bioactive compounds using the column chromatography. An example of this is the silica gel column chromatography and thin-layer chromatography (TLC) which have been used for the separation of bioactive compounds (Trakoontivakorn et al., 2001).

2.6 Physicochemical Characterization Plants Metabolites

The structural elucidation of the isolated plant constituents usually involves the use of spectroscopic data obtainable from different techniques such as Infrared (IR), mass spectroscopy, UV-visible, and Nuclear Magnetic Resonance (NMR). The basic principle of these spectroscopic techniques involves the bombardment of the plant matrix with an electromagnetic radiation. The absorption spectrum generated through the absorption of the radiation by the plant matrix helps in the measurement, identification and in an eventual elucidation of its structure. The spectra emanating from the visible, Infrared, radio frequency UV and electron beam is used for structural elucidation. In the determination of chemical constituents in an herbal extract, an organic molecule is converted to ions as a result of the atomic bombardment. A mass spectrum is generated which described the plot of relative abundance of the fragmented ion against the ratio of mass/charge (m/z). An accurate determination of the relative molecular mass can therefore be achieved through the use of mass spectrometric techniques. The exact molecular formula of the compounds can also be determined from the ionic fragmentation. In previous studies, the isolation and purification of bioactive constituents from pith were obtained using a bioactivity-guided solvent extraction, column chromatography, and HPLC techniques (Jeon et al., 2016).

Moreover, the UV-visible spectroscopy is commonly used for a quantitative determination of aromatic molecules mostly in natural product research. The presence of certain classes of compounds in any plant matrix can be analyzed using the UV-visible spectroscopy. The presence of classes of bioactive compounds such as phenolic, anthocyanins, tannins, polymer dyes, and phenols leads to the formation of complexes with iron which is usually detectable by the ultraviolet/visible (UV-Vis) spectroscopy.

This method has been found to have lesser degree of selectivity when elucidating information about the composition of total polyphenol content (TPC). The merit of this method is that it takes lesser time at a reduced cost when compared to other techniques.

Furthermore, the Fourier transform infrared spectroscopy (FTIR) is an analytical tool used in the identification and structural elucidation of the chemical constituents. Its major advantage is in the rapidness and non-destructive action on the herbal extracts during the process of spectroscopic fingerprints. It has a wide range of application in the characterization of organic and inorganic chemicals such as resins, drugs, polymers etc. It is most useful for the identification of functional groups present in the sample. The functional group identification is a function of wavelength of light absorbed and illustrated in the form of a spectrum. The chemical bonds present in a sample can therefore be determined by interpreting the infrared absorption spectrum. The frequencies are usually measured between a 4000–600 cm^{-1} wave numbers. The molecules from the extracts absorb light in the infra-red region of electromagnetic spectrum. The absorbed infra-red rays are measured in relation to the type of bond present in the extract. The initial background spectrum of the infra-red source is first measured and this is followed by the measurement of sample spectrum. The sample spectrum is obtained with respect to the background spectrum and this is proportional to the obtained absorption spectrum of the sample under investigation. The resultant absorption spectrum from the bond natural vibration frequencies indicates the presence of various chemical bonds and functional groups present in the sample.

Furthermore, the nuclear magnetic resonance spectroscopy (NMR) makes use of the magnetic properties of certain atomic nucleus of hydrogen atom, proton, carbon, and an isotope carbon. This method has made it possible for many researchers to determine the differences among various atomic nuclei. This has helped in giving a clear picture of the position these nuclei are in the molecule, while revealing the atoms are present in the adjacent groups. Hence, it has the capacity to determine the number of atoms present in each neighborhood. Many researchers had attempted using an NMR offline in the preparative/ semi preparative thin-layer chromatography, liquid chromatography, and column chromatography in isolating on an individual basic group of compounds such as phenols.

2.7 Molecular Docking

Molecular docking is a key tool in structural molecular biology and computer-assisted drug design. The goal of docking is to predict the predominant binding mode(s) of a ligand with a protein of known three-dimensional structure (Rohs, et al., 2005). Successful docking methods search high-dimensional spaces effectively and use a scoring function that correctly ranks candidate dockings. Docking can be used to perform virtual screening on large libraries of compounds, rank the results, and propose structural hypotheses of how the ligands inhibit the target, which is invaluable in lead optimization. The setting up of the input structures for the docking is just as important as the docking itself, and analysing the results of stochastic search methods can sometimes be unclear (Agarwal et al., 2015). Practical application of molecular docking requires data bank for the search of target with proper PDB format and a methodology to prepare ligand as a PDB file. To do this, there are various software's (Discovery studio, etc.,) available from where the ligand can be made in PDB format.

These tools provide the organization to ligands based upon their ability to interact with given target proteins/DNA. Molecular docking of small molecules to a target includes a pre-defined sampling of possible conformation of ligand in the particular groove of target in an order to establish the optimized conformation of the complex. This can be made possible using scoring function of software (Seeliger et al., 2010). Since the infrared spectroscopy, X-ray crystallography and Nuclear Magnetic Resonance (NMR) spectroscopy are the techniques for the investigation and establishment of three dimensional structures of any organic molecule/ biomolecular targets (Agarwal et al., 2015). Hence homology modelling makes it possible to determine the tentative structure of proteins of unknown structure with high sequence homology to known structure. This provides a substitute approach for target structure establishment, which forms starting point for in silico drug discovery (Rohs, et al., 2005).

CHAPTER 3

METHODOLOGY

3.1 Sample Preparation

A known quantity of rhizomes of *B. rotunda* was purchase from the market in Puchong, Selangor Darul Ehsan, and Malaysia. The plants voucher specimens were were authenticated by Assoc. Prof. Dr. Muhammad Nadeem Akhtar at the Faculty of Industrial Sciences and Technology (FIST), University Malaysia Pahang (UMP). The plant material was rinsed to remove the inherent dirt and was cut into small pieces. The sample was thereafter air-dried for about 76 hours in the laboratory at a controlled temperature of 27 °C. The sample was grounded into smaller size (0.1 mm) using a Grindomix grinder (GM-200 model, Germany).

3.2 Reagents

An analytical-grade methanol (99.9%), hexane, ethyl acetate, ammonium hydroxide, hydrochloric acid (5%) and distilled water were all obtained from the FKKSA chemical store, Universiti Malaysia Pahang. All reagents were used without further purification but some chemical dilutions were conducted according to the experimental protocol.

3.3 Extraction Process

The air-dried *B. rotunda* (300g) were ground into a finely-defined powder and then extracted with methanol using the Soxhlet extraction techniques. The solvent was evaporated and the residue treated with 5% HCl and then filtered. The CH₂Cl₂ extracts contain tertiary alkaloids and the terminal aqueous solution quaternary alkaloid. The last

solution was acidified with concentrated HCl and Meyers reagent/Dragendorff's reagent was added until precipitation ceased. The resulting precipitates were filtered, wash with water and suspended in MeOH-Me₂CO-H₂O (6:2:1) (Jacques *et. al.*, 2000). A complex mixture was resolved by vacuum column chromatography (VLC) with silica gel 60, packed in slurry with hexane as the initial solvent and gradually increased the polarity of a solvent. Chromatography was performed on pre-coated TLC plates Kieselgel Si 60; 0.25mm (E. Merck, Darmstadt, Germany). The separated spots were detected under UV light (256 & 366 nm). The individual components were purified by preparing TLC on a pre-coated silica-gel plates using MeOH-CHCl₃. Column Chromatography was performed on a pre-coated TLC plates Kieselgel Si-60; 0.25mm (E. Merck, Darmstadt, Germany). The separated spots were detected under UV light (256 & 366 nm). The flow diagram of the experimental procedure is illustrated in (Figure 3.1).

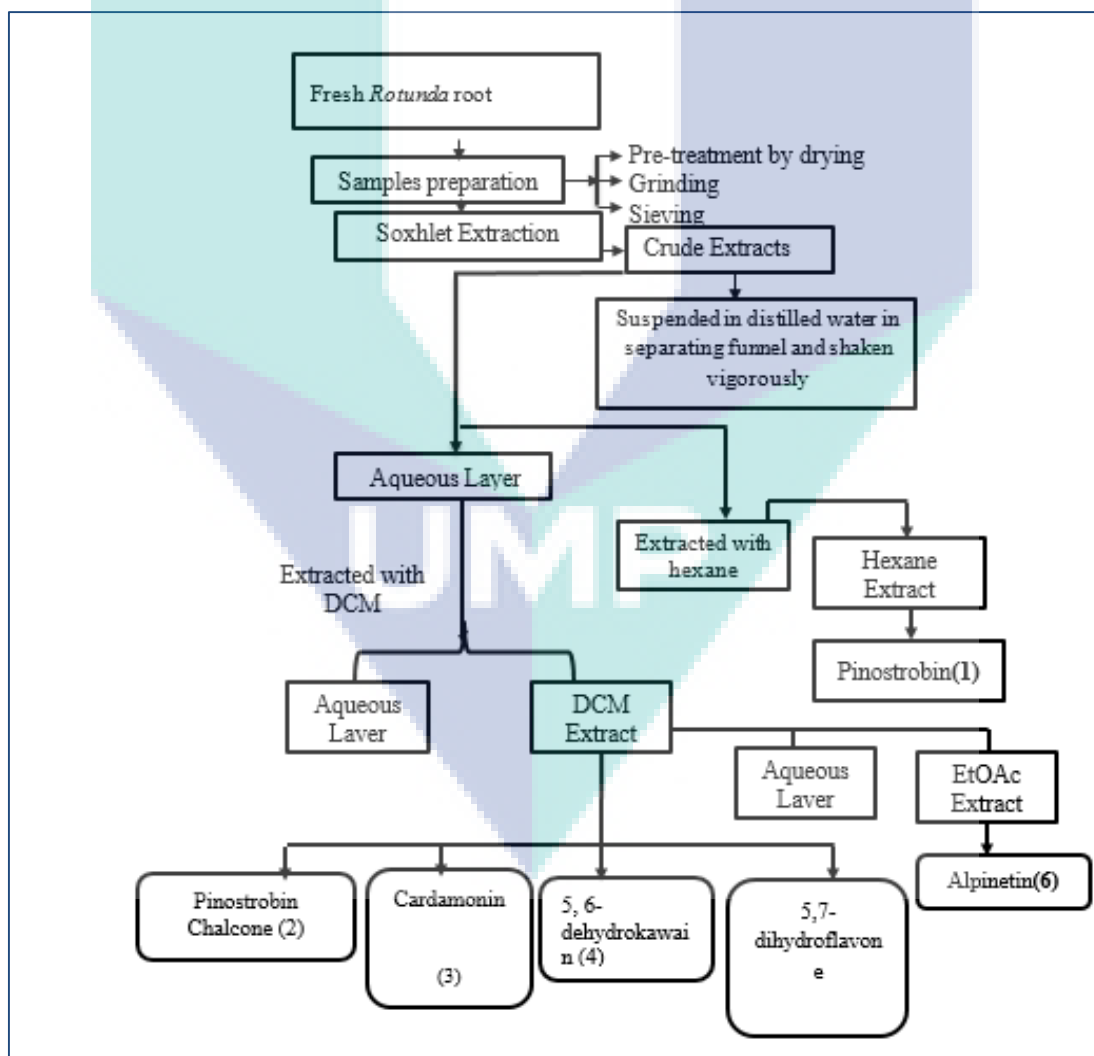


Figure 3.1 Flow diagram of extraction scheme for *B. rotunda*

3.4 Characterization of Isolated Compounds

The *B. rotunda* extracts and the isolated compounds were characterized using as discussed in the proceeding sections.

3.4.1 Ultraviolet-Visible Photometry Analysis

The Genesys 10s UV-Vis spectrometer was used in this study. Prior to the analysis is run, the solid single pure compound isolated will first dilute in solvent (acetone) and gave a pale yellowish liquid solution. The liquid solution will then be pipetted into the 1-cm path length quartz cuvettes. The preparation of the sample and the analysis will carry out under a dark environment and at the temperature of 21 ± 1 °C. The cells will close to avoid the evaporation of the solvent (acetone) and the solution will stir during the irradiation time. The solution will be irradiated at the wavelength ranged from 200 to 500 nm. The absorption spectra will display by the spectrometer and the data will collect. The wavelength of the maximum absorbance of the single pure compound will then identify.

3.4.2 Gas Chromatography-Mass Spectroscopy (GC-MS) Analysis

GC-MS analysis of the chemical constituent isolated from *B. rotunda* will performed by injecting 1 μ L of the sample on an Agilent 7890 gas chromatography coupled to a 5973 quadruple mass spectrometer equipped with a HP-5MS (30 m x 250 μ m, film thickness 0.25 μ m) capillary column. GC-MS operation conditions: injection mode – splitless; injector temperature – 300 °C; injector pressure – 12.675 psi; transfer line – 316 °C; oven temperature programme – 50 °C for 1 min, then 25 °C min^{-1} to 200 °C, then 8 °C min^{-1} to 316 °C; carrier gas –helium at 1.5 mLmin^{-1} ; ion source temperature 350 °C.

3.4.3 Fourier transform infrared spectroscopy (FTIR)

Fourier transform infrared spectroscopy (FTIR) was carried out on the extracts to determine the functional groups. A Thermo-Nicolet spectrometer (iS5 iD7 ATR, Germany) equipped with OMNIC software was employed in the spectrometry analysis. The analysis was executed using the conventional KBr standard procedure with wavenumber ranging from 4000-600 cm^{-1} . Under this study, the spectrum of the observed

bond and associated group frequencies were compared with the table of expected absorption bands (Carol 2000; Gupta et al., 2013).

3.4.4 Nuclear Magnetic Resonance Spectroscopy

The further confirmation of the structure of the isolated chemical constituent isolated will perform by the analysis of ^1H NMR. The sample will first be diluted in the solvent, deuterated chloroform (CDCl_3) and then transferred to NMR tube. The tube will then place in the NMR and the test was carried out. Based on the NMR spectra, the area under each pattern obtained from the integration of the signal will studied to determine and to identify the structure of the compound.

3.5 Cell Viability Assay

The MTT assay was conducted on different cancer cell lines to evaluate the anti-cancer activities of the extracts using H-29 and MDA-MB231 cell lines. The detail of the experimental procedure is presented in the succeeding sub-sections.

3.5.1 Cell Line and Culture

In the H-29 colon, the medium use for this cell line was DMEM supplemented with fetal bovine serum in a 5% CO_2 incubator at 37 °C supplemented with penicillin (100 U/mL) and streptomycin (100 $\mu\text{g}/\text{mL}$). MDA-MB231 (Human breast adenocarcinoma cell line) the medium use for this cell line was DMEM supplemented with fetal bovine serum in a 5% CO_2 incubator at 37 °C supplemented with penicillin (100 U/mL) and streptomycin (100 $\mu\text{g}/\text{mL}$).

The human triple-negative MDA-MB-231 breast cancer and HT-29 colon cancer cell lines were purchased from the American Type and Culture Collection (ATCC, Manassas, VA, USA). The cells were grown in RPMI-1640 supplemented with 10% foetal bovine serum as well as 1% penicillin-streptomycin (complete growth culture media). Cells used for this experiment were less than 20 passage number. Cancer cells were seeded in 96-well flat-bottomed plates with 5,000 cells per well, followed by incubation at 37 °C for 24 hours to allow cell attachment. They were subsequently treated with the compounds for 48 hours. Control cells (0.1% of DMSO) were also included in

this experiment. At the end of the experiment, 20 μL of MTT (5 mg/mL in PBS) was added into each well and incubated for 3 hours. Excess MTT was aspirated and the formazan crystals formed were dissolved using 150 μL of DMSO. The absorbance which is proportional to cell viability was measured at 570 nm and a reference wavelength of 630 nm by using Microplate Reader (BioTek Instrument Inc., Vermont USA). A bar chart of the percentage of cell viability versus concentration of compounds was constructed. The IC_{50} values were also determined.

3.5.2 Validation and Detection of Cell Viability Using MTT Assay

The validation of MTT assay was performed to establish the relationship between cell number and absorbance. This is basically required to judge the accuracy of pipetting technique before moving to chemo-sensitivity assays. The MTT assay was conducted in accordance to Mossman (1983) with slight modifications. The cells were seeded in 96-well plates at a concentration of 0.8×10^5 cells/well. The cells were then incubated in a 37 °C CO_2 incubator overnight. The following day, the synthesized chalcones compound was added to the wells with seven different concentrations.

The cell viability was measured at 72 hours post-treatment. MTT solution (5 mg/mL) was added at a volume of 20 μL in each well and was incubated for three hours. Afterwards, the solution was discarded, and 100 μL of DMSO was added to each well to solubilize the crystals. Finally, the plates will be read at 570 nm as reference wavelength by using $\mu\text{-Quant}$ ELISA Reader (Bio-tech Instruments, USA). The results of the compound-treated cells will be compared with the standard doxorubicin. Each compound control will be assayed in triplicates in three independent experiments. The percentage of inhibition will be calculated by using graph pad and expressed in $\mu\text{g/mL}$ (Nadiyah et al., 2014).

3.6 Computational Molecular Docking Studies

The structures of the compounds were sketched using the builder module in MOE 2016.0801 (Molecular Operating Environment (MOE), 2016.08; Chemical Computing Group Inc., 1010 Sherbrooke St. West, Suite #910, Montreal, QC, Canada, H3A 2R7, 2016). The compounds were then charged and minimized using the MMF94x forcefield (Halgren, T. 1996). The compounds were converted into their respective smiles and

subjected to PASS online server to predict their biological spectrum (Lagunin et al., 2000) After careful inspection of the results, the molecular docking studies were carried out using the crystal structure of the human Janus Kinase available under the accession code 3KRR in the Protein Data Bank (Yang, 2001, Berman et al., 2000). The protein was prepared, charged and minimized using the AMBER10EHT force field. The water molecules were removed and the active site was identified using the cognate ligand DQX. The docking studies were carried out using the default placement, refinement and scoring protocol; tabulated below as Table 3.1.

Table 3.1 The placement and refinement methods and scoring functions used in the docking studies of the FKB derivatives **2,3** and FKB in the active site of the human Janus Kinase B; PDB: 3KRR.

	Method	Score
Placement	Triangle Matcher	London dG
Refinement	Rigid Receptor	GBVI/WSA dG

The resulting poses, five in total were arranged according to the score and analysed visually. The protein-ligand interactions were observed using the PLIP web server (Salentin et al., 2015). All the visuals were sketched using MOE and raytraced using the POVRAY implemented in the MOE (MOE, 2016).

CHAPTER 4

RESULTS AND DISCUSSION

4.1 Overview of Preliminary Estimation of Extract Yield and Purified Fractions

From the extraction process, (35.5±0.01) g of orange coloured semi-solid extract was extracted from 300 g of *B.rotunda* sample using n-hexane as the extracting solvent. The higher percentage yield (Eq.4.1) obtained confirmed the higher efficiency of n-hexane when compared with other solvents as reported by Shan et al., (2016).

$$\text{Percentage of oil yield} = \frac{W_0 - W_1}{W_0} = \frac{300 - 25.9}{300} \times 100\% = 88.16\% \quad 4.1$$

where W_0 is the mass of *B.rotunda* sample loaded into the Soxhlet apparatus and W_1 is the semi-solid extract obtained from the process. The extraction process was conducted in triplicates. Moreover, the extracts was separated into colourless semi crystalline compound sub fraction (11-13g) using thin layer column chromatography. The compound was further purified by crystallization using methanol. The compound was identified by the several spectroscopic techniques such as UV, FT-IR, GC-MS, $^1\text{H-NMR}$ and $^{13}\text{C-NMR}$ spectroscopic techniques. The research was then continued with the identification and characterization of the major chemical constituent of the chemical constituents as presented in the preceding sections.

4.2 Results of Pinostrobin (1) Characterization

4.2.1 UV-Vis Spectrometry Analysis of Pure Pinostrobin (1)

The highest absorption wavelength, λ_{max} of the chemical constituent isolated from *B. rotunda* was observed at 290 nm as illustrated in Figure 4.1. The results show the presence of a chromophore or a C=O bond in the compound with π -electrons in the double

bond but also has lone pairs on the oxygen atom. The electron in chromophore excited from a π (pi bonding orbital) to a π^* (pi anti-bonding orbital). The π has a higher energy level than the π^* , which leads to less energy in jumping from n (non-bonding orbital) to π^* . Hence, the light was absorbed at a lower frequency and yielded a higher wavelength. The UV-Vis spectrum also shows the similarity with the UV-Vis analysis result of pinostrobin in previous studies where the value of $\lambda_{\text{max}} = 290 \text{ nm}$ (Jaipetch et al. 1982; Yap et al., 2007).

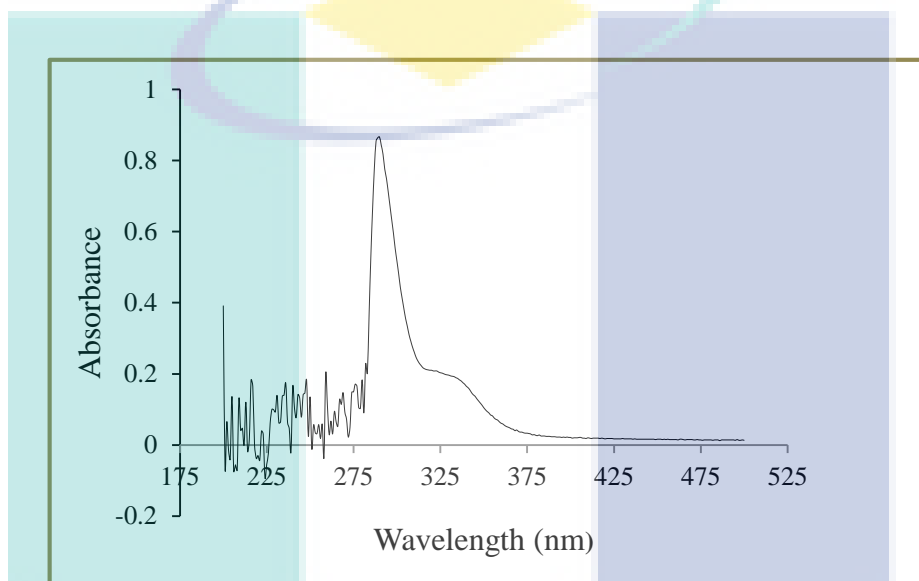


Figure 4.1 UV-Vis spectrum of the chemical constituent isolated from *B. rotunda*

4.2.2 Functional Group Analysis of Single Pure Pinostrobin (1)

In this study, the functional group analysis was conducted to determine the band attributes of single pure compounds isolated from *B. rotunda* was characterized Figure 4.3 shows the IR spectra of pure chemical constituent isolated from *B. rotunda*. FTIR instrument is used in this study for the analysis of functional groups present in the chemical constituent isolated from *B. rotunda*. The present of a broad peak of 3434 cm^{-1} shows the present of O-H bond of hydrogen bonded alcohol and phenol groups. The C-H bond of alkene and aromatic functional groups is found at 3060 cm^{-1} and 3032 cm^{-1} . These peaks are sharp and have medium strength of intensity. Besides that, the spectrums at 2973 , 2938 , 2894 and 2845 cm^{-1} show the presence of the C-H bond of alkanes group which have the strong intensity (Table 4.1). The spectrums at both these range of bonds also shows the presence of strong and broad peaks of carboxylic acids O-H bonds. The presence of aromatic C=C bond with medium-weak strength intensity is found at 1580

cm^{-1} . Furthermore, the presence of C-H bond of aliphatic alkanes with medium strength intensity is found at 1444 cm^{-1} .

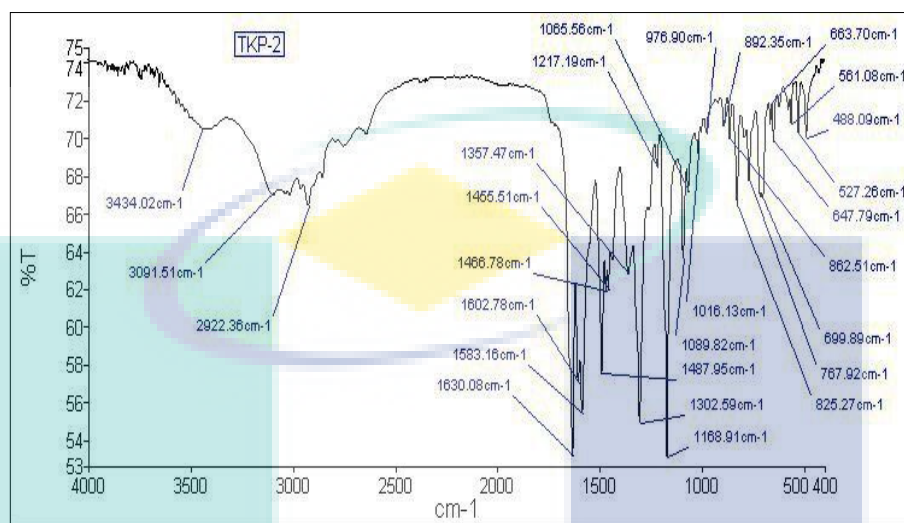


Figure 4.2 FT-IR functional groups in pure compound

Moreover, the data result shows the presence of medium strength intensity O-H bond of alcohol n phenol groups at 1381 and 1339 cm^{-1} and the presence of strong intensity C-O bond of alcohol and phenol groups at 1210 , 1160 and 1093 cm^{-1} . Additionally, the IR spectrum displayed a C-H band at 743 cm^{-1} . These IR spectra suggested that the chemical constituent isolated to be a flavonoid derivative, which is similar to the previous studies (Jaipetch et al. 1982; Yap et al., 2007). Further assignment of the structure was done by the proton nuclear magnetic resonance spectroscopy (^1H NMR) analysis and will be discussed in the proceeding sections.

Table 4.1 FTIR characteristics of a single pure pinostrobin (**1**)

Band attributes	Wavenumber (cm^{-1})
O-H: Alcohol, Phenol	3225
C-H: Alkene, Aromatic	3060, 3032
C-H: Alkanes	2973, 2938, 2894, 2845
O-H: Carboxylic	3060, 3032, 2973, 2938, 2894, 2845
C=O: Alkenes	1646, 1621
C=C: Aromatic	1580
C-H: Aliphatic Alkane	1444, 1381
O-H: Alcohol, Phenol	1381, 1339

4.2.3 ^1H Nuclear Magnetic Resonance (NMR) for a Pure Pinostrobin (I)

The structure of the single pure compound isolated from *B. rotunda* was further evaluated using ^1H NMR. The informative NMR parameters with the chemical shift, multiplicities, coupling constant and their correlations were succinctly determined. The structure of 5-hydroxy-7-methoxy-2-phenylchroman-4-one or pinostrobin (single pure compound) is shown in Figure 4.4.

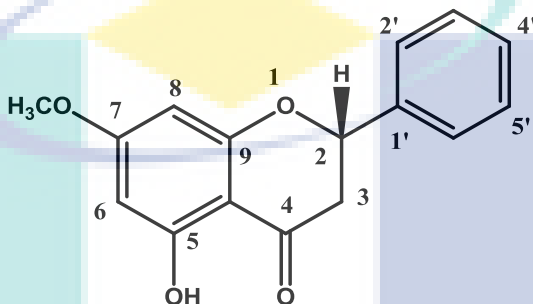


Figure 4.3 The structure of pinostrobin (1)

Based on the ^1H NMR (CDCl_3 , 600 MHz) spectrum of the chemical constituent isolated, a sharp singlet at δ 12.04 ppm was observed due to a strong hydrogen-bonded hydroxyl group. The multiplet at the range of 7.0-7.5 ppm shows that the protons on a monosubstituted benzene ring (H-2', H-3', H-5', H-6') where the aromatic ring is an electron-withdrawing group with less shielding effect. A doublet at 6.07 ppm assigned to H-6 and H-8 indicates the protons on the second aromatic ring with a coupling constant, J of 1.25 Hz calculated. The signal corresponding to the proton attached to the methine group in the chromane ring resonated centred at 5.43 ppm with the J of 15.6, 3.6 Hz.

The presence of methoxyl protons (7-OMe) at 3.83 ppm appeared as a sharp singlet in the spectrum. Two signals which arose centred at 3.08 ppm and 2.84 ppm appeared as doublet of doublet (dd) suggested the presence of the protons attached to the methyl group (H-3) and have the value of coupling constant, J of 15.6 Hz, 3.6 Hz and 1, 3.5 Hz, respectively. Atoms C8 and C9 in TK4 were disordered with refined sites occupancy ratio of 0.846 (9) and 0.154 (9) as illustrated in Figure 4.5. However, both C9 and C9X bounded H atoms are at axial position.

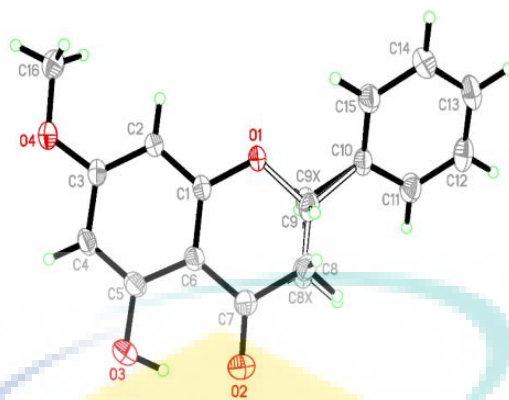


Figure 4.4 ORTEP diagram of Pinostrobin (1)

The summary of the ^1H NMR spectral data were tabulated in Table 4.3. The ^1H NMR spectroscopic data of the single pure compound isolated was compared and showed similarity to the previous investigation (Jaipetch et al. 1982; Yap et al., 2007). Further elucidation of the chemical constituent was done by UV-Vis and the assignment is presented and discussed in proceeding sections.

Table 4.2 ^1H & ^{13}C NMR data of Pinostrobin compound (1)

Position	^{13}C (δ)	^1H (δ)	^1H (m, J/Hz)	Assignment
2	79.24	5.43	(dd, $J = 3.6, 15.6, 1\text{H}$)	C2-H
3	43.40	2.84,	(dd, $J = 3.6, 15.6, 2\text{H}$)	C3 α , β -H
4	195.77	-	-	-
5	164.15	-	-	-
6	95.16	6.09	(d, $J = 2.7, 1\text{H}$)	C6-H
7	167.99	-	-	-
8	94.28	6.10	(d, $J = 2.7, 1\text{H}$)	C8-H
9	162.79	-	-	-
10	103.16	-	-	-
1'	138.37	-	-	-
2'/6'	126.14	7.40	(m, 2H)	C2'/6'-H
3'/5'	128.89	7.43	(m, 2H)	C3'/5'-H
4'	128.89	7.43	(m, 1H)	C4'-H
7-OCH ₃	55.71	3.83	(s, 3H)	OCH ₃ (C7)
5-OH	-	12.05	(s, 1H)	OH (C5)

Source: Shoja et al., (1989); Yamovoi et al., (2001)

4.2.4 Gas Mass Spectrometry Determination of Pinostrobin (1)

The gas chromatography mass spectrometer (GC-MS) was used in this study as one of the spectroscopic data source of the chemical constituent isolated from *B. rotunda*.

The identification of the chemical constituent is also done by the National Institute of Standards and Technology (NIST) database matching and published data comparing. GC-MS instrument is used to identify the molecular weight of the compound and its chemical structure by analysing the ions present in the molecules. Previous studies reported that 5-hydroxy-7-methoxy-2-phenylchroman-4-one (pinostrobin (**1**)) with the molecular formula of $C_{16}H_{14}O_4$ and molecular ion peak at $m/z = 270$ was found to one of the flavonoids isolated from *B. rotunda* (Jaipetch et al. 1982; Yap et al., 2007).

The highest peak with 95 % at retention time of 14.279 min indicates the presence of the highest content of the compound at its respective retention time through the GC-MS analysis. At 14.279 min, the respective mass spectrum shows the molecular ion peak at $m/z = 270$ (Figure 4.2). These GC-MS spectroscopic data information claimed that the chemical constituent isolated from *B. rotunda* has a molecular weight of 270 and $C_{16}H_{14}O_4$ as its molecular structure.

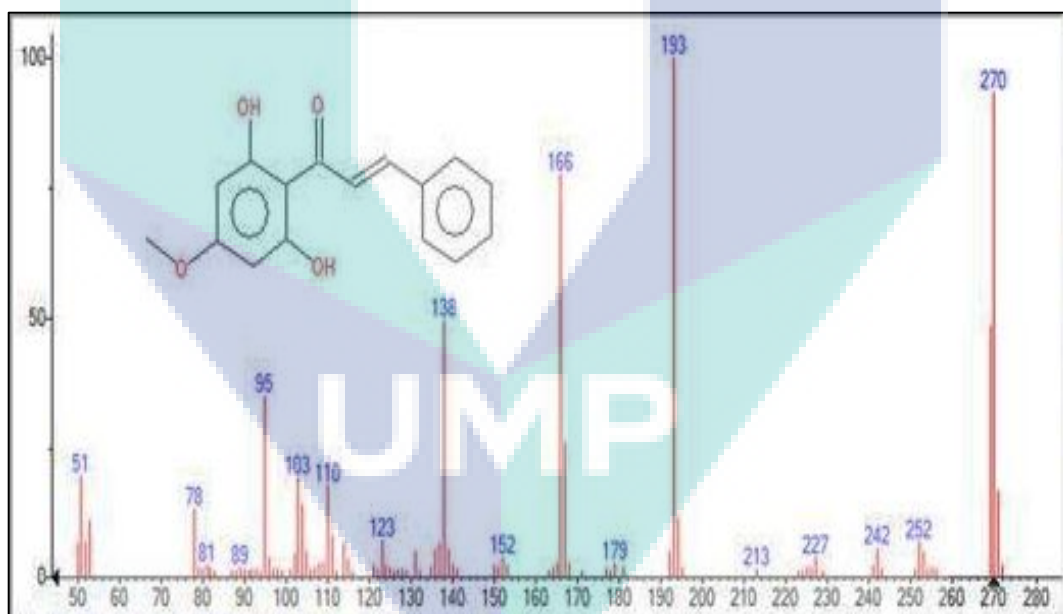


Figure 4.5 GC-MS spectrum of single pure compound isolated from *B. rotunda*

The GC-MS analysis result is found similar to the previous investigations by Jaipetch et al. (1982) and Yap et al. 2007). Further elucidations of the isolated compound from *B. rotunda* were succinctly discussed in the preceding section.

4.2.5 Results of X-ray Crystallography Analysis of Pinostrobin (1)

The X-ray analysis for all these samples was performed using Bruker APEX II DUO CCD diffractometer, employing MoK α radiation ($\lambda = 0.71073 \text{ \AA}$) with φ and ω scans, at room temperature. Data reduction and absorption correction were performed using the SAINT and SADABS programs (Bruker, 2012). All structures were solved by direct methods and refined by full-matrix, least-squares techniques on F^2 using the SHELXTL software package (Sheldrick, 2008, Sheldrick, 2015). All C- bound H atoms were placed in geometrically idealized positions and constrained to ride on their parent atoms with C-H distance in the range of 0.93-0.97 and $U_{\text{iso}}(\text{H}) = 1.2 U_{\text{eq}}(\text{C})$, while $U_{\text{iso}}(\text{H})$ for methyl H atoms were set at $1.5 U_{\text{eq}}(\text{C})$ and each groups were allowed to rotate freely about its C—C bond. The O- bound atoms were located from difference Fourier maps and were refined freely. The ORTEP (Oak Ride Thermal Ellipsoid Plot Program) of 1 and TKA is shown in Figure 4.5 The X-ray crystallographic data presented in Table 4.2.

Table 4.3 Crystal data and parameters for the structure refinement of Pinostrobin (1)

Compound	Pinostrobin
CCDC Number	-
Molecular Formula	C ₁₆ H ₁₄ O ₄
Molecular Weight	270.27
Crystal System	Monoclinic
Space Group	<i>P</i> 2 ₁ / <i>c</i>
<i>a</i> (Å)	10.1897 (17)
<i>b</i> (Å)	16.105 (3)
<i>c</i> (Å)	8.1037 (13)
β (°)	91.745 (2)
<i>V</i> (Å ³)	1329.2 (4)
<i>Z</i>	4
<i>D</i> _{calc} (Mg m ⁻³)	1.351
Crystal dimensions (mm)	0.40 x 0.29 x 0.23
μ (mm ⁻¹)	0.10
<i>T</i> _{min} / <i>T</i> _{max}	0.640,0.946
Reflections measured	21562
Ranges/indices (<i>h</i> , <i>k</i> , <i>l</i>)	-13→13; -22→21; -10→11
θ limit (°)	2.0-29.1
Unique reflections	3546
Observed reflections	2251
Parameters	205
Goodness of fit on F^2	1.03
<i>R</i> ₁ , <i>wR</i> ₂ [<i>I</i> ≥ 2 σ (<i>I</i>)]	0.050, 0.133

Source : Bruker (2012) ;Sheldrick (2015); Sheldrick (2008)

Crystallographic data for the reported structures have been deposited at the Cambridge Crystallographic Data Centre (CCDC) with the CCDC deposition numbers of 1548733 and 1548734. Copies of available material can be obtained free of charge on application to the CCDC, 12 Union Road, Cambridge CB2 1EZ, UK, (Fax: +44-(0)1223-336033 or e-mail: deposit@ccdc.cam.ac.uk).

4.3 Isolation and purification of Pinostrobin Chalcone (**2**)

Pinostrobin chalcone ((*E*)-1-(2',6'-dihydroxy-4'-methoxyphenyl)-3-phenylprop-2-en-1-one) was isolated from the chloroform fraction. Then the compound was purified after several column chromatographic operations and purification of compound was monitored by thin layer of column chromatography. The sub fraction of the chloroform fraction was yielded again semi pure compound, which was further redo the small column chromatography and yielded the title compound.

4.3.1 UV-Vis Spectrophotometry Analysis of Pinostrobin Chalcone (**2**)

Pinostrobin chalcone (**2**) absorbed UV light in the wavelength range of 250-380 nm, which corresponded to the conjugated α,β -unsaturated carbonyl (C=O) chromophore (Hufford et al., 1982). Figure 4.6 shows the UV-Visible spectrum of compound **2** with maximum absorption at wavelength, λ_{max} of 340 nm.

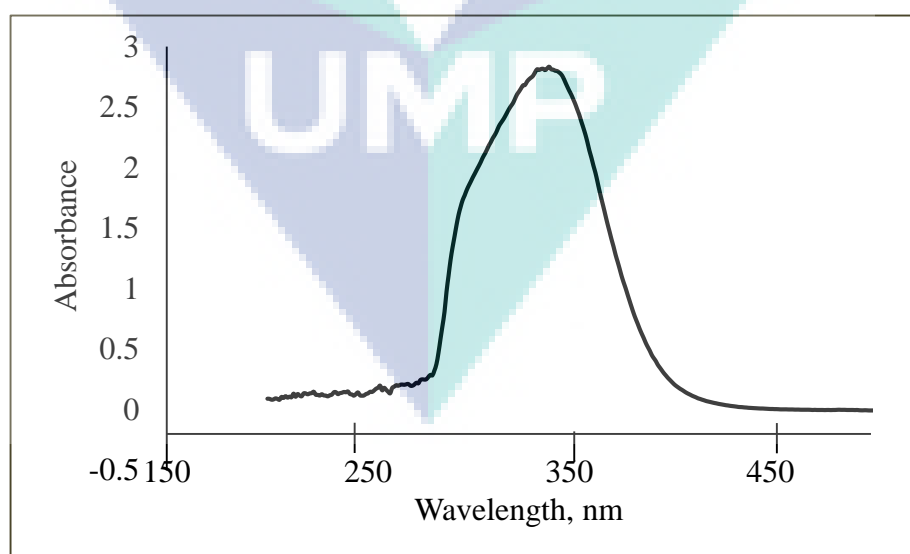


Figure 4.6 UV spectrum of pure pinostrobin chalcone (**2**)

4.3.2 Functional Group Analysis of Single Pure Pinostrobin chalcone

IR spectrum of compound 2 in Figure 4.8 shows absorption band at 3456 cm^{-1} which corresponded to hydroxy (O-H) and between $2940\text{--}3092\text{ cm}^{-1}$ which corresponded to aromatic C-H stretch. Absorption band at 1623 cm^{-1} and between $1416\text{--}1439\text{ cm}^{-1}$ was indicated the presence of carbonyl (C=O) and aromatic ring C=C, respectively. Absorption band appeared in the range of $1158\text{--}1219\text{ cm}^{-1}$ corresponded to (C-O) moiety (Akhtar et al., 2015).

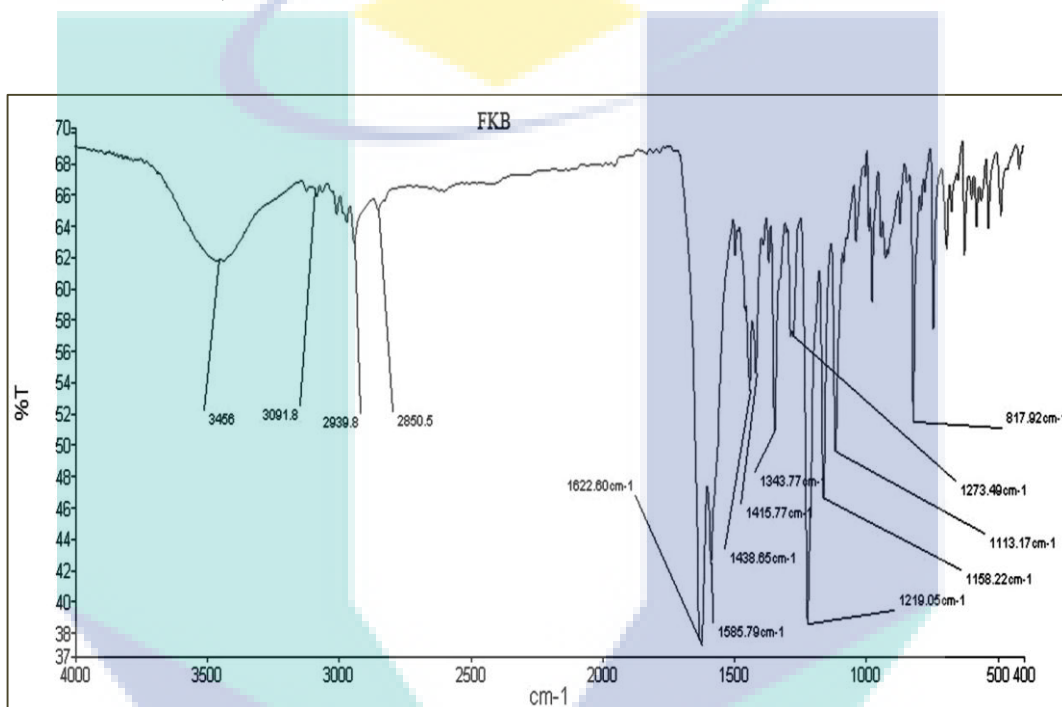


Figure 4.7 IR spectrum of pure pinostrobin chalcone (2)

4.3.3 ^1H Nuclear Magnetic Resonance (NMR) for Pinostrobin chalcone (2)

The ^1H -NMR spectrum (600 MHz, CDCl_3) of compound 2 in Figure 4.9 (Appendix A1) shows a singlet at δ 3.84, which was assigned to the methoxy protons at C-4'. Two doublets that appeared at 5.96 (d, $J = 2.46\text{ Hz}$) and 6.11 (d, $J = 2.40\text{ Hz}$) were assigned to C-5' and C-3' protons, respectively.

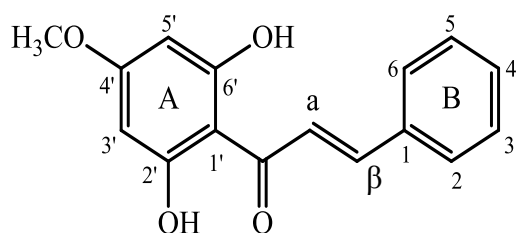


Figure 4.8 Structure of pure pinostrobin chalcone (2)

A broad multiplet that appeared in the range of 7.38-7.42 was assigned to C-3, C-4 and C-5 protons. Two doublets observed at 7.62 (d, $J = 8.04$ Hz) and 7.60 (d, $J = 8.04$ Hz) were assigned to C-2 and C-6 protons, respectively. A downfield doublet at 7.78 (d, $J = 15.55$ Hz) was assigned to proton at α -carbon and another doublet observed at 7.90 (d, $J = 15.55$ Hz) was assigned to proton at β -carbon, which data is supported by previous publication (Jing et al., 2011; Sukari et al., 2017). A downfield singlet that appeared at 14.30 was assigned to C-2' hydroxyl proton chelated to carbonyl group. Further details of $^1\text{H-NMR}$ and $^{13}\text{C-NMR}$ spectra are shown in Table 4.4.

Table 4.4 NMR data of pure pinostrobin chalcone (2)

Carbon	^{13}C (δ)	^1H (δ)	Multiplicity	Designation
1'	108.14	-	-	-
2'	168.90	-	-	-
3'	93.60	6.11	(d, $J = 2.40$ Hz, 1H)	C3'-H
4'	166.70	-	-	-
5'	90.94	5.96	(d, $J = 2.46$ Hz, 1H)	C5'-H
6'	162.50	-	-	-
1	132.90	-	-	-
2	130.20	7.62	(d, $J = 8.04$ Hz, 1H)	C2-H
3	128.10	7.38-7.42	(m, 3H)	C3-H
4	141.00	7.38-7.42	(m, 3H)	C4-H
5	128.10	7.38-7.42	(m, 3H)	C5-H
6	130.20	7.60	(d, $J = 8.04$ Hz, 1H)	C6-H
A	126.60	7.78	(d, $J = 15.55$ Hz, 1H, H- α)	C α -H
B	142.51	7.90	(d, $J = 15.55$ Hz, 1H, H- β)	C β -H
OCH ₃	55.70	3.84	(s, 3H)	OCH ₃ (C4')
OH	-	14.30	(s, 1H)	OH (C2')
OH(C6')				
C=O	192.22	-	-	-

4.3.4 Gas Mass Spectrometry Determination of Pure Pinostrobin chalcone (2)

GC-MS spectrum of compound (2) shown in Figure 4.7 displays the main fragment ion at $m/z = 270$, 226, 198, 141, 115, 131, 103 and 77. The abundance of molecular peak at $m/z = 141$ was about 100. Loss of H_2O from the molecular ion produced fragment ion at $m/z = 252$. The base peak at $m/z = 207$ was produced due to loss of phenyl group while another fragment formed at $m/z = 77$ due to β -cleavage.

The fragment ion at $m/z = 181$ could be the radical ketone moiety formed due to α -cleavage. Formation of fragment ion at $m/z = 152$ could be due to the cleavage of bond next to $C=O$ and subsequent rearrangement; the other part formed a fragment ion at $m/z = 131$.

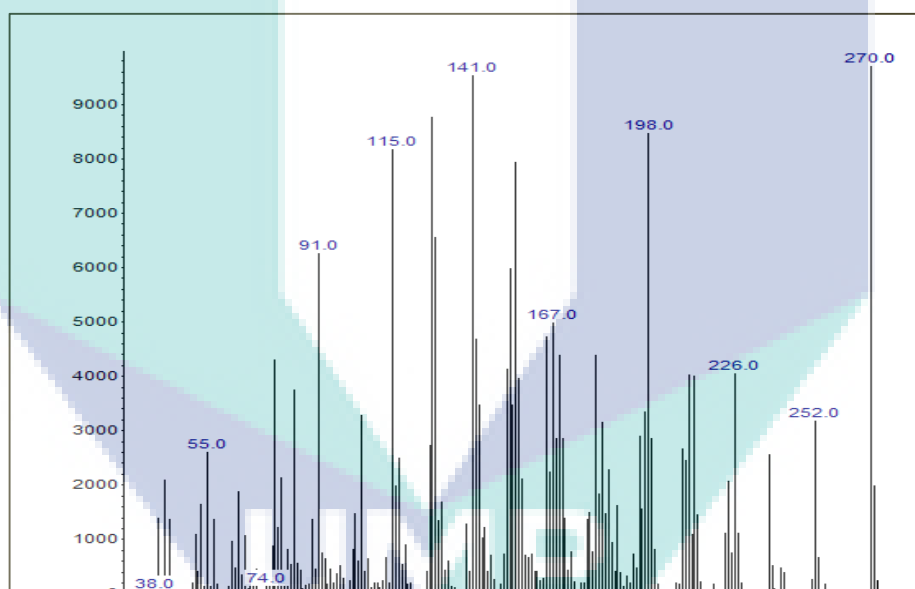


Figure 4.9 GC-MS spectrum of pure pinostrobin chalcone (2)

4.4 Characterization Results for Cardamonin (3)

Compound (3) (i.e. (*E*)-1-(2',4'-dihydroxy-6'-methoxyphenyl)-3-phenylprop-2-en-1-one) was isolated from the chloroform fraction. Then, fraction from the isolation and purification of this hexane extract had yielded a single pure compound which was a 130.5 mg of crystalline solid with a yellow colour. Then the compound was purified after several column chromatographies and purification of compound was monitored by thin layer of column chromatography.

4.4.1 UV-Vis Spectrometry Analysis of Cardamomin (3)

The compound **3** absorbed UV light in the wavelength range of 290-380 nm, which corresponded to the conjugated α,β -unsaturated carbonyl (C=O) chromophore (Hufford et al., 1982). Figure 4.10 shows the UV-Visible spectrum of compound **3** with maximum absorption at wavelength, λ_{max} of 340 nm.

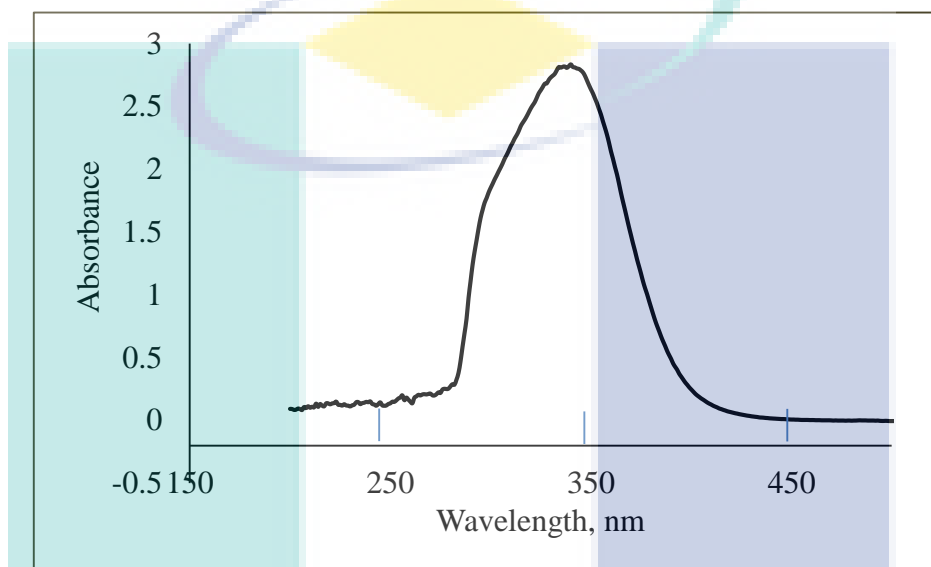


Figure 4.10 UV spectrum of compound (3)

4.4.2 Functional Group Analysis of Single Pure Cardamomin (3)

IR spectrum of compound **3** in Figure 4.11 shows absorption band at 3456 cm^{-1} which corresponded to hydroxy (O-H) and between $2940\text{-}3092\text{ cm}^{-1}$ which corresponded to aromatic C-H stretch. Absorption band at 1623 cm^{-1} and between $1416\text{-}1439\text{ cm}^{-1}$ was indicated the presence of carbonyl (C=O) and aromatic ring C=C, respectively. Absorption band appeared in the range of $1158\text{-}1219\text{ cm}^{-1}$ corresponded to (C-O) moiety (Akhtar et al., 2015).

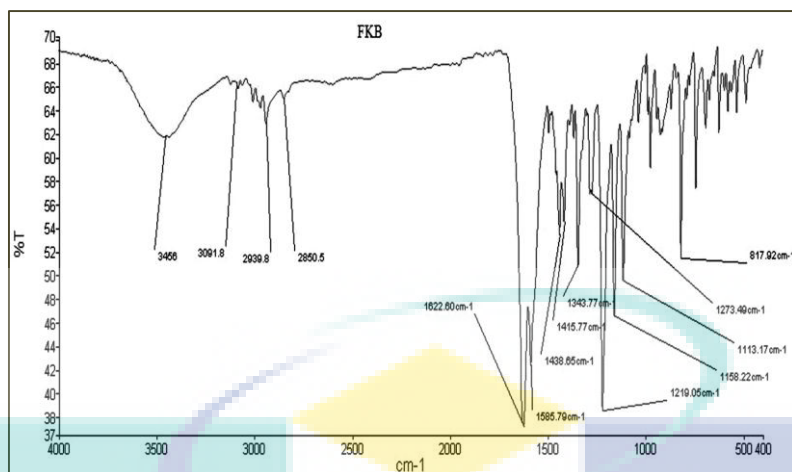


Figure 4.11 IR spectrum of compound (3)

4.4.3 ¹H Nuclear Magnetic Resonance (NMR) for a Pure Cardamomin (3)

The ¹H-NMR spectrum (600 MHz, CDCl₃) of compound **3** in Figure 4.12 (Appendix A1) showed a singlet at δ 3.84, which was assigned to the methoxy protons at C-6' atom.

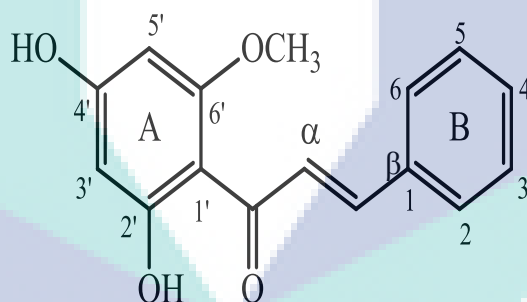


Figure 4.12 Structure of pure Cardamomin (3)

Two doublet that appeared at 5.96 (d, $J = 2.46$ Hz) and 6.11 (d, $J = 2.40$ Hz) were assigned to C-5' and C-3' protons, respectively. A broad multiplet that appeared in the range of 7.38-7.42 was assigned to C-3, C-4 and C-5 protons. Two doublets observed at 7.62 (d, $J = 8.04$ Hz) and 7.60 (d, $J = 8.04$ Hz) were assigned to C-2 and C-6 protons, respectively. A downfield doublet at 7.78 (d, $J = 15.55$ Hz) was assigned to proton at α -carbon and another doublet observed at 7.90 (d, $J = 15.55$ Hz) was assigned to proton at β -carbon, which data is supported by previous publication (Abu et al., 2016; Seo et al., 2013). A downfield singlet that appeared at 14.30 was assigned to C-2' hydroxyl proton chelated to carbonyl group. Further details of ¹H-NMR and ¹³C-NMR spectra are shown in Table 4.5.

Table 4.5 NMR data of Cardamonin (**3**)

Carbon	¹³ C (δ)	¹ H (δ)	Multiplicity	Designation
1'	108.14	-	-	-
2'	168.90	-	-	-
3'	93.60	6.11	(d, <i>J</i> = 2.40 Hz, 1H)	C3'-H
4'	166.70	-	-	-
5'	90.94	5.96	(d, <i>J</i> = 2.46 Hz, 1H)	C5'-H
6'	162.50	-	-	-
1	132.90	-	-	-
2	130.20	7.62	(d, <i>J</i> = 8.04 Hz, 1H)	C2-H
3	128.10	7.38-7.42	(m, 3H)	C3-H
4	141.00	7.38-7.42	(m, 3H)	C4-H
5	128.10	7.38-7.42	(m, 3H)	C5-H
6	130.20	7.60	(d, <i>J</i> = 8.04 Hz, 1H)	C6-H
A	126.60	7.78	(d, <i>J</i> = 15.55 Hz, 1H, H-α)	Cα-H
B	142.51	7.90	(d, <i>J</i> = 15.55 Hz, 1H, H-β)	Cβ-H
OH (C4')	-	-	-	OH (C4')
OCH ₃ (C6')	55.53	3.92	(s, 3H)	OCH ₃ (C6')
OH (C2')	-	14.30	(s, 1H)	OH (C2')
C=O	193.20	-	-	-

4.4.4 Gas Mass Spectrometry Determination of Cardamonin (**3**)

GC-MS spectrum of compound **3** shown evaluated the main fragment ion at $m/z = 284, 267, 207, 181, 152, 131, 103$ and 77 . The abundance of molecular peak at $m/z = 284$ was about 50%. Loss of $\cdot\text{OH}$ radical from the molecular ion produced fragment ion at $m/z = 267$. The base peak at $m/z = 207$ was produced due to loss of phenyl group while another fragment formed at $m/z = 77$ due to β -cleavage. The fragment ion at $m/z = 181$ could be the radical ketone moiety formed due to α -cleavage. Formation of fragment ion at $m/z = 152$ could be due to the cleavage of bond next to C=O and subsequent rearrangement; the other part formed a fragment ion at $m/z = 131$. The fragment ion at $m/z = 103$ was probably the C_8H_7^+ ion, formed after cleavage of bond next to C=O in structure of fragment ion observed at $m/z = 131$.

4.5 Results of Pure 5, 6-dehydrokawain (4) Characterization

The physicochemical characterization conducted on compound (4) is carefully discussed in the proceeding sub-sections.

4.5.1 UV-Vis Spectrometry Analysis of 5,6-dehydrokawain (4)

The highest absorption wavelength, λ_{\max} of the chemical constituent isolated from *Boesenbergia rotunda* was observed at 290 nm (Figure 4.13). The π has a higher energy level than the π^* , which leads to less energy in jumping from n (non-bonding orbital) to π^* . Hence, the light was absorbed at a lower frequency and yielded a higher wavelength. The UV-Vis spectrum also shows the similarity with the UV-Vis analysis result of 5,6-dehydrokawain in previous studies where the value of $\lambda_{\max} = 290$ nm (He et al. 1997, Hansel et al. 1968)

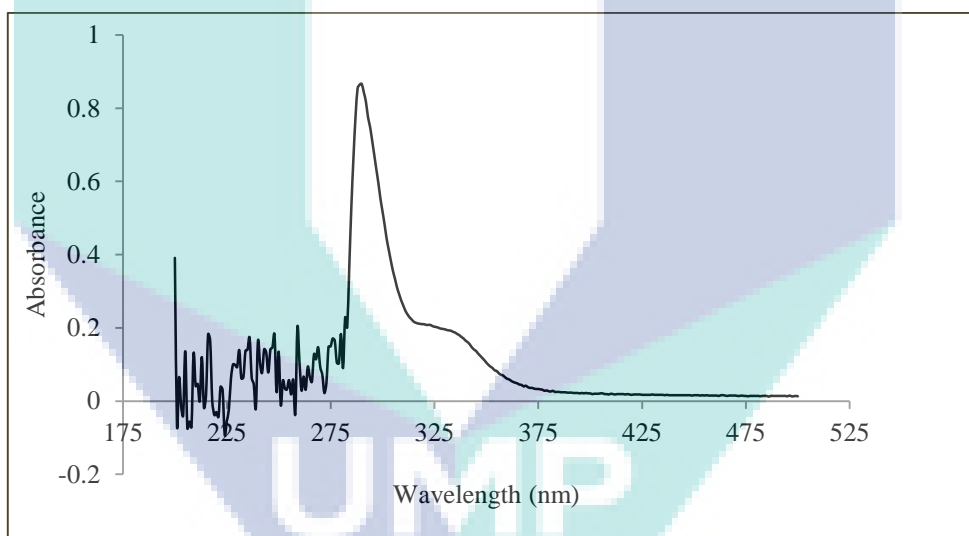


Figure 4.13 UV-Vis spectrum of pure 5,6-dehydrokawain (4)

4.5.2 Functional Group Analysis of Single Pure 5,6-dehydrokawain (4)

FTIR instrument was used in this study for the analysis of functional groups present in the chemical constituent isolated from *B. rotunda*. The presence of C=O bond with variable intensity is found at 1646 cm^{-1} and 1621 cm^{-1} while that of aromatic C=C bond with medium-weak strength intensity is found at 1580 cm^{-1} . C-H bond of alkene and aromatic functional groups is found at 3060 cm^{-1} and 3032 cm^{-1} . These peaks are sharp and have medium strength of intensity. Additionally, the IR spectrum displayed a

C-H band at 743 cm^{-1} . IR (KBr disc, V_{max} , cm^{-1}): 1714, 1639, 1553 & 1451. These IR spectra suggested that the chemical constituent isolated to be a flavonoid derivative, which is similar to the previous studies (Jaipetch et al. 1982; Yap et al., 2007). Further assignment of the structure was done by the proton nuclear magnetic resonance spectroscopy (^1H NMR) analysis and will be discussed in the next sub-section.

4.5.3 ^1H Nuclear Magnetic Resonance (NMR) for a Pure 5,6-dehydrokawain (4)

The structure of the single pure compound isolated from *B. rotunda* was further determined by ^1H NMR. The informative NMR parameters including chemical shift, multiplicities, coupling constant and their correlations were tabulated in Table 4.6. The structure of 5,6-dehydrokawain (single pure compound) is shown in Figure 4.15.

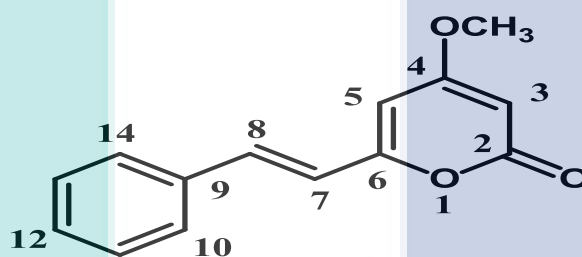


Figure 4.14 The structure of 5,6-dehydrokawain (4)

Based on the ^1H NMR spectrum of the chemical constituent isolated, one multiplet at the range of 7.23 - 7.28 ppm shows the protons on a mono substituted benzene ring (5H, H-10, 11, 12, 13 & 14) where the aromatic ring is an electron-withdrawing group with less shielding effect. A doublet at 5.51 and 6.12 ppm assigned to H-3 and H-5 indicates the protons on the second aromatic ring with a coupling constant, J of 2.1 Hz calculated. The presence of methoxyl protons (4-OMe) at 3.78 ppm appeared as a sharp singlet in the spectrum. Two protons assigned signals which arose centred at 6.77 ppm and 7.33 ppm suggested the presence of the protons attached to the olefinic protons (H-6 and H-7) and have the value of coupling constant, J of 16.0 Hz and 16.01 Hz respectively. The ^1H NMR spectral data were tabulated in Table 4.6 below (also refer to Appendix A1 for the NMR spectra). The ^1H NMR spectroscopic date of the single pure compound isolated was compared and showed similarity to the previous investigation (Jaipetch et al. 1982; Yap et al., 2007, Itokawa et al., 1981).

Table 4.6 ^1H & ^{13}C NMR data of 5,6-Dehydrokawain (**4**).

Position	^{13}C (δ)	^1H (δ)	^1H (m, J/Hz)	Assignment
2	158.61	-	-	-
3	88.85	5.51	(d, $J = 2.1$, 1H)	C3-H
4	171.2	-	-	-
5	101.36	6.12	(d, $J = 2.1$, 1H)	C5-H
6	164.05	-	-	-
7	118.62	6.77	(d, $J = 16.0$, 1H)	C7-H
8	135.78	7.33	(d, $J = 16.01$, 1H)	C8-H
9	135.20	-	-	-
10/14	127.44	7.23-7.28	(m, 2H)	C10/14-H
11/13	128.90	7.23-7.28	(m, 2H)	C11/13-H
12	129.44	7.23-7.28	(m, 1H)	C12-H
4-OCH ₃	55.95	3.78	(s, 3H)	OCH ₃ (C4)

4.5.4 Gas Mass Spectrometry Determination of Pure 5,6-dehydrokawain (**4**)

GC-MS spectrum of compound **4** shown in Figure 4.14 displays the main fragment ion at $m/z = 228$, 211, 200, 186, 115, 131, 103 and 77. The abundance of molecular peak at $m/z = 228$ was about 100. The main fragment at $m/z = 103$ was appeared due to the loss of lactone ring ($\text{C}_6\text{H}_5\text{O}_3$) $m/z = 125$ form the molecular ion [$\text{M}^+ 228$]. Another fragment ion appeared 185 appeared due to loss of CO_2 . The fragment ion at $m/z = 78$ could be the loss of phenyl ring. Formation of fragment ion at $m/z = 157$ could be due to the cleavage of bond next to $\text{C}=\text{O}$ and subsequent rearrangement (Koppel and Tenczer 1991).

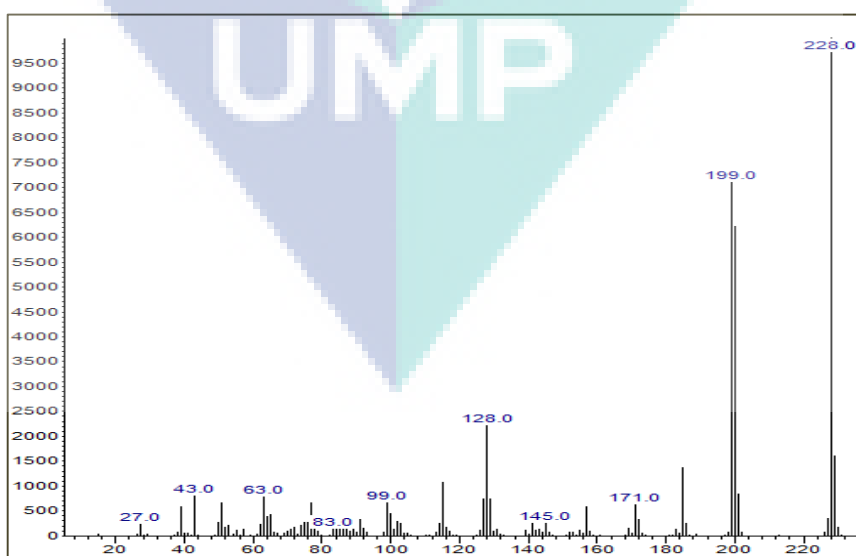


Figure 4.15 GC-MS spectrum of 5,6-dehydrokawain (**4**)

4.6 Results of Pure 5,7-dihydroxyflavanone (5) Characterization

5,7-dihydroxyflavanone isolated out from CC fraction 30-39. The interpretation of the spectral analysis is discussed in the following subsections

4.6.1 UV-Vis Spectrometry Analysis of 5,7-dihydroxyflavanone (5)

After melting point of the compound is determined, the characterization of the isolated compound is continued with UV-VIS analysis. Figure 4.16 here displays the spectrum of UV-VIS.

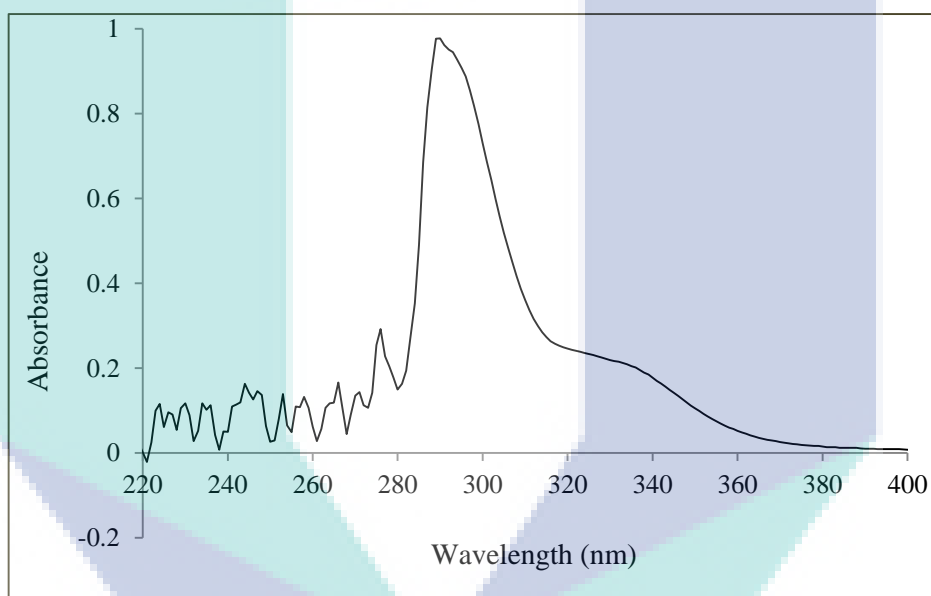


Figure 4.16 UV-VIS spectrum of pure 5,7-dihydroxyflavanone (5)

Based on the result of UV-VIS, the λ_{max} for purified single compound isolated from polar extracts of BR rhizome is at 288 nm. According to Pavia et al. (2001), typical carbonyl chromophore will experience a $n \rightarrow \pi^*$ transition at the range of 280 nm to 290nm. This implies that, the purified compound contains C=O chromophore where a λ_{max} at 289 nm is observed in the UV-VIS spectrum.

The λ_{max} of the compound is occurred near the upper range of a C=O chromophore. This might be due to the presence of substituents in the compound which resulted in a red shift. A red shift is a shift which affects the absorption band of chromophore to longer wavelength or lower energy. Other than the presence of substituents caused a red shift, the extent of conjugation in a double bond system also give rise to a red shift.

4.6.2 Functional Group Analysis of 5,7-dihydroxyflavanone (5)

KBr pellet method was used to prepare the solid sample for FTIR spectroscopy. Figure 4.19 show the infrared spectrum of transmittance percentage versus wavenumber. The frequencies that correspond with the specific functional groups present in the purified single compound are listed along with its peak intensity.

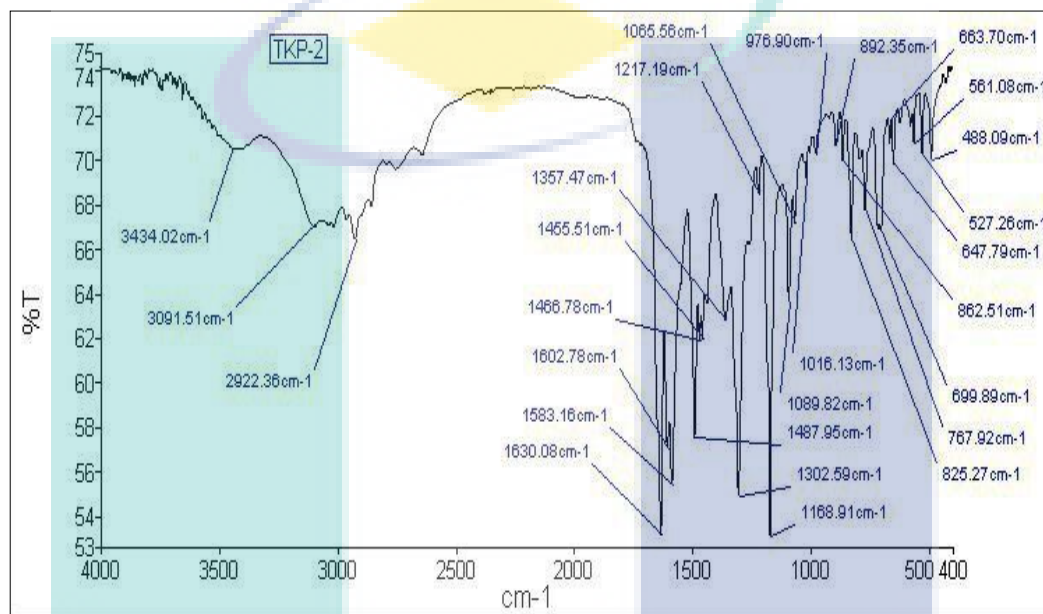


Figure 4.17 FTIR spectrum of purified 5,7-dihydroxyflavanone (5)

From UV-VIS, presence of C=O in the compound is assured. In FTIR, a strong intensity C=O stretch normally falls between the range of 1850 cm⁻¹ to 1630 cm⁻¹ (Pavia et al., 2001). In the FTIR spectrum, the strong C=O stretch is occurred at 1638 cm⁻¹. In UV-VIS part, it is proposed that the extent of conjugation affected the λ_{\max} wavelength. Similarly, in FTIR, the effect of conjugation will decrease the frequency of particular functional group. The presence of this conjugation effect is supported by the occurrence of aromatic C=C stretch that spotted at 1583 and 1488 cm⁻¹. Lampman et al. (2010) said that the C=C aromatic stretch is usually occurring in pair, at 1600 and 1475 cm⁻¹. In addition the aromatic =C-H is occurred at 3091.51 cm⁻¹. Another noticeable functional group present in the isolated compound is the O-H group. An O-H band is a strong and broad peak happens at 3400-3300 cm⁻¹ (Lampman et al. 2010). From the result, O-H occurred as a broad and weak stretch band at 3445 cm⁻¹. Functional group C-O is spotted in the FTIR spectrum as well, which is at 1302 and 1168 cm⁻¹ as presented in Table 4.7.

Table 4.7 Major functional groups present in 5,7-dihydroxyflavanone (5)

Functional group	Wavenumber (cm ⁻¹)	Intensity
O–H	3445	Weak
Aromatic =C–H	3091.51	Medium
C=O	1638	Strong
Aromatic C=C	1583 and 1488	Strong
C–O	1302 and 1168	Strong

4.6.3 ¹H Nuclear Magnetic Resonance for 5,7-dihydroxyflavanone (5)

Table 4.8 listed out the chemical shifts (δ) observed in the ¹H NMR spectrum and the chemical shift is assigned to each proton accordingly. The coupling constant, J is calculated in hertz (Hz). The result is shown in Table 4.2 whereas ¹H NMR spectra. Based on the result tabulated, there are 8 protons with different environment are found in the compound. The assignment for each of the chemical shift to respective protons is by referring to the simplified correlation chart for proton chemical shift attached in Appendix B. One proton singlet is observed at δ 12.06 which is from the 5-OH. At δ 7.46 - 7.49 ppm, multiplet is spotted where this confirmed the presence of non-substituted benzene ring in the structure.

A set of broad singlet at δ 6.02 ppm is assigned to two different protons integration at position H-6 and H-8. In addition, there are two doublet-doublet observed at δ 3.08 ppm ($J = 15.78$ Hz) and δ 2.83 ppm ($J = 3.6$ Hz) attribute to H-3(α) and H-3(β), respectively. Whereas, H-2 attributed to the doublet-doublet at δ 5.43 ($J = 15.6, 3.6$ Hz). However, 7-OH is failed to notice in the ¹H NMR. This may be due to the amount of the compound isolated is not enough.

Table 4.8 ¹H & ¹³C NMR data of compound (5)

Position	¹³ C (δ)	¹ H (δ)	¹ H (m, J/Hz)	Assignment
2	79.22	5.43	(dd, $J = 3.6, 15.6$, 1H)	C2-H
3	43.33	3.08, 2.83	(dd, $J = 3.6, 15.78$, 2H)	C3 α,β -H
4	195.79	-	-	-
5	164.33	-	-	-
6	96.76	6.02	(brs, 1H)	C6-H
7	163.15	-	-	-
8	95.50	6.02	(br s, 1H)	C8-H

Table 4.8 Continued

Position	^{13}C (δ)	^1H (δ)	^1H (m, J/Hz)	Assignment
9	164.70	-	-	-
10	103.18	-	-	-
1'	138.28	-	-	-
2'/6'	126.14	7.46-7.49	(m, 2H)	C2'/6'-H
3'/5'	128.91	7.46-7.49	(m, 2H)	C3'/5'-H
4'	132.13	7.46-7.49	(m, 1H)	C4'-H
5-OH	-	12.06	(brs, 1H)	OH (C5)

4.6.4 Gas Mass Spectrometry Determination of 5,7-dihydroxyflavanone (5)

Figure 4.17 depict the result of mass spectroscopy. The spectrum shows molecular ion peak at 256 m/z with relative abundance as high as 99.9 %. This implies the chemical formula for the isolated compound is $\text{C}_{15}\text{H}_{12}\text{O}_4$.

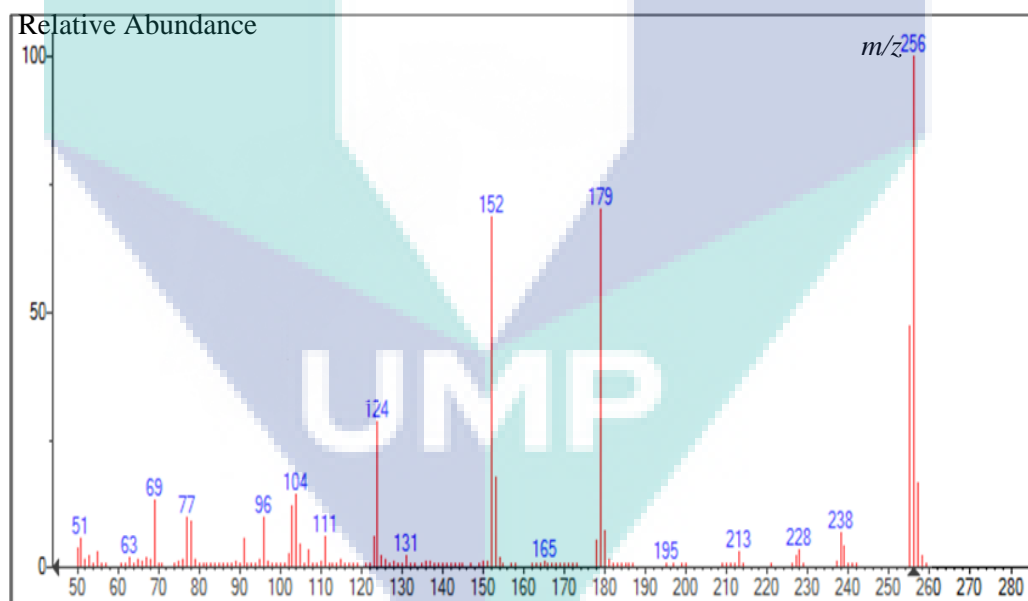


Figure 4.18 Mass spectrum of single pure 5,7-dihydroxyflavanone

By referring and comparing to the result published in Yap et al. (2007) and Tanjung et al. (2013) research, the isolated compound obtained is recognized as 5,7-dihydroxyflavanone (pinocembrin) which have the same MS result showed a base peak of 256 m/z with relative abundance 100%. The structure of 5,7-dihydroxyflavanone is show in Figure 4.18

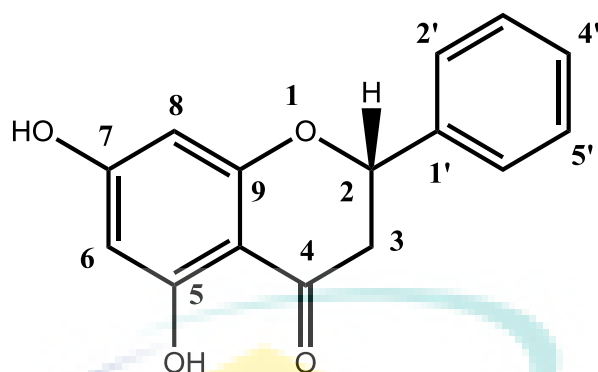


Figure 4.19 Chemical structure of 5,7-dihydroxyflavanone (5).

Apart from the base peak, there is also some others fragments of molecular ion peak at $179\ m/z$ with relative abundance of 69.8 %, $152\ m/z$ relative abundance of 68.5 % and $124\ m/z$ relative abundance of 37.4 %. Peak at $179\ m/z$ is from the molecular $C_9H_7O_4$ ion where this indicated the removal of a phenyl ring (ring B) from the chemical compound. Meanwhile, peak $152\ m/z$ and $124\ m/z$ are resulting from the cleavage of heterocyclic pyran ring (ring C) in the structure.

4.7 Results of Alpinetin (6) Characterization

The physicochemical characterization conducted on alpinetin (6) is carefully discussed in the proceeding sub-sections.

4.7.1 UV-Vis Spectrometry Analysis of Pure Alpinetin (6)

After melting point of the compound is determined, the characterization of the isolated compound is continued with UV-VIS analysis. Figure 4.20 here displays the spectrum of UV-VIS.

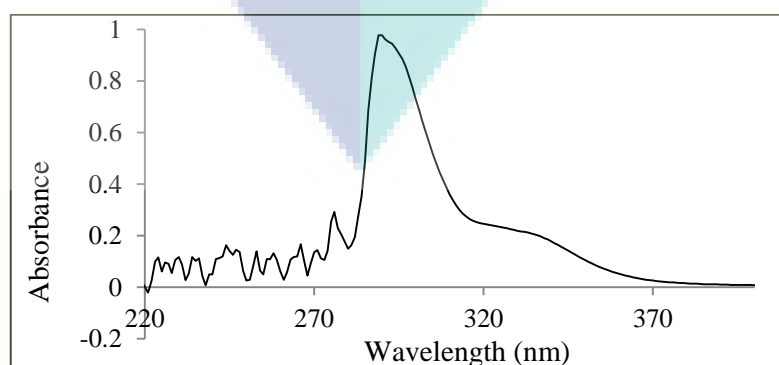


Figure 4.20 UV-VIS spectrum of single alpinetin (6)

Based on the result of UV-VIS, the λ_{max} for purified single compound isolated from polar extracts of BR rhizome is at 289nm. According to Pavia et al. (2001), typical carbonyl chromophore will experience a $n \rightarrow \pi^*$ transition at the range of 280 nm to 290nm. This implies that, the purified compound contains C=O chromophore where a λ_{max} at 289 nm is observed in the UV-VIS spectrum. The λ_{max} of the compound is occurred near the upper range of a C=O chromophore. This might be due to the presence of substituents in the compound, which resulted in a red shift. A red shift is a shift, which affects the absorption band of a chromophore to longer wavelength or lower energy. Other than the presence of substituents caused a red shift, the extent of conjugation in a double bond system also give rise to a red shift.

4.7.2 Functional Group Analysis of Single Pure Alpinetin (6)

KBr pellet method was used to prepare the solid sample for FTIR spectroscopy. Figure 4.22 show the infrared spectrum of transmittance percentage versus wavenumber. The frequencies that correspond with the specific functional groups present in the purified single compound are listed along with its peak intensity in Table 4.9.

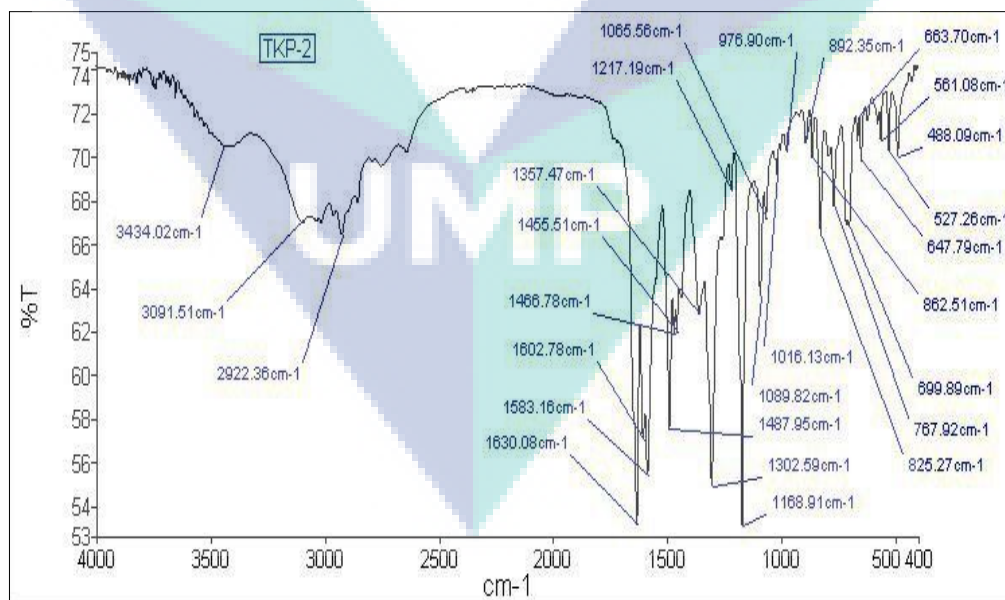


Figure 4.21 FTIR spectrum of purified Alpinetin (6)

Table 4.9 Major functional groups present in Alpinetin (6)

Functional group	Wavenumber (cm^{-1})	Intensity
O–H	3434.02	Weak
Aromatic =C–H	3091.51	Medium
C=O	1630.08	Strong
Aromatic C=C	1602.78 and 1487.85	Strong
C–O	1583.16, 1357.47, 1168.91	Strong

From UV-VIS, presence of C=O in the compound is assured. In FTIR, a strong intensity C=O stretch normally falls between the range of 1850cm^{-1} to 1630cm^{-1} (Pavia et al., 2001). In the FTIR spectrum, the strong C=O stretch is occurred at 1630.08cm^{-1} . In UV-VIS part, it is proposed that the extent of conjugation affected the λ_{max} wavelength. Similarly, in FTIR, the effect of conjugation will decrease the frequency of particular functional group. The presence of this conjugation effect is supported by the occurrence of aromatic C=C stretch that spotted at 1602.78cm^{-1} and 1487.85cm^{-1} .

Lampman et al. (2010) said that the C=C aromatic stretch is usually occur in pair, at 1600cm^{-1} and 1475cm^{-1} . In addition the aromatic =C – H is occurred at 3091.51cm^{-1} . Another noticeable functional group present in the isolated compound is the O–H group. An O–H band is a strong and broad peak happens at $3400\text{--}3300\text{cm}^{-1}$ (Lampman et al. 2010). Form the result, O–H occurred as a broad and weak stretch band at 3434.02cm^{-1} . Functional group C–O is spotted in the FTIR spectrum as well, which is at 1583.16cm^{-1} , 1357.47cm^{-1} , and 1168.91cm^{-1} .

4.7.3 ^1H Nuclear Magnetic Resonance (NMR) of Alpinetin (6)

Table 4.10 listed out the chemical shifts (δ) observed in the ^1H NMR spectrum and the chemical shift is assigned to each proton accordingly. The coupling constant, J is calculated in hertz (Hz).

The result is shown in Table 4.10 whereas ^1H NMR spectra are shown in Appendix C₁-C₆. Based on the result tabulated, there are 8 protons with different environment are found in the compound. The assignment for each of the chemical shift to respective protons is by referring to the simplified correlation chart for proton chemical shift.

Table 4.10 ^1H & ^{13}C NMR data of Alpinetin

Position	^{13}C (δ)	^1H (δ)	^1H (m, J/Hz)	Assignment
2	78.49	5.47	(dd, $J = 3.48, 14.84, 1\text{H}$)	C2-H
3	45.29	3.02	(dd, $J = 14.88, 19.62, 1\text{H}$)	C3 α -H
		2.60	(dd, $J = 19.62, 3.72, 1\text{H}$)	C3 β -H
4	187.82	-	-	-
5	164.72	-	-	-
6	96.08	6.08	(d, $J = 2.52, 1\text{H}$)	C6-H
7	164.81	-	-	-
8	93.80	6.01	(d, $J = 2.52, 1\text{H}$)	C8-H
9	162.66	-	-	-
10	104.94	-	-	-
1'	139.60	-	-	-
2'/6'	126.88	7.60	(d, $J = 8.07, 2\text{H}$)	C2'/6'-H
3'/5'	128.96	7.30-7.42	(m, 2H)	C3'/5'-H
4'	128.78	7.30-7.42	(m, 1H)	C4'-H
5-OCH ₃	56.08	3.74	(s, 3H)	OCH ₃ (C5)

One proton singlet is observed at $\delta 12.18$ which is from the 5-OH. At $\delta 7.42-7.49$ ppm, multiplet is spotted where this confirmed the presence of non-substituted benzene ring in the structure. Two doublets at $\delta 5.99$ and 6.03 ppm are assigned to two different protons at position H-6 and H-8 with $J = 2.5$ Hz and $J = 2.0$ Hz, respectively. In addition, there are two doublet-doublet observed at $\delta 2.82$ ppm ($J = 3.0$ Hz) and $\delta 3.16$ ppm ($J = 12.5$ Hz) attribute to H-3(*cis*) and H-3(*trans*), respectively. Whereas, H-2 attributed to the doublet-doublet at $\delta 5.58$ ($J = 3$ Hz). However, 7-OH is failed to notice in the ^1H NMR. This may be due to the purity of the compound isolated is not high enough. The ORTEP structure of alpinetin (6) is illustrated in Figure 4.23.

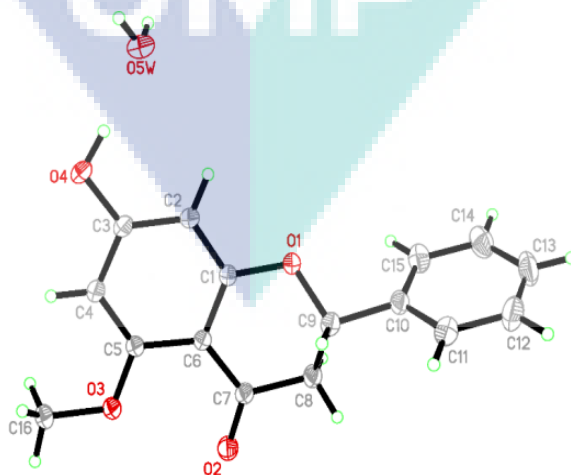


Figure 4.22 ORTEP diagram of alpinetin (6).

Source: Ren-Wang et al., (2001)

4.7.4 Gas Mass Spectrometry Determination of Pure Alpinetin (6)

Figure 4.21 depict the result of mass spectroscopy. The spectrum shows molecular ion peak at 256 m/z with relative abundance as high as 99.9 %. This implies the chemical formula for the isolated compound is $C_{15}H_{12}O_4$. By referring and comparing to the result published in Yap et al. (2007) and Tanjung et al. (2013) research, the isolated compound obtained is recognized as 5-methoxy-7-hydroxyflavanone 5,7-dihydroxyflavanone (pinocembrin) which have the same MS result showed a base peak of 256 m/z with relative abundance 100%.

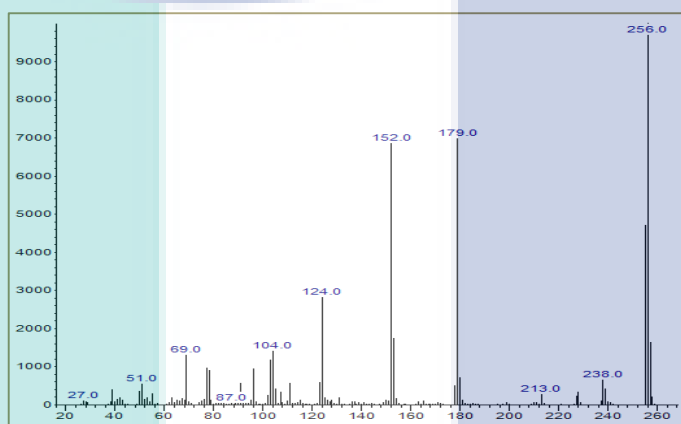


Figure 4.23 Spectrum of compound Alpinetin

Apart from the base peak, there is also some others fragments of molecular ion peak at 179 m/z with relative abundance of 69.8 %, 152 m/z relative abundance of 68.5 % and 124 m/z relative abundance of 37.4 %. Peak at 179 m/z is from the molecular $C_9H_7O_4$ ion where this indicated the removal of a phenyl ring (ring B) from the chemical compound. Meanwhile, peak 152 m/z and 124 m/z are resulting from the cleavage of heterocyclic pyran ring (ring C) in the structure.

4.8 Results of Flavokawain B (FKB) (7)

Chalcone FKB was synthesized 2'-hydroxy-4',6'-dimethoxyacetophenone (1.00 mmol) and 4-hydroxybenzaldehyde (1.00 mmol) diluted in 5 mL MeOH, catalysed by 40% KOH and stirred at room temperature for 48 hr, gave product after purification by silica gel column chromatography, (*E*)-1-(2'-hydroxyl-4',6'-dimethoxyphenyl)-3-(4-methoxyphenyl)prop-2-en-1-one (**7**) (72.5%) (109-110°C) (Boeck et al., 2006) as yellow flat crystal shaped.

4.8.1 UV-Vis Spectrometry Analysis of Pure FKB (7)

Compound **7** absorbed UV light in the wavelength range of 290-405 nm, which corresponded to the conjugated α,β -unsaturated carbonyl (C=O) chromophore (Jing et al., 2011). Figure 4.24 shows the UV-Visible spectrum of compound **7** with maximum absorption observed at wavelength, λ_{max} of 364-365 nm.

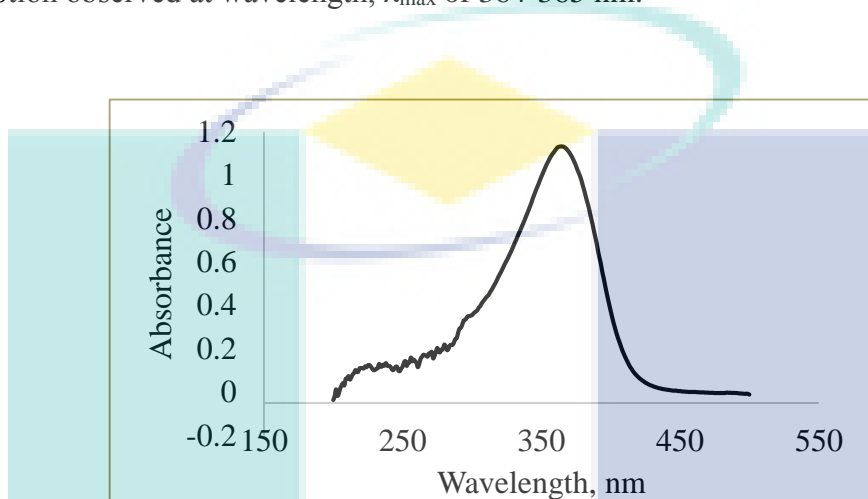


Figure 4.24 UV spectrum of FKP (7)

4.8.2 Functional Group Analysis of FKB (7)

IR spectrum of compound **5** shown in Figure 4.25 shows the absorption bands at 3389 cm^{-1} and between $2860\text{--}3006\text{ cm}^{-1}$, which corresponded to hydroxyl (O-H) group and aromatic C-H stretch, respectively. The absorption bands at 1603 cm^{-1} and $1426\text{--}1513\text{ cm}^{-1}$ corresponded to carbonyl (C=O) group and aromatic ring C=C, respectively.

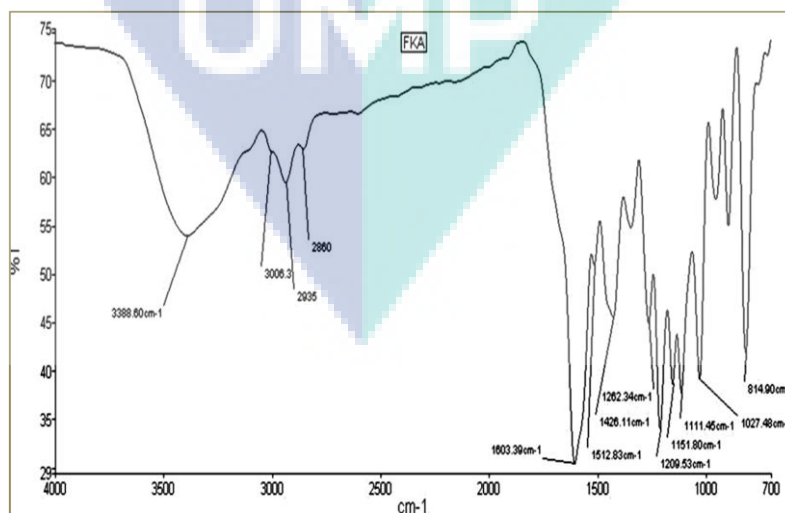


Figure 4.25 IR spectrum of pure (FKB)

4.8.3 ^1H Nuclear Magnetic Resonance (NMR) of FKB (7)

The ^1H -NMR spectrum (600 MHz, CDCl_3) of compound **7** shown in Figure 4.26 shows that a signal appeared as doublet at δ 6.09 (d, $J = 2.40$ Hz), and assigned to the C-3' proton.

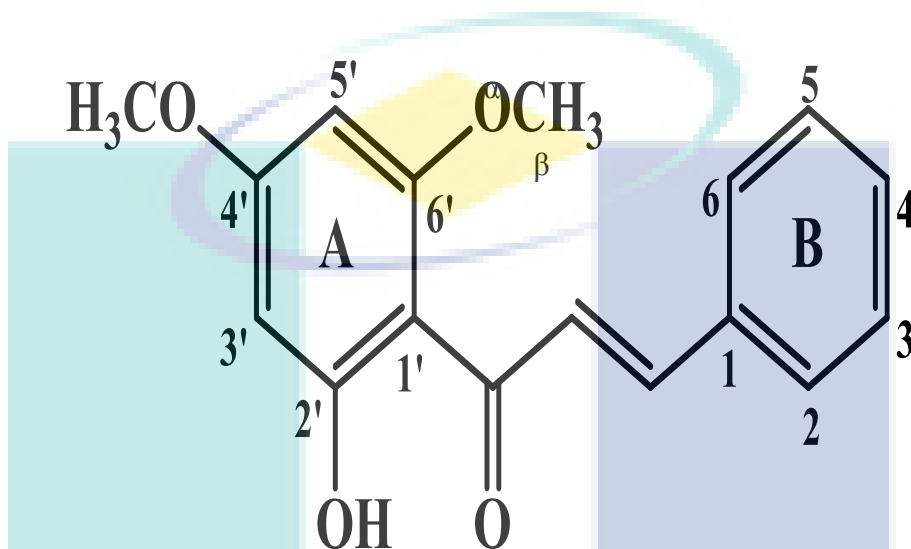


Figure 4.26 Structure pure FKB (7).

A doublet appeared at 5.94 (d, $J = 2.40$ Hz) and was assigned to the C-5' proton. Two doublets appeared at 7.56 (d, $J = 8.76$ Hz) and 7.54 (d, $J = 8.76$ Hz) were assigned to the C-2 and C-6 proton, respectively. Another doublet appeared at 6.92 (d, $J = 8.70$ Hz) and 6.91 (d, $J = 8.70$ Hz) were assigned to the C-3 and C-5 proton, respectively. Three signals of singlet that appeared at 3.82 (s, 3H), 3.84 (s, 3H) and 3.90 (s, 3H) were assigned to the methoxy protons at C-4' and C-6', respectively.

A signal of doublet which appeared at 7.78 (d, $J = 15.48$ Hz) was assigned to proton α -carbon and a doublet at 7.79 (d, $J = 15.48$ Hz) was assigned to proton β -carbon. A downfield singlet that appeared at 14.45 was assigned to the C-2' hydroxyl proton chelated to carbonyl group, which data is supported by previous journal (Abu et al., 2014). The details of ^1H -NMR and ^{13}C -NMR spectra are shown in Table 4.11.

Table 4.11 NMR data of pure FKB (7)

Carbon	¹³ C (δ)	¹ H (δ)	Multiplicity	Designation
1'	130.10	-	-	-
2'	168.70	-	-	-
3'	93.56	6.09	(d, <i>J</i> = 2.40 Hz, 1H)	C3'-H
4'	166.20	-	-	-
5'	91.40	5.94	(d, <i>J</i> = 2.40 Hz, 1H)	C5'-H
6'	163.10	-	-	-
1	127.50	-	-	-
2	130.10	7.56	(d, <i>J</i> = 8.76 Hz, 1H)	C2-H
3	114.30	6.92	(d, <i>J</i> = 8.70 Hz, 1H)	C3-H
4	160.90	-	-	-
5	114.30	6.91	(d, <i>J</i> = 8.70 Hz, 1H)	C5-H
6	130.10	7.54	(d, <i>J</i> = 8.76 Hz, 1H)	C6-H
α	125.40	7.78	(d, <i>J</i> = 15.48 Hz, 1H, H-α)	Cα-H
β	141.60	7.79	(d, <i>J</i> = 15.48 Hz, 1H, H-β)	Cβ-H
OCH ₃	55.79	3.84	(s, 3H)	OCH ₃ (C4')
OCH ₃ (C6')	55.53	3.90	(s, 3H)	OCH ₃ (C6')
OH (C2')	-	14.45	(s, 1H)	OH (C2')
C=O	192.60	-	-	-

4.9 Cytotoxic Effects on Colon H-29 and Breast MDA-MB-231 Cancer Cell Line

The half-inhibitory concentration (IC₅₀) values were also estimated and a bar chart (Figure 4.29, and 4.30) of the percentage of cell viability versus concentration of compounds was constructed from Table 4.12. Compound 2 and 3 showed good cytotoxicity on both cancer cell lines as compared to cisplatin (6.73 ± 0.30 IC₅₀ µg/mL) and (6.02 ± 0.54 µg/mL), while the other compounds exhibited more than 100 µg/mL.

Table 4.12 IC₅₀ values of 1-6 and Flavokavain B types against H-29 and MDA-MB-231 cell lines.

Compound	IC ₅₀ values (µg/mL)	
	H29	MDA-MB-231
1	>100	>100
2	22.51 ± 0.42	(20.42 ± 2.23)
3	(4.44 ± 0.66)	(5.62 ± 0.61)
4	>100	>100
5	>100	>100
6	>100	>100
FKB	(6.50 ± 0.40)	(9.60 ± 0.52)

Compound **2** and **3** (Figure 4.27) showed good cytotoxicity on both cancer cell lines as compared to cisplatin (6.73 ± 0.30 IC₅₀ $\mu\text{g/mL}$) and (6.02 ± 0.54 $\mu\text{g/mL}$), while the other compounds exhibited more than 100 $\mu\text{g/mL}$. Figure 4.29 and 4.30 showed the IC₅₀ values of flavokawain B type chalcone against H-29 and MDA-MB-231.

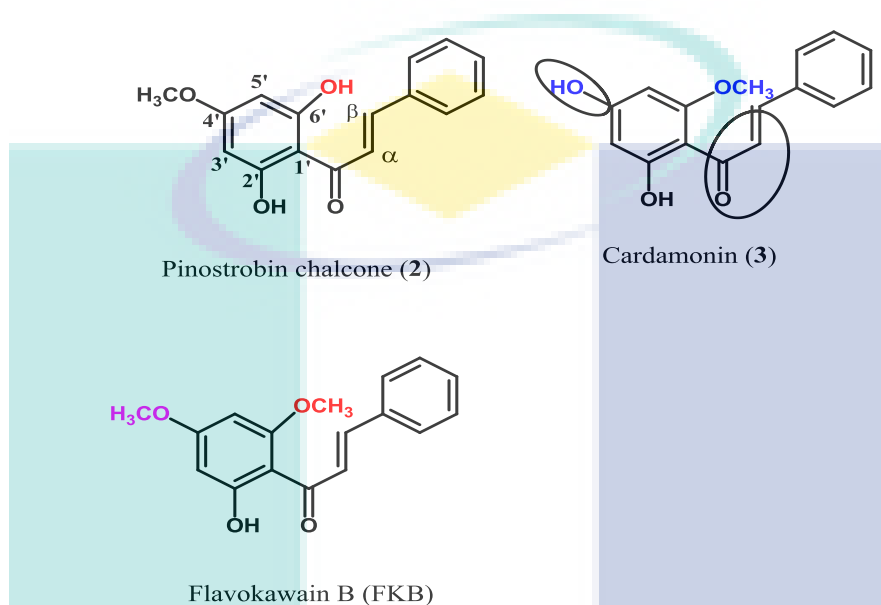


Figure 4.27 Structure of compound **2**, **3** and **4**

It is well established that chalcones exhibiting potential anticancer properties because of the presence of α,β -unsaturated ketone moiety in the skeleton. Among the tested chalcones, the 2' hydroxyl group in ring A is an essential against several biological assays predominantly anticancer properties. The presence of electron-withdrawing and electron-donating groups effects on α,β -unsaturated system which eventually effects on the cytotoxic properties. Generally, the electron-donating in ring A improved the cytotoxic properties as it effects acidity of 2' hydroxyl group in ring A.

While compounds **1**, **4**, **5**, **6** did not showed the significant activity against colon cancer cell lines H-29 and breast cancer cell lines MDA-MB-231 (Figure 4.28). Compound **2** and **3** are chalcones, while other compounds are flavonoids in nature. Chalcones are bioactive compounds, which could be possibly assumed the effects of electron-effect on the α, β -unsaturated. In this way, α, β -unsaturated system become more nucleophile and Michael receptor or protein bind effectively thus activity is increase. However, compounds **2** and **3** showed the slightly better activity because selective position of methoxy groups at 2 and 6 (Figure 4.29).

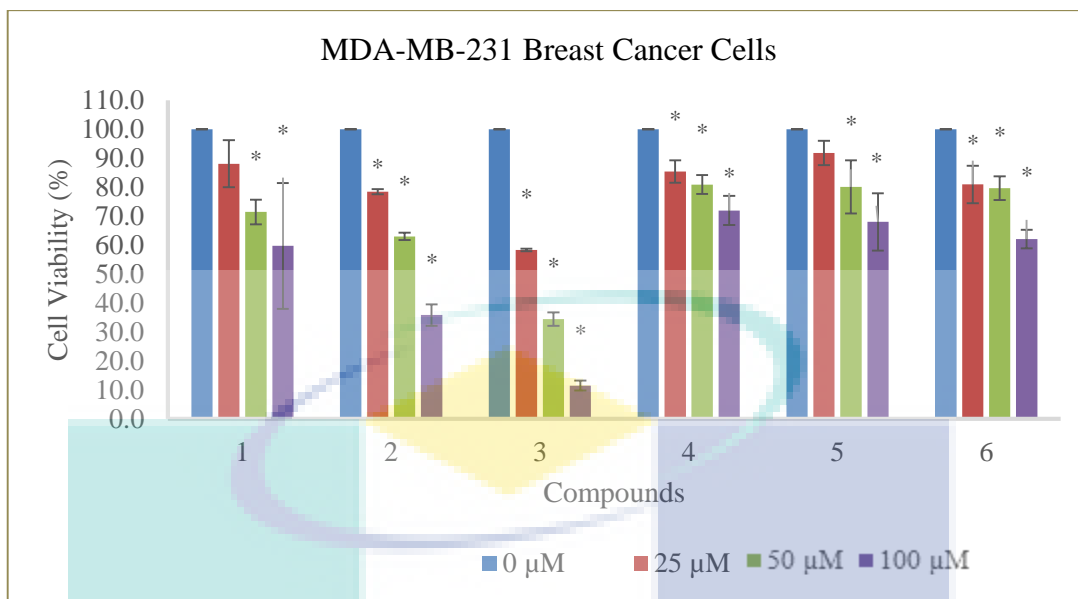


Figure 4.28 Effect of natural compounds on the viability of MDA-MB-231 breast cancer cell line at 48 hours as determined by MTT assay. Each data point represents the mean of two independent experiments \pm SD. *significantly different from the control ($p < 0.05$).

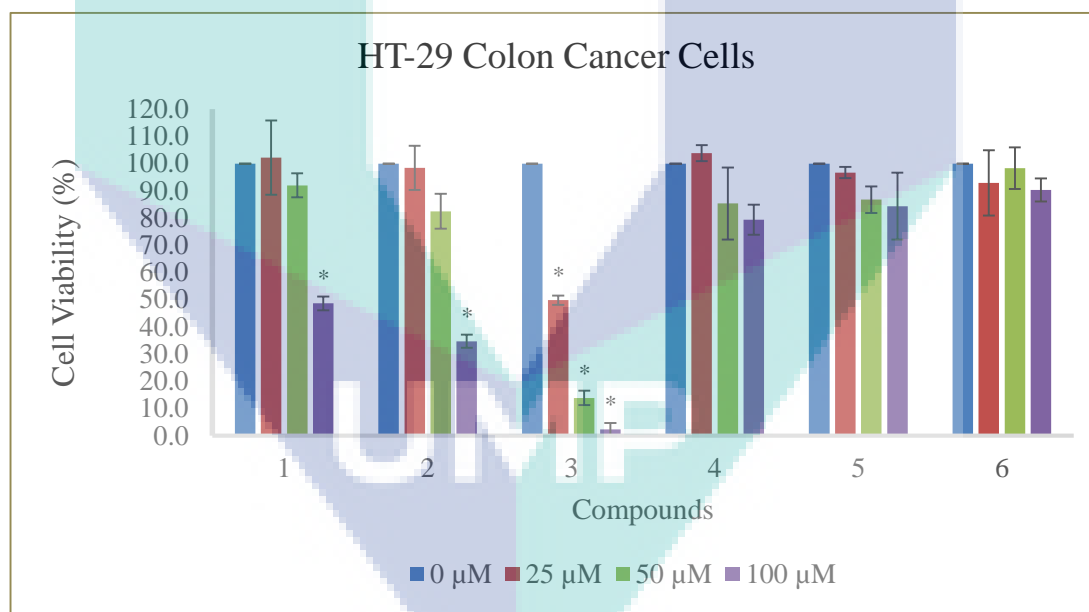


Figure 4.29 Effect of natural compounds on the viability of HT-29 colon cancer cell line at 48 hours as determined by MTT assay. Each data point represents the mean of two independent experiments \pm SD. *significantly different from the control ($p < 0.05$).

4.10 Results of Molecular Docking Studies

The biological spectrum of the selected compounds 2, 3, and FKB was predicted using the PASS online server. The prediction of the activity value was set to 0.7, and the results were analysed critically to comprehend the observed anticancer activity of the compounds. The results of PASS prediction were found to be consistent with the previous studies, which highlight, anti-leukemic, anti-inflammatory, and antibacterial activity of these compounds. Furthermore, the PASS online server highlight that the observed anticancer activity of these compounds could be attributed to their activity as the caspase-3 stimulant, and JAK2 expression inhibitors.

Herein, we have carried out molecular docking studies to predict the likely binding mode of the active compounds of the series within the binding site of the human Janus Kinase. The results of the docking studies suggest that all the compounds present similar binding profile with hydrogen bonding interactions mediated by the methoxy and hydroxyl groups. The hydrogen bond is presented as yellow dashed lines. The residues involved in interaction are depicted as sticks. The images were rendered using the Pymol-Educational Use Only version. The presence of OH group at position 3 allowed compound 2 to mediate hydrogen bonding interaction with Asn859 (Figure 4.30).

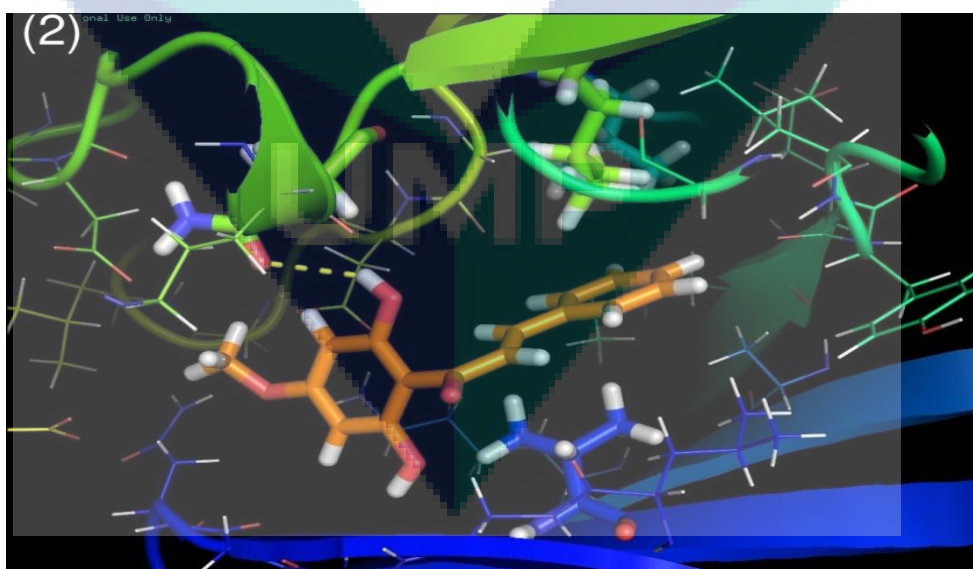


Figure 4.30 The simulated binding mode of the pinostrobin chalcone (2) in the active site of Human Janus Kinase.

However, switching the position of the moieties resulted in a slightly different binding mode of compound 3, in which the two hydroxyl groups are involved in hydrogen bonding interactions with the residues Asn859, Asp976 and Asn981 (Figure 4.31).

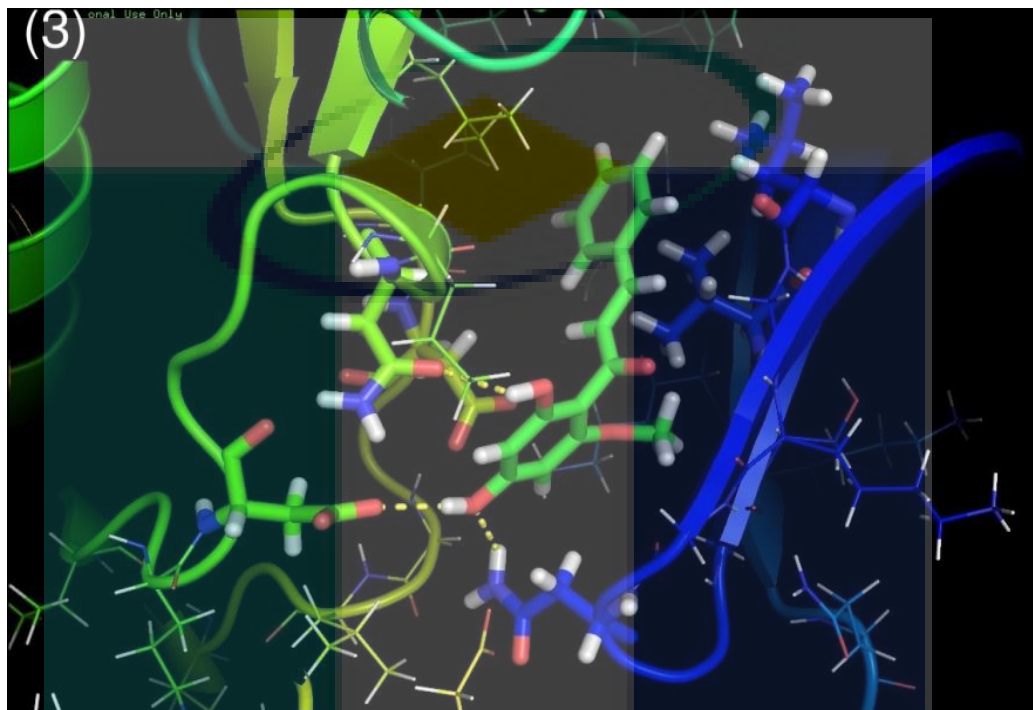


Figure 4.31 The simulated binding mode of the cardamonin (3) in the active site of Human Janus Kinase.

As already mentioned in SAR of FKB, which lacks the OH at position 4, demonstrate only polar interactions with the Val863. Both the methoxy groups of the compound were not involved in any interaction, which explains the relatively compromised activity of FKB when compared to the compound 3 (Figure 4.32). The evidence underpins the importance of the hydroxyl group in the observed anticancer activity of the compounds.

Further, all the three compounds anchored to the active site via hydrophobic interactions mediated by their aromatic ring system. The benzene was found to complement the surrounding hydrophobic residues; making hydrophobic interactions with the Val863, Ala880, Leu983, and Asp994.

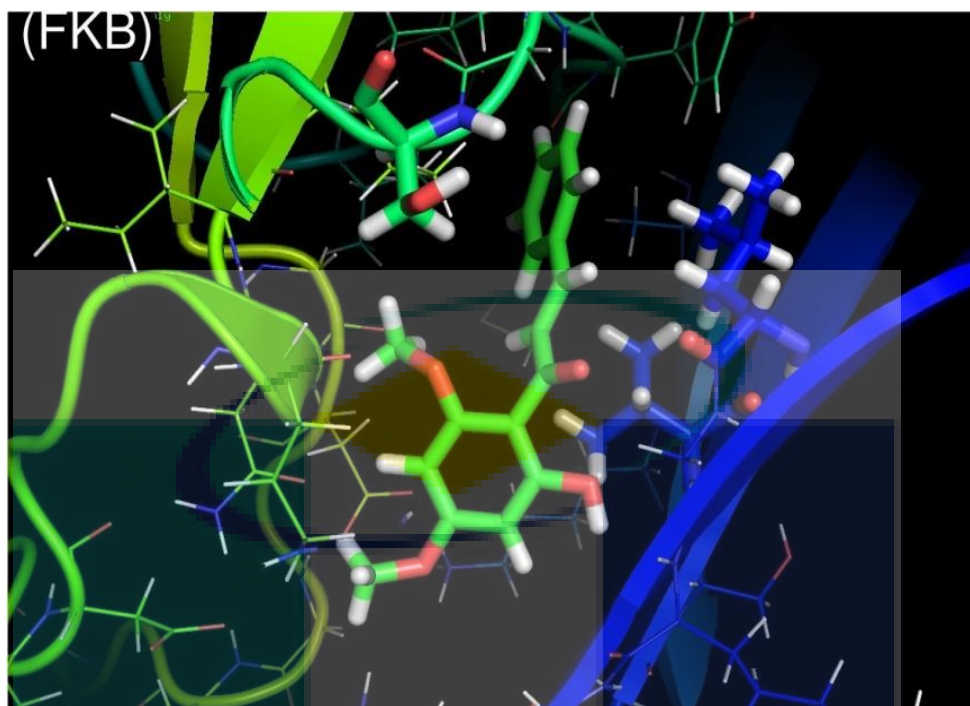


Figure 4.32 The simulated binding mode of the flavokawain B, (FKB) in the active site of Human Janus Kinase.

UMP

CHAPTER 5

CONCLUSION

5.1 Conclusion

As the conclusion, six natural and one synthetic compound flavokawain B were presented in the current studies. The flavokawain B synthesized by Claisen-Schmidt condensation reaction using 2'-hydroxy-4',6'-dimethoxyacetophenone reacted with benzaldehydes and purified by column chromatography. The compounds were elucidated by using different spectroscopic techniques such as UV-Vis, FTIR, GC-MS, NMR and single X-ray crystallography. All compounds were tested for their cytotoxicity against colon cancer H-29 and human breast cancer MDA-MB-231 breast cancer cell lines. Among the natural compounds, pinostrobin chalcone (**2**), caradamonin (**3**) and chalcone derivatives FKB were found to be significant cytotoxic activity against H29 and human breast cancer MDA-MB-23 cell lines. Pinostrobin chalcone (**2**), caradamonin (**3**) exhibited (22.51 ± 0.42 IC₅₀ $\mu\text{g/mL}$) and (20.42 ± 2.23 $\mu\text{g/mL}$), respectively.

The naturally occurring synthetic chalcone flavokawain B (FKB) showed the (6.50 ± 0.40 IC₅₀ $\mu\text{g/mL}$) and (9.60 ± 0.52 $\mu\text{g/mL}$) against H29 and human breast cancer MDA-MB-23 cell lines. So the role of methoxy group in all three compounds is important. Over all the compound **2**, **3** and FKB showed good cytotoxicity on both cancer cell lines as compared to cisplatin (6.73 ± 0.30 IC₅₀ $\mu\text{g/mL}$) and (6.02 ± 0.54 $\mu\text{g/mL}$), while the other compounds exhibited more than 100 $\mu\text{g/mL}$.

The objectives of this work have been largely achieved and the results showed a synergistic correlation among the extraction process, isolation of bioactive compounds, physicochemical characterization of isolated compounds, anti-cancer activities and established a structure-activity relationship of the bioactive compounds using molecular docking.

5.2 Recommendation

Based on the results extraction process, isolation of bioactive compounds, physicochemical characterization, cytotoxic assay activities molecular docking studies, it is suggested that the following recommendations be carried out for any future work:

- i. It is recommended to focus on compound 2 and 3 due to their good anti-cancer activity against breast cancer cell line. It also recommended to conduct the cytotoxicity test by MTT assay using tamoxifen as the positive control and to perform the cytotoxicity test on normal breast cell line to check the compound selectivity. The study of structure-activity relationship between the compound derivatives and anti-cancer activity should be more detail.
- ii. The compound pinostrobin chalcone (2), caradamonin (3) and naturally chalcone derivatives FKB were found to be significant cytotoxic activity against H29 and human breast cancer MDA-MB-23 cell lines. So in future synthetic derivatives based on pinostrobin chalcone (2), caradamonin (3) and chalcone derivatives FKB could be obtained and investigate on different cancer cell lines.



UMP

REFERENCES

- Abdelwahab, S. I. (2013). In vitro inhibitory effect of *Boeserngin A* on human acetylcholinesterase: Understanding its potential using in silico ADMET studies”, *Journal of Applied Pharmaceutical Science*, 3 (3), 30-35.
- Ackerknecht, E.H., (1973). *Therapeutics: from the Primitives to the Twentieth Century*. Hafner Press, New York.
- Agarwal S, Chadha D, Mehrotra R (2015) Molecular modeling and spectroscopic studies of semustine binding with DNA and its comparison with lomustine–DNA adduct formation. *J Biomol Struct Dyn* 33: 1653-1668.
- Aishwarya, S. (2017). Therapeutic Effects of *Boesenbergia rotunda*, 6(8), *International Journal of Science and Research*, 6(8), 1323-1327.
- Alara, O. R. *et al.* (2017). Effect of drying methods on the free radicals scavenging activity of *Vernonia amygdalina* growing in Malaysia’, *Journal of King Saud University - Science*. doi: 10.1016/j.jksus.2017.05.018.
- Atun, S., Handayani, S. and Frindryani, L. F. (2017). Identification and antioxidant activity test of bioactive compound produced from ethanol extract of temukunci (*Boesenbergia rotunda*). *AIP Conference Proceedings*, 1868, 1-7.
- Ayoola, G. *et al.* (2008). Phytochemical Screening and Antioxidant Activities of Some Selected Medicinal Plants Used for Malaria Therapy in Southwestern Nigeria. *Tropical Journal of Pharmaceutical Research*, 7(3), 1019–1024.
- Badwaik, L. S., Borah, P. K. and Deka, S. C. (2015). Optimization of Microwave Assisted Extraction of Antioxidant Extract from *Garcinia pedunculata* Robx. *Separation Science and Technology*, 50(12), 1814–1822.
- Barnes J., Anderson L.A., Phillipson J.D., (2007). *Herbal medicine*. 3rd Edition, *Pharmaceutical Press*, London. 1-23.
- Baquar S.R., (1995). The Role of Traditional Medicine in Rural Environment, In: *Traditional Medicine in Africa*, Issaq, S. (Editor), East Africa Educational Publishers Ltd. Nairobi, 141-142.
- Bhamarapravati S., Chaiprasong M., Laotavornkijkul C., Dancharoenkij A., Reutrakul V., (2000). Antidermatophytic compound from the root of *Boesenbergia rotunda* (L.) Mansf. A validation of a local wisdom in Thai traditional medicine. *Proceedings of the TRF First Postdoctoral Research Conference*, 28-30, 209-212.
- Bhamarapravati S., Mahady G.B., Pendland S.L., (2003). In Vitro Susceptibility of *Helicobacter pylori* to Extracts from the Thai Medicinal Plant *Boesenbergia rotunda* and Pinostrobin. *Proceedings of the 3rd World Congress on Medicinal and Aromatic Plants for Human Welfare*, Chiang Mai Thailand, 521.

- Bhamarapavati S., Juthapruth S., Mahachai W., Mahady G., (2006). Antibacterial activity of *Boesenbergia rotunda* (L.) Mansf. and *Myristica fragrans* Houtt. Against *Helicobacter pylori*. *Nutraceutical and Functional Food*, 1,28.
- Boonjaraspinyo S., Boonmars T., Aromdee C., Kaewsamut B. Effect of fingerroot on reducing inflammatory cells in hamster infected with *Opisthorchis viverrini* and N-nitrosodimethylamine administration. *Parasitology Research*, 106, 1485-1489, 2010.
- Bruker (2012). *Bruker AXS Inc., Madison. Wisconsin, USA.*
- Chatsumpun, N., Sritularak, B. and Likhitwitayawuid, K. (2017). New Biflavonoids with α -Glucosidase and Pancreatic Lipase Inhibitory Activities from *Boesenbergia rotunda*. *Molecules*, 22(11), 862.
- Cheenpracha S., Karalai C., Ponglimanont C., Subhadhirasakul S., Tewtrakul S. Anti-HIV-1 protease activity of compounds from *Boesenbergia pandurate*. *Bioorganic & Medicinal Chemistry*, 14, 1710–1714, 2006.
- Ching A.Y.L., Tang S.W., Sukari M.A., Lian G.E.C., Rahmani M., and Khalid K., (2007). Characterization of flavonoid derivatives from *Boesenbergia rotunda* (L.). *The Malaysian Journal of Analytical Sciences*, 11(1), 154–159.
- Cosa, P., Vlietinck, A.J., Berghe, D.V., Maes, L. (2006). Anti-infective potential of natural products: How to develop a stronger in vitro 'proof-of-concept'. *Journal of Ethnopharmacology* 106, 290–302.
- Cuvelier, M. E. and Berset, C. (1995) 'Use of a Free Radical Method to Evaluate Antioxidant Activity. *Antioxidants*, 30, 25–30.
- Eikani, M. H. *et al.* (2013) 'An Experimental Design Approach for Pressurized Liquid Extraction from Cardamom Seeds', *Separation Science and Technology*, 48(8), 1194-1200.
- Eng-Chong T., Yean-Kee L., Chin-Fei C., Choon-Han H., Sher-Ming W., Thio Li-Ping C., Gen-Teck F., Khalid N., Abd Rahman N., Karsani S. A., Othman S., Othman R., Yusof R. (2012). *Boesenbergia rotunda*: From Ethnomedicine to Drug Discovery. *Evidence-Based Complementary and Alternative Medicine*, 1-26, 345-350.
- Fabricant, D.S. and Farnsworth, N.R. (2001). The value of plants used in traditional medicine for drug discovery. *Environ. Health Perspective*. 109, 69–75.
- Ghasemzadeh, A. and Ghasemzadeh, N. (2011). Flavonoids and phenolic acids : Role and biochemical activity in plants and human. *Basic structure of flavonoids*. 5(31), 6697-6703.
- Halliwell, B. (2001). Free Radicals and other reactive species in Disease. *Radicals*, 3,1-7.

- Hansel R., Weiss D. and Schmidt B. (1968). Kawalaktone; Kettenlage und fungistatische Wirkung, Mitt. Über Inhaltsstoffe aus Piper-Artern. *Archive der Pharmazie*, 301, 369-373.
- Haroune, L. (2015). Liquid chromatography-tandem mass spectrometry determination for multiclass pesticides from insect samples by microwave-assisted solvent extraction followed by a salt-out effect and micro-dispersion purification. *Analytica Chimica Acta*, 891,160-170.
- He X., Lin L. and Lian J. (1997). Electrospray high performance liquid chromatography mass spectrometry in phytochemical analysis of kava (*Piper methysticum*) extract. *Planta Medica*, 63, 70-74.
- Huie, C.W. (2002). A review of modern sample-preparation techniques for the extraction and analysis of medicinal plants. *Analytical Bioanalytical Chemistry*, 373, 23-30.
- Hwang J.-K., Shim J.-S., Chung J.-Y. (2004). Anticariogenic activity of some tropical medicinal plants against *Streptococcus mutans*. *Fitoterapia* 75, 596-598.
- Ibrahim, H, Nugroho, A. *Boesenbergia rotunda* (L.) Mansfeld. In: de Guzman CC, Siemonsma J. (1999). Plant resources of South-East Asia 13. Spices. Leiden: *Backhuys* ,8, 83-85.
- Ibrahim B. J., Basni I., A. S. N. M Ahmad, A. Ali, Ahmad, A. R. and Ibrahim, H. (2001). Constituents of the rhizome oils of *Boesenbergia pandurata* (Roxb.) Schlecht from Malaysia, Indonesia and Thailand. *Flavour and Fragrance Journal*, 16, (2), 110–112.
- Isa, N.M., Abdelwahab, S.I., Mohan, S., Abdul, A.B., Sukari, M.A., Taha, M.M.E., Syam, S., Narrima, P., Cheah, S.C., Ahmad, S. and Mustafa, M.R. 2012. In vitro anti-inflammatory, cytotoxic and antioxidant activities of boesenbergia A, a chalcone isolated from *Boesenbergia rotunda* (L.) (fingerroot). *Brazilian Journal of Medical and Biological Research*, 45(6), 524-530.
- Jaipetch, T., Kanghae, S., Pancharoen, O., Patrick, V.A., Reutrakul, V., Tuntiwachwuttikul, P., and White, A. H. (1982). Constituents of *Boesenbergia pandurata* (syn. *Kaempferia pandurata*) : Isolation, Crystal Structure and Synthesis of (\pm)-Boesenbergin A. *Australian Journal of Chemistry*. 35, 351-361.
- Jeon, J. S. *et al.* (2016). Simultaneous Detection of Glabridin, (-)- α -Bisabolol, and Ascorbyl Tetraisopalmitate in Whitening Cosmetic Creams Using HPLC-PAD. *Chromatographia*, 79 (13-14), 851-860.
- Jing L. J., Abu Bakar M. F., Mohamed M., Rahmat A., (2011) Effects of Selected *Boesenbergia* Species on the Proliferation of Several Cancer Cell Lines, *Journal of Pharmacology and Toxicology* 6 (3), 272-282.

- Kiat T.S., Phippen R., Yusof R., Ibrahim H., Khalid N., Rahman N.A., (2006). Inhibitory activity of cyclohexenyl chalcone derivatives and flavonoids of fingerroot, *B. rotunda* (L.), towards dengue-2 virus NS3 protease. *Bioorganic. Medicinal Chemistry. Letters*, 16, 3337-3340.
- Kim D., Lee M.-S., Jo K., Lee K.-E., Hwang J.-K. (2011). Therapeutic potential of panduratin A, LKB1-dependent AMP-activated protein kinase stimulator, with activation of PPAR α/δ for the treatment of obesity. *Diabetes, Obesity and Metabolism*, 13, 584-593.
- Kirana C., Jones G.P., Record I.R., McIntosh G.H., (2007). Anticancer properties of panduratin A isolated from *B. pandurata* (Zingiberaceae). *Journal of Natural Medicine*, 61, 131-137.
- Koppel C. and Tenczer J. (1991) Characterization of urinary metabolites of D, L-kavain. *Journal of Chromatography*, 591, 207-211.
- Kress, W.J., DeFilipps, R.A., Farr, E. & Kyi, Y.Y. (2003). A checklist of the trees, shrubs, herbs and climbers of Myanmar. *Contr. U.S. National Herbs*, 45, 1-590.
- Kunle, Folashade O., Egharevba, Omoregie H. and Ochogu A.P, (2012). *International Journal of Biodiversity and Conservation*. 4(3), 101-112.
- Lampman, G. M., Pavia, D. L., Kriz, G. S., and Vyvyan, J. R. 2010. *Spectroscopy*. (4th ed.). Belmont, CA: Brooks/Cole Cengage Learning. 3453,7543-7559.
- Mahmood A. A., Mariod A.A., Siddig Ibrahim Abdelwahab S.I., Ismail S., and Al-Bayaty F. (2010). Potential activity of ethanolic extract of *Boesenbergia rotunda* (L.) rhizomes extract in accelerating wound healing in rats. *Journal of Medicinal Plants Research*, 4(15), 1570-1576.
- Mageed, (2000). The medicinal uses of pepper'. *International Pepper News*, 25(1), 1-9.
- Morikawa T., Funakoshi K., Ninomiya K., Yasuda D., Miyagawa K., Matsuda H., Yoshikawa M. (2008). Structures of New Prenylchalcones and Prenylflavanones with TNF- α and Aminopeptidase N Inhibitory Activities from *Boesenbergia rotunda*. *Chemical Pharmacy Bulletin*. 56(7), 956-962.
- Pavia, D. L., Lampman, G. M., and Kriz, G. S. (2001). *Introduction to Spectroscopy*. 3rd ed. Bellingham, Washington: Brooks Cole.
- Phongpaichit S., Subhadhirasakul S., Wattanapiromsakul C. (2005). Antifungal activities of extracts from Thai medicinal plants against opportunistic fungal pathogens associated with AIDS patients. *Mycoses*, 48, 333-338.
- Ren-Wang J., Zhen-Dan H., P.Pui-Hay B., Yiu-Man C., Shuang-Cheng M., Mak, T. C. W. (2001). New Antiviral Cassane Furanoditerpenes from *Caesalpinia minax*. *Chemica. Pharmacy. Bulletin*, 49, 1166.

- Rohs R, Bloch I, Sklenar H, Shakked Z (2005) Molecular flexibility in ab-initio drug docking to DNA: binding-site and binding-mode transitions in all-atom Monte Carlo simulations. *Nucl Acids Res* 33: 7048-7057.
- Rho H.S., Ghimeray A.K., Yoo D.S., Ahn S.M., Kwon S.S., Lee K.H., Cho D.H., and Cho J.Y., (2011). Kaempferol and kaempferol rhamnosides with depigmenting and anti-inflammatory properties. *Molecules*, 16(4), 3338-3344.
- Rukayadi Y., Han S., Yong D., Hwang J.-K. (2010). In Vitro Antibacterial Activity of Panduratin A against Enterococci Clinical Isolates. *Biological Pharmacy Bulletin*, 33(9), 1489-1493.
- Salama S.M., Bilgen M., Al Rashdi A.S., and Abdulla M.A., (2012). Efficacy of *Boesenbergia rotunda* Treatment against Thioacetamide-Induced Liver Cirrhosis in a Rat Model. *Evidence-Based Complementary and Alternative Medicine*, 20(12), 137083.
- Saralamp P., Chuakul W., Temsiririrkkul R., Clayton T., (1996). *Medicinal Plants in Thailand*, , Amarin Printing and Publishing Public Co., Ltd., Bangkok, 1, 49.
- Sasidharan S., Chen Y., Saravanan D., Sundram K.M., Yoga Latha L., (2011). Extraction, isolation and characterization of bioactive compounds from plants' extracts. *African Journal of Traditional, Complementary and Alternative Medicines*, 8(1), 1-10.
- Sawangjaroen N., Subhadhirasakul S., Phongpaichit S., Siripanth C., Jamjaroen K., Sawangjaroen K. (2005). "The in vitro anti-giardial activity of extracts from plants that are used for self-medication by AIDS patients in southern Thailand. *Parasitology Research*, 95, 17-21.
- Sahin U. (2017). Personalized RNA mutanome vaccines mobilize poly-specific therapeutic immunity against cancer. *Nature*, 547(7662), 222-226.
- Seeliger D, de Groot BL (2010) Ligand docking and binding site analysis with PyMOL and Autodock/Vina. *J Comput Aided Mol Des* 24: 417-422.
- Shan, T. C., Al Matar, M., Makky, E. A., & Ali, E. N. (2017). The use of *Moringa oleifera* seed as a natural coagulant for wastewater treatment and heavy metals removal. *Applied Water Science*, 7(3), 1369-1376.
- Sheldrick, G. M. (2008). *A short history of SHELX*, A64, 112–122.
- Shim, J.S., Kwon, Y.Y., Han, Y.S. and Hwang, J.K. 2008. Inhibitory effect of panduratin A on UV-induced activation of mitogen-activated protein kinases (MAPKs) in Dermal Fibroblast Cells. *Plant Medica*, 74(12), 1446-1450.
- Shim, J. S., Han, Y.S. and Hwang, J.K. 2009. The effect of 4-hydroxypanduratin A on the mitogen-activated protein kinase-dependent activation of matrix metalloproteinase-1 expression in human skin fibroblasts. *Journal of Dermatological Science* ,53, 129-134.

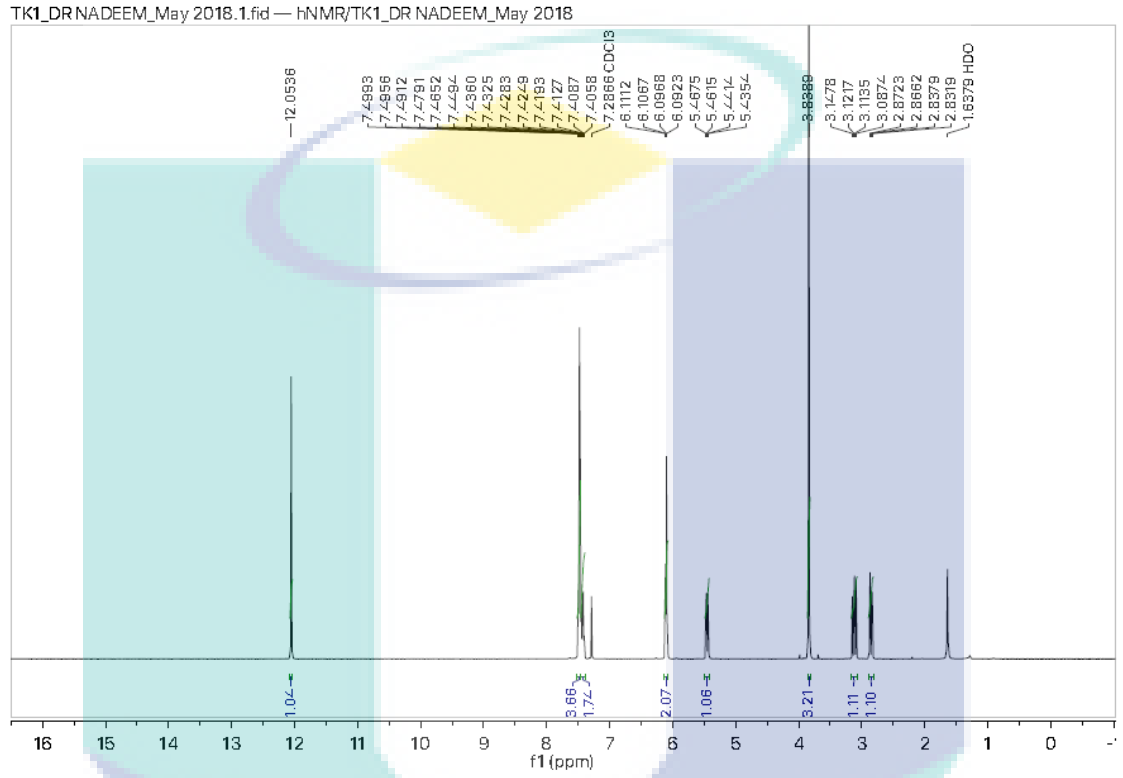
- Shindu K., Kato M., Kinoshita A., Kobayashi A., Koike Y., (2006). Analysis of antioxidant activities contained in the *B. rotunda* Schult. Rhizome. *Bioscience Biotechnology Biochemistry*, 70, 2281-2284.
- Sukari M. A., Ching A. Y. L., Lian G. E. C., Rahmani M., Khalid K. (2017). Cytotoxic Constituents from *Boesenbergia pandurata* (Roxb.) Schltr. *Natural Product Sciences*, 13(2), 110-113.
- Stevenson P.C., Veitch N.C. Simmonds M.S., (2007). Polyoxygenated cyclohexane derivatives and other constituent from *Kaempferia rotunda* L. *Phytochemistry*, 68, 1579-1586.
- Tanjung, M., tjahjandarie, T. S., and Sentosa, M. H. (2013). Antioxidant and cytotoxic agent from the rhizomes of *Kaempferia pandurata*. *Asian Pacific Journal of Tropical Disease*, 3(5), 401-404.
- Thermo Fisher Scientific. (2008). IA9000 Series Digital Melting Point Apparatus: *Operation and Safety Instructions*. Essex, UK: Thermo Fisher Scientific Inc.
- Tewtrakul, S., Subhadhirasakul, S., Karalai, C., Ponglimanont, C., and Cheenpracha, S. (2009). Anti-inflammatory effects of compounds from *Kaempferia parviflora* and *Boesenbergia pandurata*. *Food Chemistry*. 115, 534-538.
- Tewtrakul S., Subhadhirasakul S., Puripattanavong J., Panphadung T. (2011). HIV-1 protease inhibitory substances from the rhizomes of *Boesenbergia pandurata* Holtt. *Journal of Science Technology*, 25,(4), 56-78.
- Tewtrakul S., Subhadhirasakul S., Kummee S. HIV-1 protease inhibitory effects of medicinal plants used as self-medication by AIDS patients. *Songklanakarin Journal of Science and Technology*, 25(2), 239-243, 2003b.
- Trakoontivakorn G., Nakahara K., Shinmoto H., Takenaka M., OnishiKameyama M., Ono H., Yoshida M., Nagata T., Tsushida T., (2001). Structural analysis of a novel antimutagenic compound, 4-hydroxypanduratin A, and the antimutagenic activity of flavonoids in a Thai spice, Fingerroot (*Boesenbergia pandurata* Schult.) against mutagenic heterocyclic amines. *Journal of Agriculture Food Chemistry*, 49, 3046-3050.
- Tuchinda P., Reutrakul V., Claeson P., Pongprayoon U., Sematong T., Santisuk T., Taylor W.C., (2002). Anti-inflammatory cyclohexenyl chalcone derivatives in *Boesenbergia pandurata*. *Phytochemistry*, 59, 169-173.
- United States Pharmacopeia and National Formulary, (2002). *United States Pharmacopeial Convention Inc.*, Rockville. USP 25, NF 19.
- Voravuthikunchai S.P., Phongpaichit S., Subhadhirasakul S., (2005). Evaluation of antibacterial activities of medicinal plants widely used among AIDS patients in Thailand. *Pharmaceutical Bioogy*, 43, 701-706.
- Wu, D., and Kai, L. (2000). Zingiberaceae. *Flora of China*. 24, 322-377.

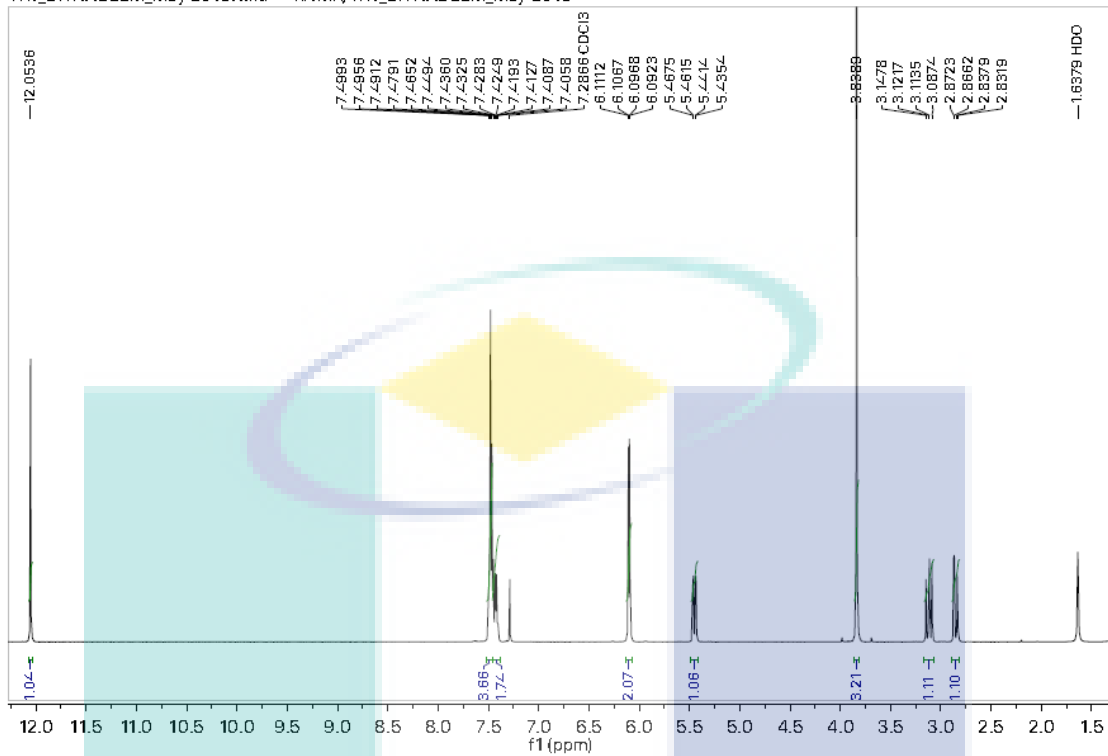
- Yamovoi V.I., Kul'magambetova E.A., Kulyyasov A.T., Turdybekov K.M., Adekenov S.M., Molecular structure of a novel polymorphic modification of pinostrobin. *Chemistry of Natural Compounds*, 37(5), 424-427.
- Yap, A. L. C, Tang, S. K., Sukari, M. A., Ee, G. C. L., Rahmani, M., and Khalid, K. (2007). Characterization of flavonoid derivatives from *Boesenbergia rotunda* (L.). *The Malaysian Journal of Analytical Sciences*, 11(1), 154-159.
- Yun J.-M., Kweon M.-H., Kwon H., Hwang J.-K., Mukhtar H. (2006). Induction of apoptosis and cell cycle arrest by a chalcone panduratin A isolated from *Kaempferia pandurata* in androgen-independent human prostate cancer cells PC3 and DU145. *Carcinogenesis*. 27 (7), 1454-1464.
- Zanariah U., Nurul I.N., Thavamanithevi S. (2016). Ginger Species and their Traditional uses in Modern Applications. *Journal of Industrial Technology*, 2 (6), 45-55.

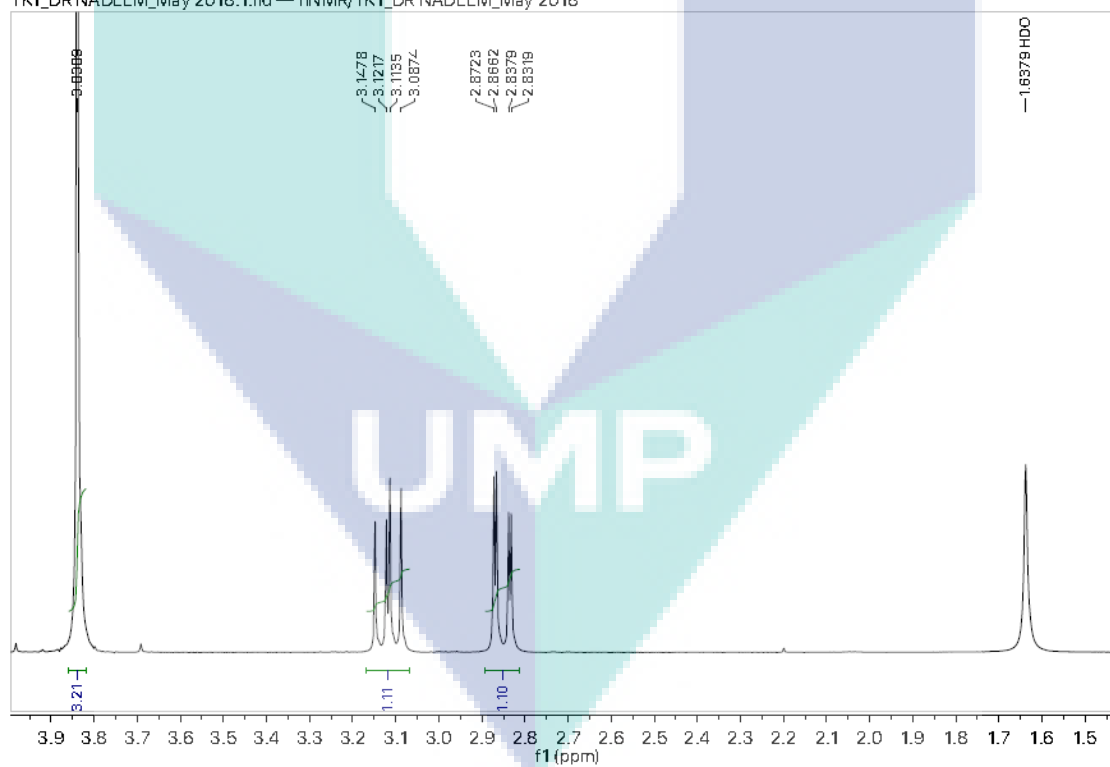
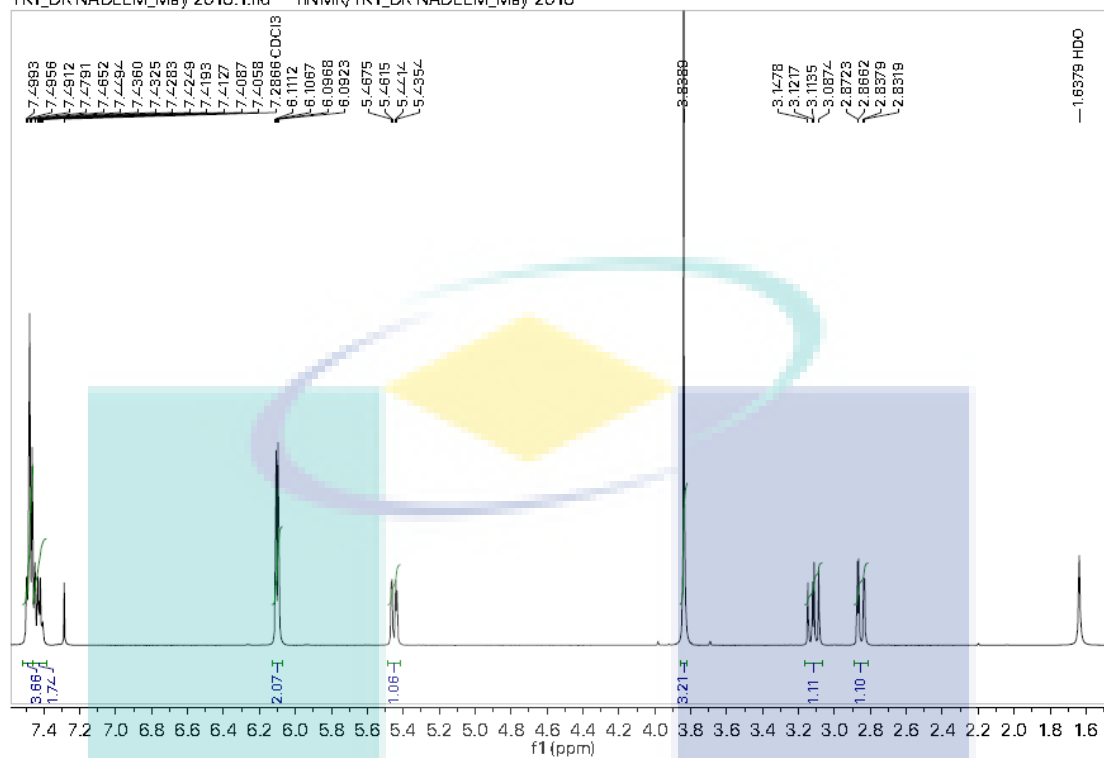
The logo of UMPU (Universiti Malaysia Perlis) is a large, downward-pointing arrow shape. It is composed of four colored segments: a light blue segment on the top left, a light purple segment on the top right, a teal segment on the bottom left, and a light blue segment on the bottom right. The letters 'UMPU' are written in white, bold, sans-serif font across the center of the arrow.

UMPU

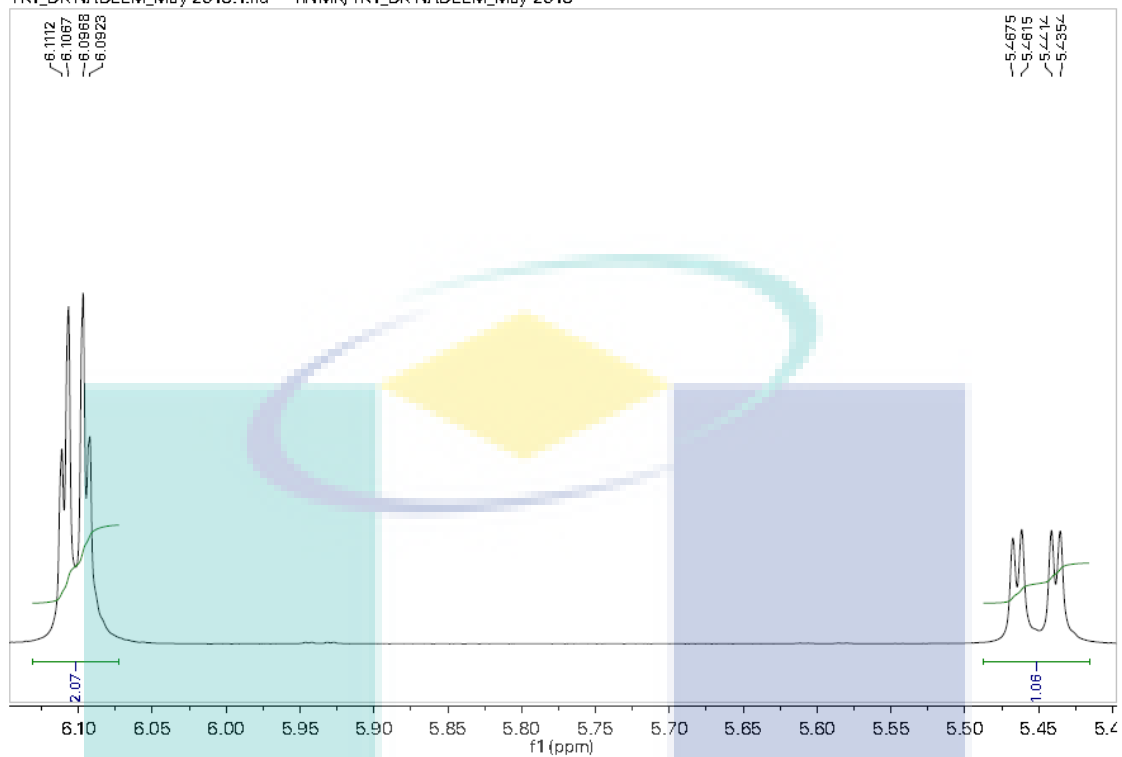
APPENDIX A
RESULT OF ¹H NUCLEAR MAGNETIC RESONANCE NMR



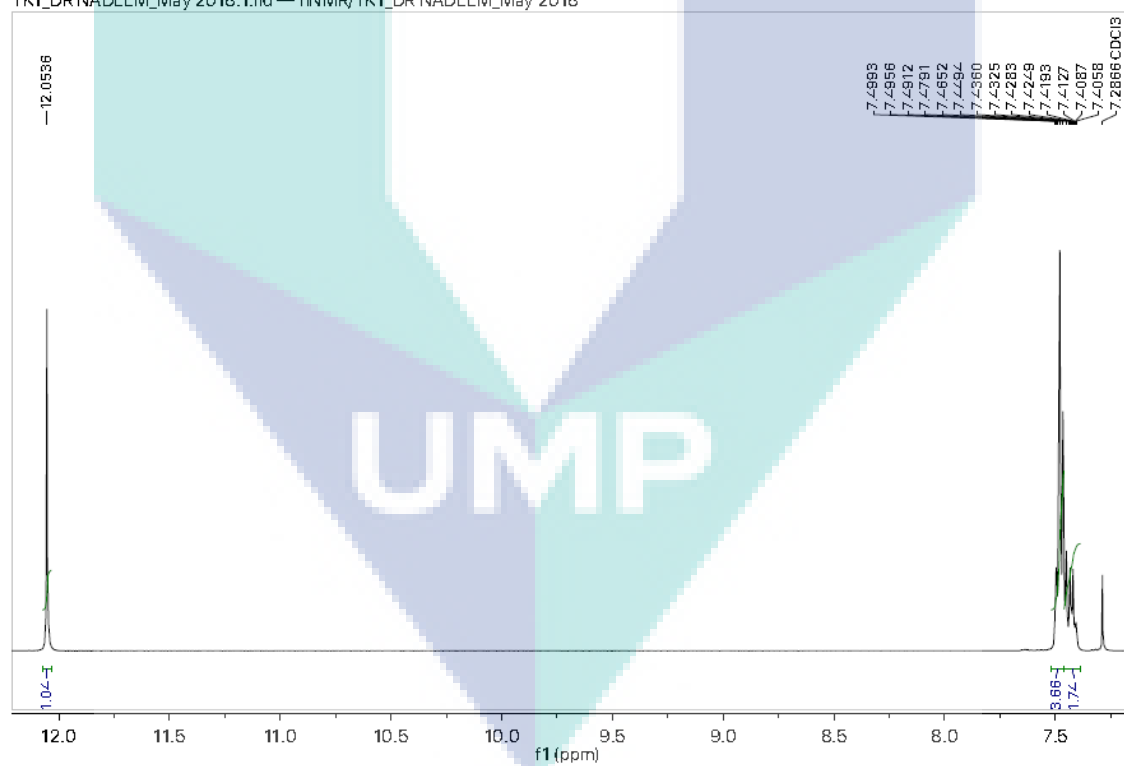




TK1_DR NADEEM_May 2018.1.fid — hNMR/TK1_DR NADEEM_May 2018

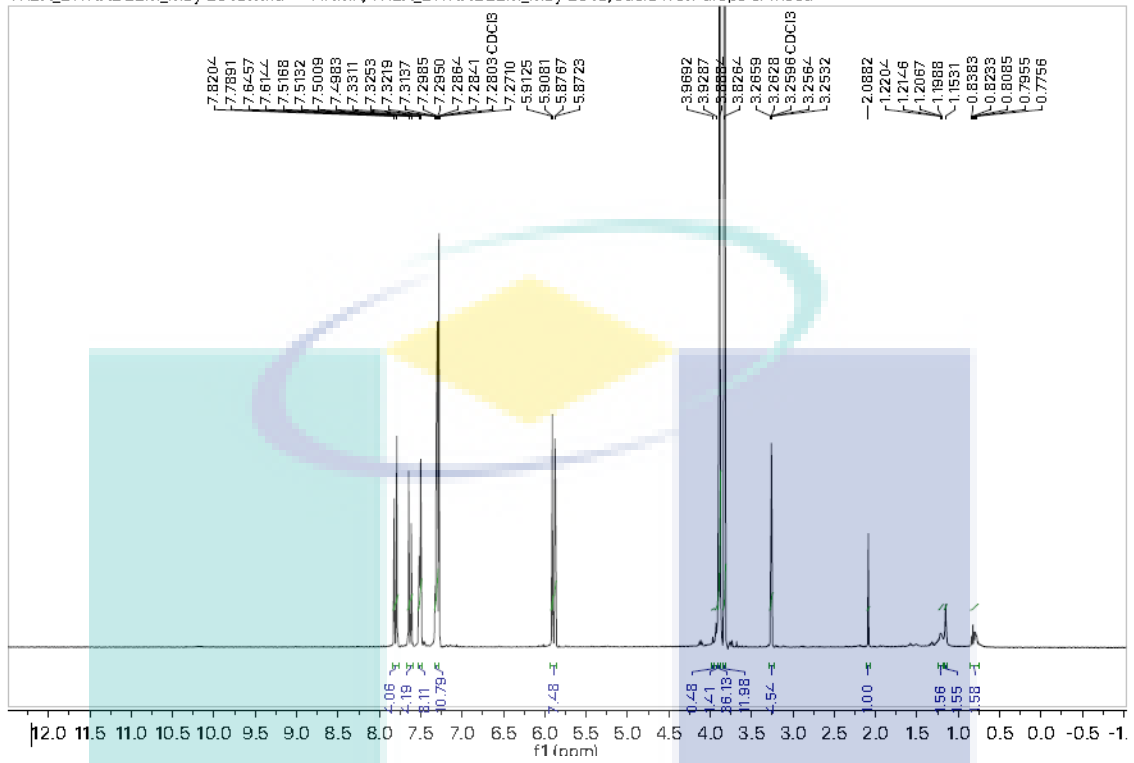


TK1_DR NADEEM_May 2018.1.fid — hNMR/TK1_DR NADEEM_May 2018

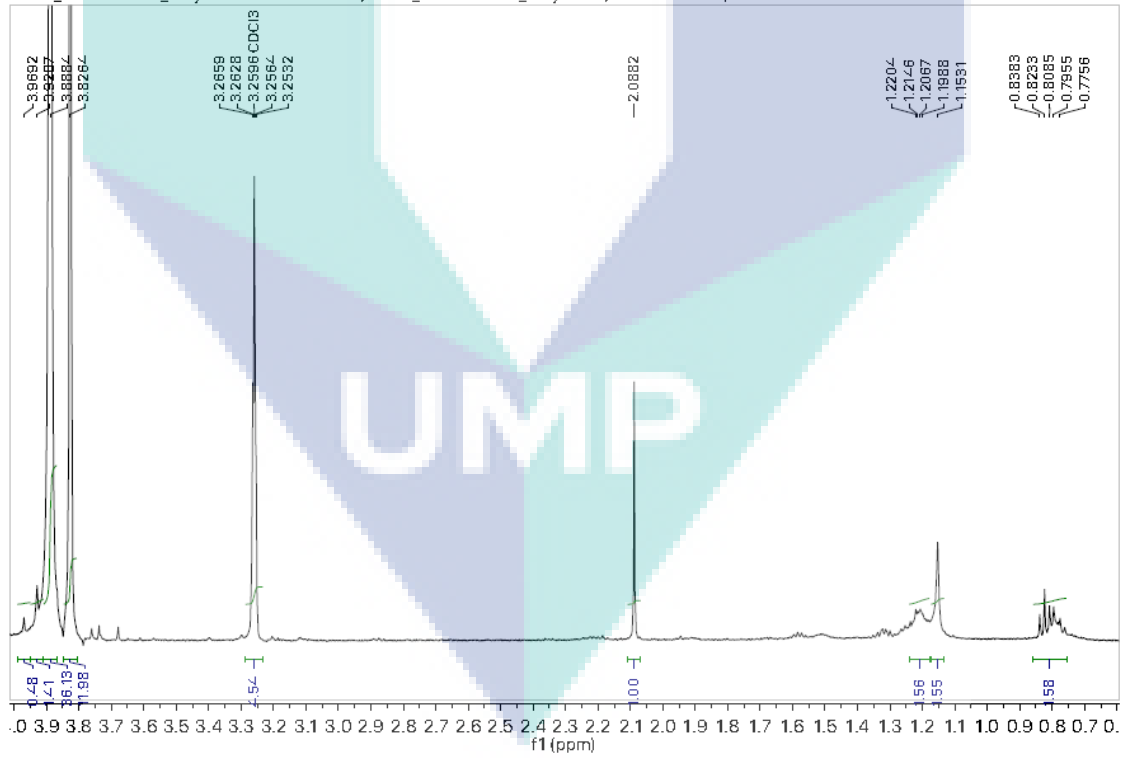


TK2A

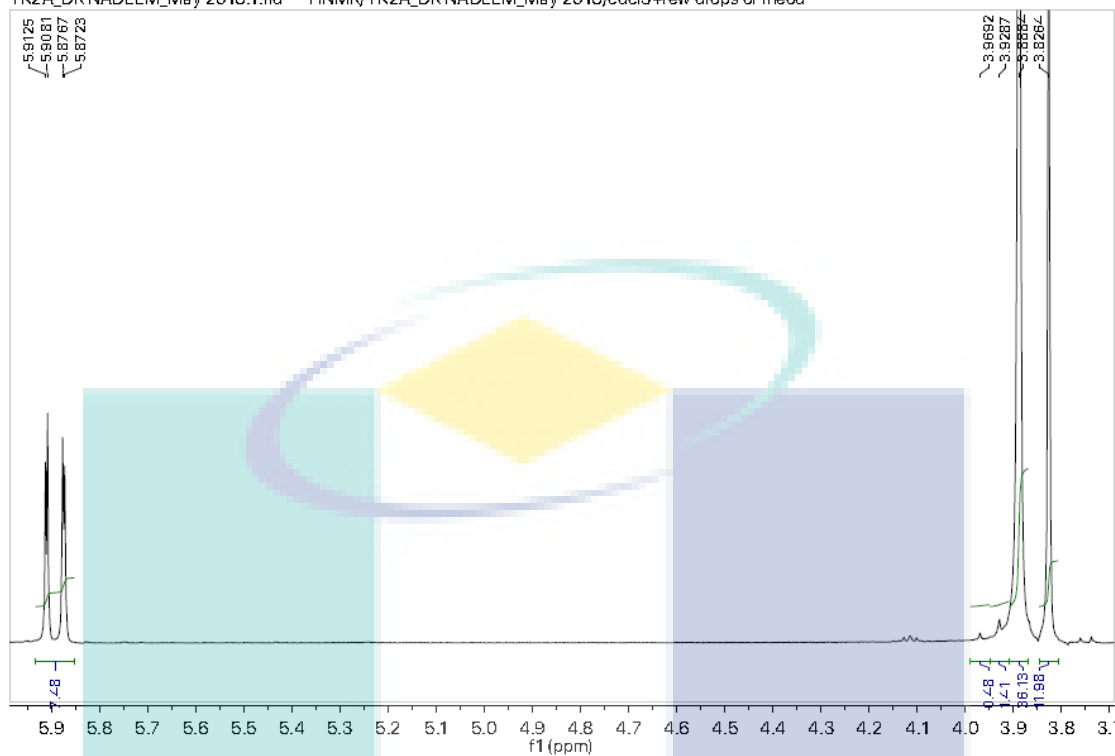
TK2A_DRNADEEM_May 2018.1.fid — HNMR/TK2A_DRNADEEM_May 2018/cdcl3+few drops of meod



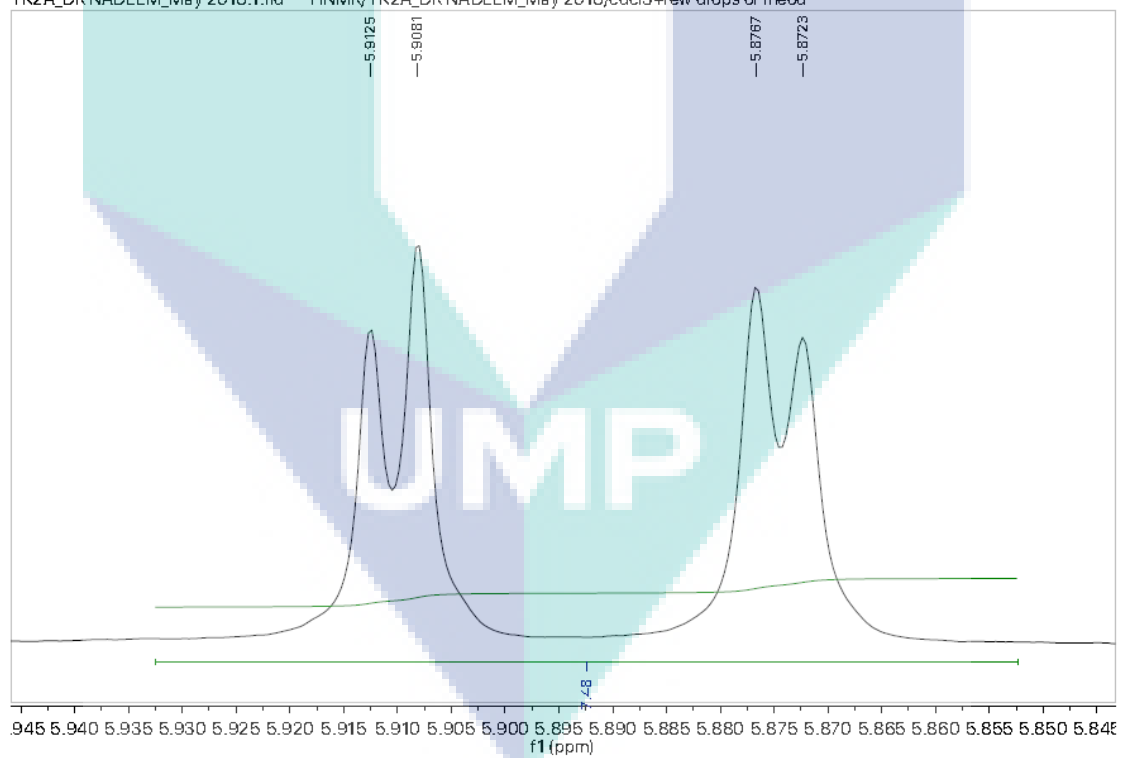
TK2A_DRNADEEM_May 2018.1.fid — HNMR/TK2A_DRNADEEM_May 2018/cdcl3+few drops of meod



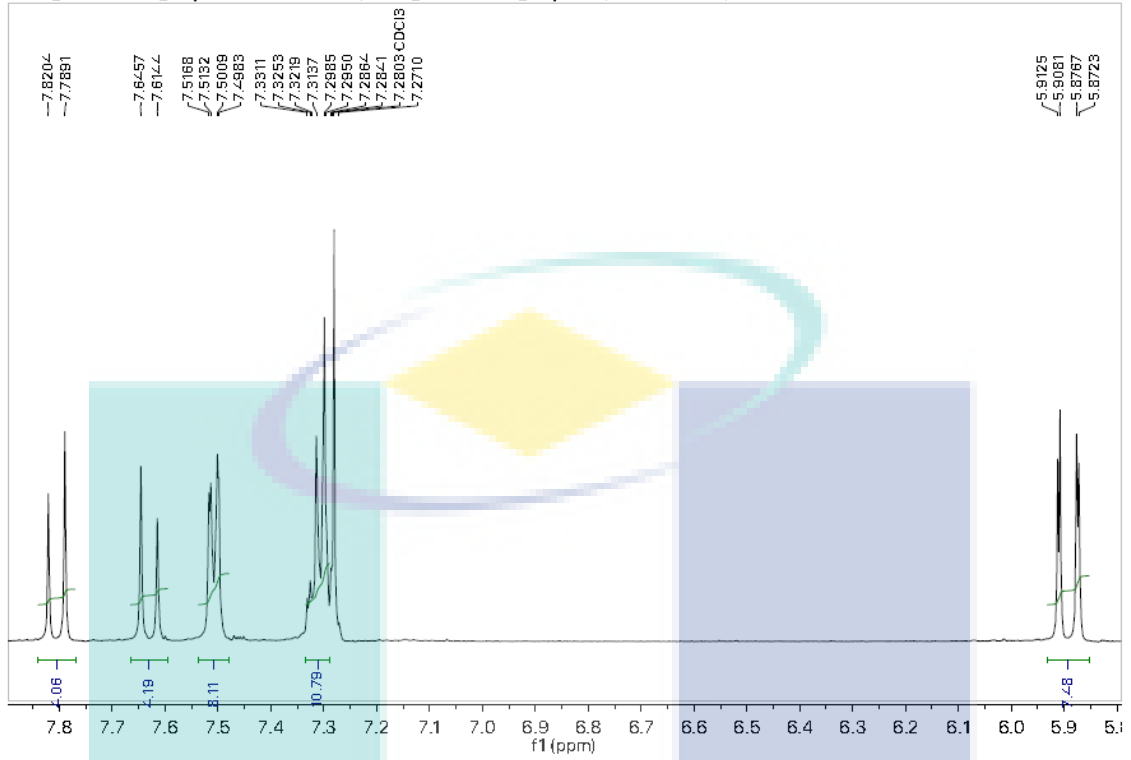
TK2A_DR NADEEM_May 2018.1.fid — HNMR/TK2A_DR NADEEM_May 2018/cdcl3+few drops of meod



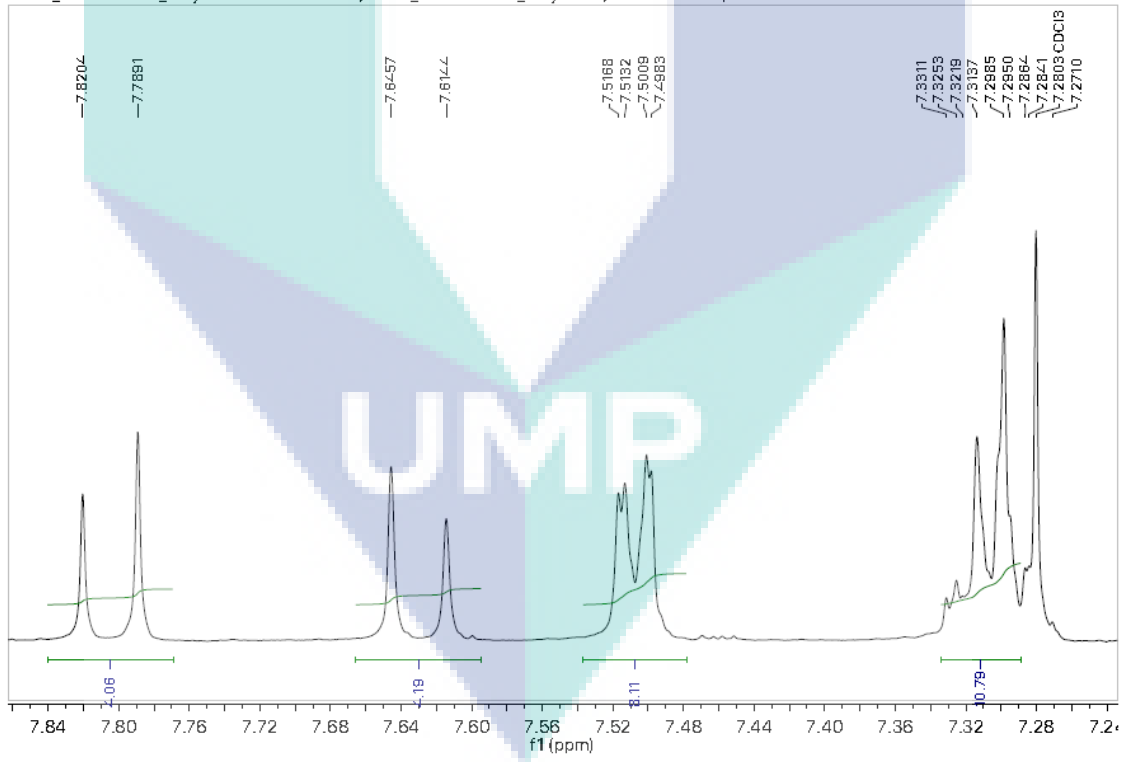
TK2A_DR NADEEM_May 2018.1.fid — HNMR/TK2A_DR NADEEM_May 2018/cdcl3+few drops of meod



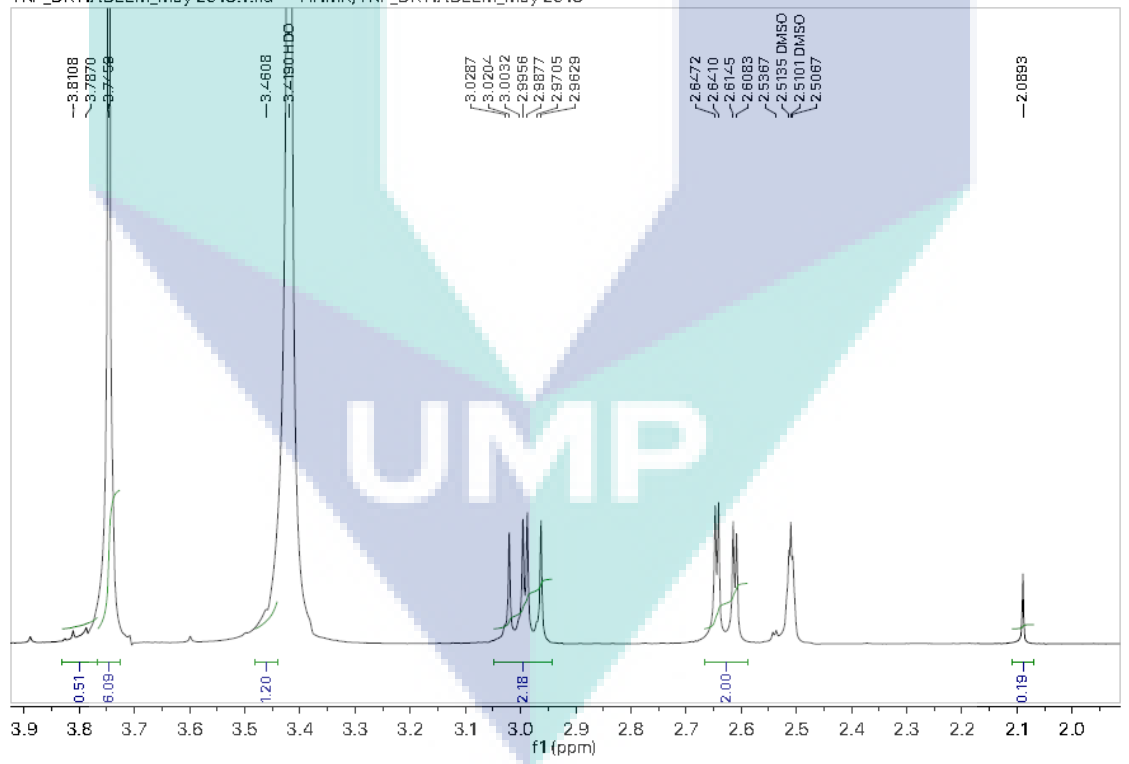
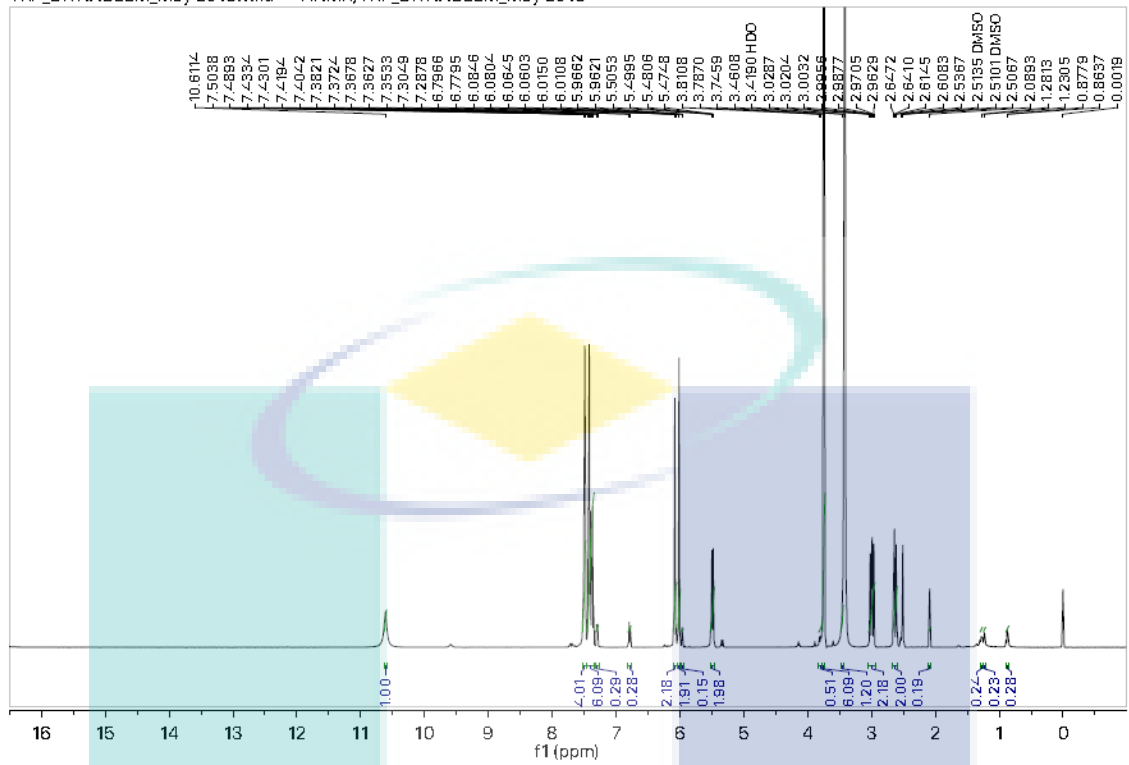
TK2A_DRNADEEM_May 2018.1.fid — HNMR/TK2A_DRNADEEM_May 2018/cdcl3+few drops of meod



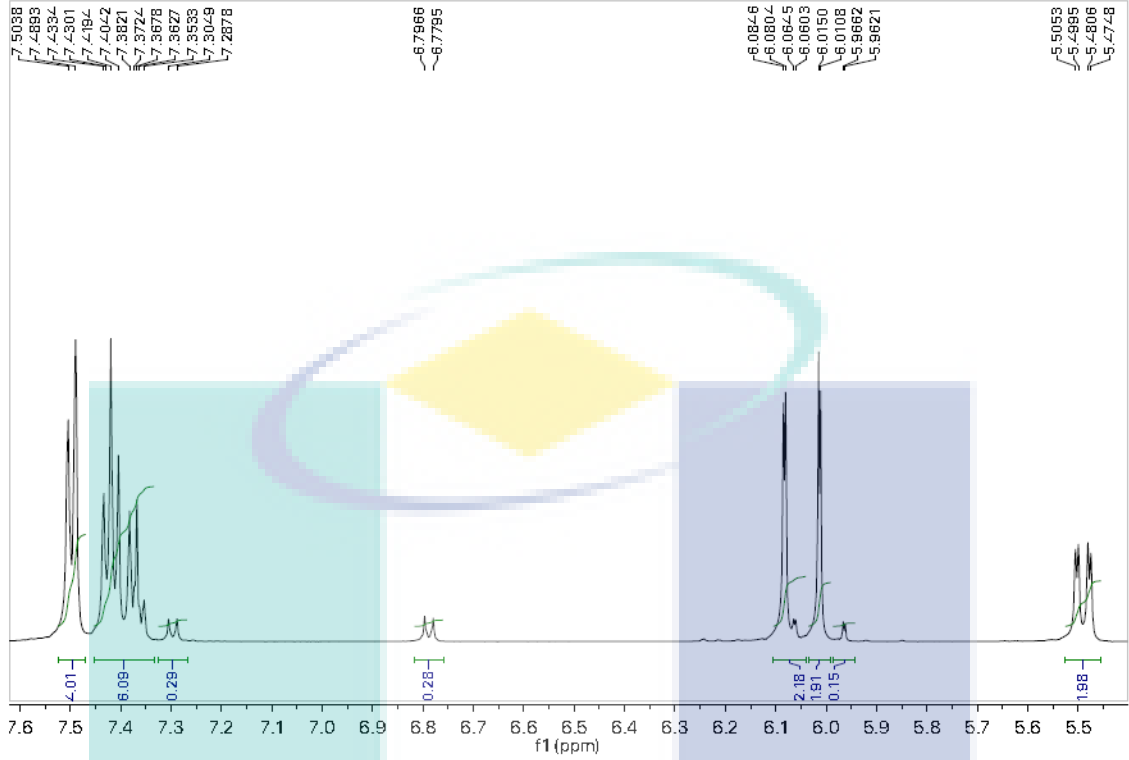
TK2A_DRNADEEM_May 2018.1.fid — HNMR/TK2A_DRNADEEM_May 2018/cdcl3+few drops of meod



TKP



TKP_DRNADEEM_May 2018.1.fid — HNMR/TKP_DRNADEEM_May 2018



TKP_DRNADEEM_May 2018.1.fid — HNMR/TKP_DRNADEEM_May 2018

